University of Stavanger

Faculty of Science and Technology

Master thesis

Study program/Specialization: Petroleum Engineering (Well Engineering)	Spring semester, 2016 Open
Author: Omar Salem Alani	..... (signature author)

Faculty supervisor: Dan Sui (UiS)

External supervisor: Eric Cayeux (IRIS)

Title:

Drillbotics 2016:

Management of drilling incidents while drilling heterogeneous formation rocks.

Study points: 30

Keywords:

Rig design	Machine control	Drilling control
Drilling performance	Drilling incident	Drilling parameters

Pages: 98

+ enclosure: 16

Stavanger, 28. June. 2016

Drillbotics 2016:

Management of drilling incidents while drilling heterogeneous formation rocks.

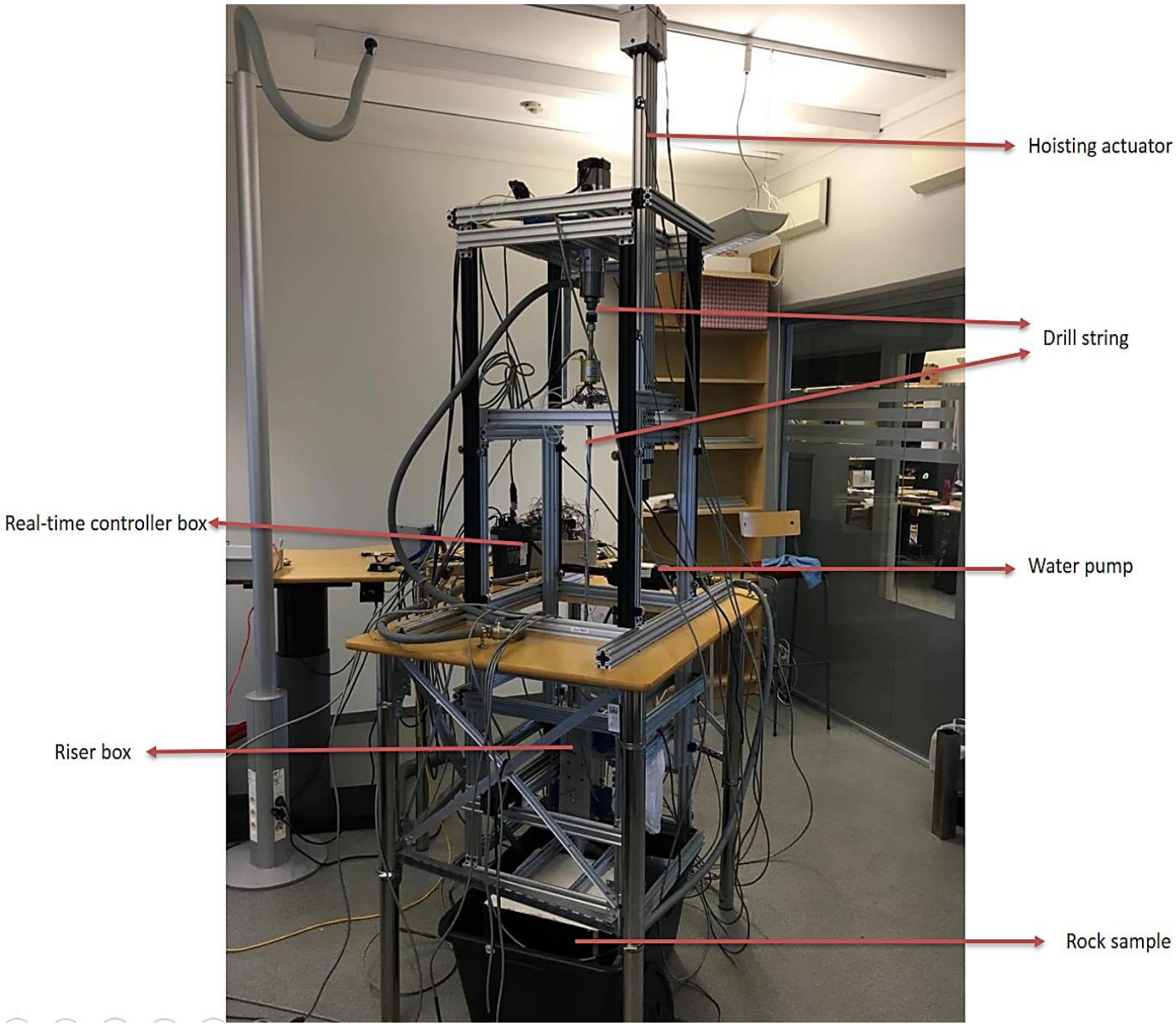

Acknowledgments

Above all, I want to thank my God that gave me strength to make this master thesis to reality. This thesis is a result of a large research and building in the laboratory in addition to writing work. This challenge changed me as a person and made me more responsible person.

I would like to give a special gratitude to my external supervisor **Eric Cayeux** that helped me despite his busy schedule. I also want to thank my internal supervisor **Dan Sui** for her support when I needed. Moreover, I am really grateful and blessed to have my teacher **Mesfin Belayneh** by my side that always was there to encourage and help me when I needed.

I will also thank my family and friends for their love, support and prayers that gave me the motivation to stand on my feet and complete this thesis.

Abstract

The purpose of the thesis is to analyse the abnormal incidents on the drill pipe. The reason for this research is to apply the learned theories into the reality by building an automated rig and detect the problems. Also, to participate in Drillbotics competition 2016. Drillbotics 2016 is an international competition arranged by Drilling Systems Automation Technical Section (DSATS) that is a part of the Society of Petroleum Engineers (SPE), to encourage students to build a small and fully automated rig to drill safety and efficiency a rock sample as vertically and fast as possible.

Using literature backgrounds of circumstances combined with theories makes it easier to get an estimated overview of the failures that might occur while applying different drilling parameters. Moreover, which parameters used in term of drilling to drill more safety without failures.

The analysis that performed based on the design such twisting, buckling, vibration and leakage, and overpressure testing. Optimising the rotational speed and weight on bit applied; reduces problems such twisting, buckling and vibrational movements. The choice of the rotational speed and the weight on bit is based on the type of drill pipe materials which is the weakest component of the drill string, with respect to the maximum yield and ultimate torque of the drill pipe material.

The next step is to build the design and see if it is working properly with the chosen values. Tests like leakage, overpressure, and over-torque performed after calibrating the load cells to evaluate the reaction of the real-time controller, to be able to stop the rotation in case of:

- Low circulation pressure, leakage
- High circulation pressure, overpressure
- Over-torque, sticking

Later buckling tests by applying weight on the 2.20 mm thick and 1 m long pipe, to determine the maximum weight that buckles the pipe. In the end, vibrations are observed after rotating at 180 rpm. The rig design is working fine and safe in term of torque, buckling and circulation system, but there are quite high vibrations that made it difficult to read the signal from the accelerometers.

Table of Contents

List of figures

List of tables

List of Abbreviations

WOB	Weight on bit
ROP	Rate of penetration
RPM	Revolution per minute
DSATS	Drilling System Automation Technical Section
PDC	Polycrystalline diamond composite or compact
DP	Drill pipe
UCS	Unconfined Compressive Strength
CCS	Confined Compressive Strength
MSE	Mechanical Specific Energy
PLC	Programmed Logic Controller
NP	Neutral point

Nomenclatures

σ	Axial stress	F	Axial force
A	Area	ε	Normal strain
ΔL	Elongation	L_0	Original length
E	Young`s modulus	τ_{max}	Maximum torque
τ_y	Yield torque	$\sigma_{shearmax}$	Fracture shear stress
$\sigma_{shearyield}$	Yield shear stress	σ_r	Radial stress
σ_θ	Tangential stress	σ_a	Axial stress
Fc	Coulomb`s friction force	μ	Friction coefficient
N	Normal force	Fv	Viscous friction force
f	Viscous coefficient	Ft	Total friction force
τ_{total}	Total torque	W_{BHA}	Weight of the BHA
$W_{applied}$	Weight on bit		

Chapter 1: Introduction

1.1 Background

Optimising drilling parameters in such way to drill through rock formation without failures is a bit of a challenge in oil and gas industries. Controlling drilling parameters like the weight on bit (WOB) applied and the rotational speed (RPM) are the key increasing the probability of managing to drill successfully through different formation layers without problems. The drill string is the element that is responsible for drilling where the drill pipe is the weakest component. The most mechanical failures occur on drill pipe, failures that pull the pipe apart like twisting and axial loads combined with rotation. Accumulation of cuttings causes pack off, which is a dangerous scenario in drilling starting with a reduced hole diameter, then develops to sticking problems. Pack off indicated by a noticeable increase in standpipe pressure where a remedial action required. If standpipe pressure reduces without changing any of drilling parameters like rotational speed or mud weight, there is a possibility of pipe washout which may occur due to drill pipe failure. So any failure in drill pipe during drilling causes other failures like leaks which are very dangerous for the crew and environment.

Such incidents are quite expensive to deal with, where the major issue those oil and gas industries have in mind is maximising the economic profit. Drilling failures cost the industry because of the lost time due to fixing and fishing.

The challenge of drilling becomes tougher when formation rocks have different properties, where some of the rocks are soft, and others are hard. During drilling through soft rocks then suddenly met hard rocks, the torque that exposed to the drill pipe increases. When the torque that applied to drill pipe exceeds the materials ultimate torque, the pipe fails by twisting. Vibrations occur during rotation of the drill string and result from rapid and continuous shocks that are fatiguing the drill string, where such problem accelerates twisting the pipe off. So the rotational speed and drill string stability should be controlled to reduce such a problem.

1.2 Drillbotics

Drilling System Automation Technical Section (DSATS) has made this competition; Drillbotics 2016, encouraging students to be able to use automated systems in drilling. Many complicated problems included in such competition, an example of that is the thin drill pipe,

which twists very easily. This project is planning to make students understand how is it to be an engineering since the design is built to be aware of the most of the drilling problems such drilling parameters and drill string failures. Also, this project includes many electrical parts that need programming to make it work such stepper motor, hoisting motor, pump, and riser system. The task is to design, build and determine the various drilling failures.

Drillbotics competition arranged first time in spring 2015, where many universities from different regions of the world were participating; the three finalists were the University of Texas, Oklahoma, and Texas A&M [1]. The competition was about to be able to drill through a cubic rock with different formation layers as fast and vertically as possible, but none of the finalists was able to complete drilling through the stone. Where the three universities failed due to failures on drill pipe and connections.

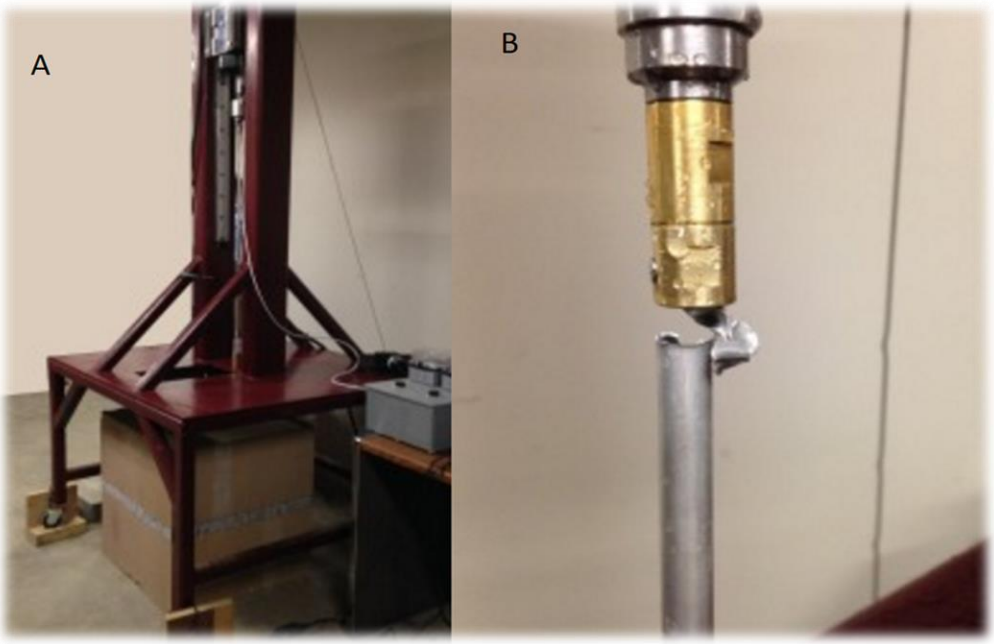

Figure 1: The rig of the University of Texas A&M. B: Failure by twisting drill pipe [1].

This spring 2016, the competition took place and we were unfortunately not qualified to the final stage, but we have arranged a local Drillbotics competition with the University of Agder. Our goal is to drill completely and as vertically as possible through the cubic rock.

This project is new of its kind, which deals with different drilling issues that every driller should have in mind. An automated drilling rig is the future of drilling, where it is an advantage to exploit new technologies. Also, an automated drilling rig makes it safer to perform drilling

operations. Such drilling rig deals with the variation of rock layers and optimises drilling parameters automatically.

Such challenge demands a good understanding of drilling parameters, like the rate of penetration (ROP), rotational speed (RPM) and weight on bit (WOB) to ensure safe drilling in the case of stick and slip and torsional oscillations. Twisting, vibrations, buckling and pump control are important issues that need to be aware of.

1.3 Objective

The project consists of a team of three students and one external supervisor. The task is about to construct and build a drilling rig to drill through a cubic rock with different layers that have dimensions of 30x30x30 cm as vertically as possible as fast as possible. The perspective of this thesis is to be able to give a simple analysis of the behaviour of the drill string regarding different drilling scenarios like the twist off (over-torque), overpressure, leakage and vibrations during drilling. Where the following studies the thesis focuses on:

- Literature study on the theory of drill string mechanics and hydraulics
- Drillbotics related engineering design calculation
- Rig design, construction, and calibrations
- Drillbotics drilling experiments

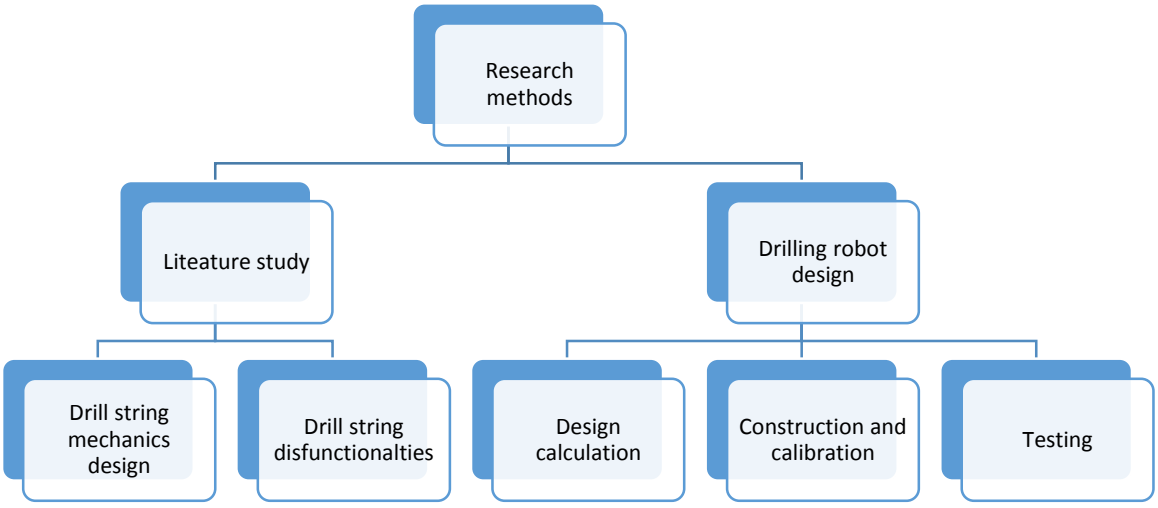

Figure 2: The summary of research methods employed in this thesis work.

Chapter 2: Literature study

During drilling in hard zones, the drill string may become forced to twist in the borehole. One of the biggest problems in drilling is drill string twist off. Understanding and eliminating such problem is an important issue. Twist off problems in real life drilling could be very dangerous for the crew who are working in oil and gas industry and the environment. When twist off occurs, a pressure drop in the drill string is noticed, in some cases water or mud comes out from the pipe. Twist off is the most breaks down scenarios during drilling in the oil field; due to the danger and stressful situations that drilling crew would meet. It is not only dangerous when twist off occurs, but the fishing job is dangerous as well as it is equipment and time demanding. In addition to all that, twist off scenarios is very expensive due to the loss of rig time during fishing. Where it could take weeks of fixing properly. The upper part of the drill string is easy to fish out, but the bottom part may not be fished then a need of side track to carry on drilling.

At the 1980s, it was noticed in many areas, for example in West Africa, 77% of the failures occur in the BHA and the remaining 23% in the drill pipe [2]. TH Hill has analysed drill string failures between 2001 and 2003 and covered 68% of drill string failure due to fatigue. Also, while overloading by a combination of tension, torque, and corrosion counted only 17% and 4% of drill string [3].

Drill string fails due to the following as illustrated in figure 3:

- Compression
- Tension
- Torsion and Tension
- Torsion and Compression [4]

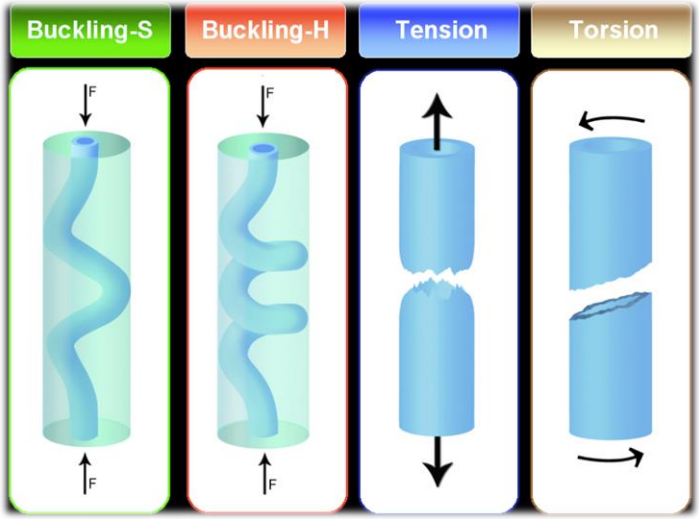

Figure 3: Typical drill pipe failures [4].

Continues loadings are damaging the drill string what is called fatigue failure. Cyclic loading may induce because of rotating while buckling or vibration caused by excessive weight on bit. The level of the cyclic loadings depends on the displacement of the drill string during drilling. In addition to the cyclic load fatigue failure of materials is quite complicated and depends on several other parameters like the type of equipment material and the environment of drilling. Notice that both inclination and vibration increase the complexity of fatigue.

2.1 Drilling bits

Depending on the kind of formation that drilled, a proper drill bit selected to do a properly drilling job which depends on the hardness and abrasiveness of the formation. During drilling the drill bit meets different types of formation; there are soft/medium formation such shale, sands or medium/hard formation like hard limestone, dolomite. Some hard/abrasive formation find a place during drilling as well such granites, basalts, and quartz.

PDC bit is one of the most used drill bits during drilling where that type of bits has fixed cutter blades as the number of cutters can vary; the fixed body made from tungsten carbide that has excellent resistance to erosion. It has a fixed head and rotates as a one-piece, and it is effective at drilling into soft to medium/hard formations, not preferable in very hard and abrasive formation [5]. Roller cone: The second type that is used the most during drilling is the roller cone, this type has a ball and roller bearing, and when the drill pipe rotates the three cones roll on the formation and crushes the rock while a certain WOB is applied. Bearings are the weak point of this type since cones can get lost, and the cutters can be worn down. Roller cone bit used where the PDC does not work in soft, medium and hard formation. Roller cone can cause axial vibrations due to three cones and lateral vibrations.

Figure 4: PDC bit with five blades (left) and roller cone bit (right) [5].

The advantage is that the torsional vibrations are much less in roller cone compared to PDC bits.

Unwanted vibrations such axial movements that make the bit bounce, lateral and torsional (twist about its axis (stick-slip)) occur during drilling. Those vibrations could lead to destroying and wear the bit quite fast. The lateral and torsional vibrations are the most common movements that PDC bits can cause, where the roller cone bit leads to more axial and lateral movements as illustrated in Table 1.

Table 1: Different motions on different bits [5].

Motion / Type	*PDC*	*Roller cone*
Axial	No	Yes
Torsion	Yes	No
Lateral	Yes	Yes

2.2 Drilling problems

The formation types are different and mixed randomly with each other what makes it harder to drill through. The formation also has different inclinations. Different rock types in the formation would cause a variety of movements like vibrations and torque would occur at the drill string. Torque and vibrations can damage the drilling system due to the huge movements of the drill string during drilling operations; that could cause damages to the drill pipe such twisting or buckling in a case of sticking while drilling with high RPM.

A study case of the drilling system before starting to drill is required, to be able to get a good overview of what could happen and how to avoid problems. A drill pipe buckled for reasons the oil industry were not aware of at the Macondo well in the Gulf of Mexico and that caused failures to seal the well which caused a disaster in 2010 [6].

Two wells near each other might have different formation layers. Therefore, a good drilling plan for every well is required. Designing a good program is the key to achieving a successfully

drilled hole through different types of rocks. The most problems that have reported are like stick-slip, lost circulation, twisting drill pipe, damaging drill bit, hole deviation, pressure problems and many other problems that come up in every single well.

2.2.1 Drill string twist off

One of the biggest problems during drilling are problems related to drill string because it is the weakest element in the drilling system. Those types of problems are related to breaking the drill pipe due to over-torque, and it is called twist off. When drill pipe fails due to twisting off in real life drilling scenario, that might cost the industry a lot because of the time spending on fishing the drill string equipment. It may take days or weeks to manage to fish the parts of the drill pipe. In fact, fishing a twisted drill pipe that is more than 500 meters or many kilometres long, needs time and workers.

Figure 5: Twisted drill pipe [7].

The materials of the drill pipe decide when the drill pipe fails. It has a specific yield shear stress and ultimate shear stress. So if the torque exceeds the shear yield stress of the drill pipe, the drill pipe deforms, and later it fractures if the torque exceeds the ultimate shear stress. The torque of the drill pipe should not exceed the yield and fracture limits during drilling. So the drill pipe should be analysed theoretically and tested before drilling.

2.2.2 Drill string vibrations

One of the major failures on drill pipe is vibration and bouncing off the drill string and has huge effects on drilling performances. Vibrations take place due to:

- The misalignment of the drill string.
- The contact between the bit and formation and the contact between stabilisers and riser/formation.

Vibrations can induce by shocks that are a sudden input of energy due to the impact to the bit, BHA or drill pipe with wellbore formation. Vibrations result from rapid and continuous shocks that are causing fatiguing of the drill string and to the point of twist off. That is why drill string failures are the result of cumulative fatigue due to vibration where shocks are measured G (force of gravity) by using accelerometers. Shocks can have very high values, which may accelerate damaging the drill string.

Shocks depends on the following as illustrated in figure 6:

- The magnitude of the shocks because of the interaction
- Duration of shocks
- Frequency of shocks

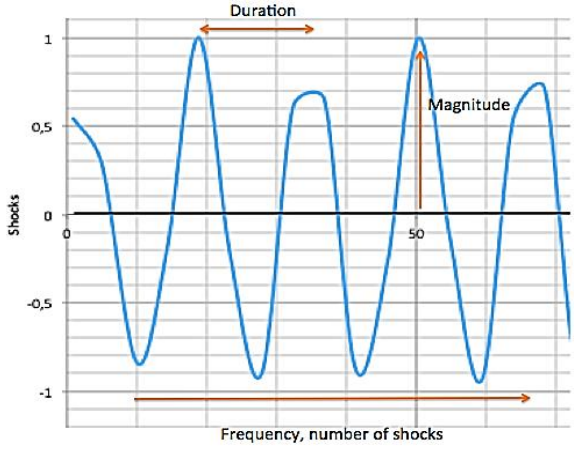

Figure 6: Parameters that determines the type of vibrational movement.

Shocks and vibrations reduce the impact of the drilling process and slowing down the ROP.

Vibrational motions

Several dynamic (BHA) bottom hole assembly vibrations/motions occur and those motions are accelerating damaging the drill string like the following proposals, where it is important to detect them to recommend the right cure. Axial, torsional and lateral vibrations occur during drilling; all those three movements cause a significant impact on the drill string and its components. In our case, those movements could easily accelerate twisting of drill pipe. The type of the bit that used considers the type of vibrations.

1. Axial movements occurred due to vibrations and WOB, and the force that induced allows for pipe hopping or bouncing. Afterwards, the shocks become absorbed by the drill string, which increases or decreases the WOB. Axial movements cause broken teeth of the drill bit, damaging downhole tools and slowing ROP.
2. Torsional shocks which resulting from momentary slowing down or stopping drill string where it is rotating irregularly in the wellbore. Torsional shocks occur when the bit digs into the formation deeply enough to slow it down about the drill string or when stabilisers dig into the formation. These types of movements lead to winding the drill string, which could fatigue drill string and causes twist off.
3. Lateral shocks induced by lateral movements from BHA, one side from the wellbore to the other reasons to dig the edge of the wellbore wall causes bigger hole diameter sometimes.

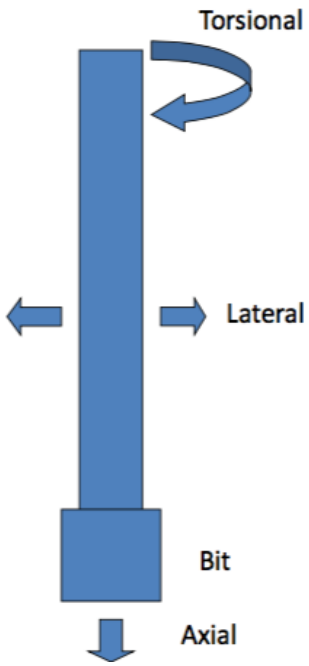

Figure 7: Vibrational motions [5].

2.2.3 BHA whirl

BHA whirl is very complex, and it results in none stabilised drill string and forces acting on the BHA. In other words, the drill string goes away from its centre of the wellbore into the wall of the well and causes enlarged borehole. Whirl occurs most frequently and limited to vertical wells. It happens when there are enough side forces to give sideways movement in the BHA to contact the wellbore wall, see figure 8 for forward and backward whirling [8].

There are three types of whirl that occurs as the following:

- Forward Whirl
- Backward Whirl
- Chaotic Whirl

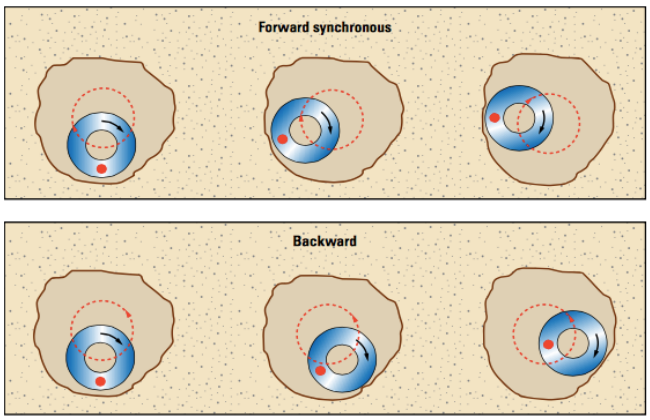

Figure 8: Forward and backwards whirl [8].

Forward whirl

When the BHA rotates along the borehole in the same direction as the rotation of drill string where the contact points to the wall of the wellbore is constant. This type of whirl causes destroying the components of the BHA.

Backward Whirl

Backward Whirl is very similar to forward whirl, except that the friction on backward whirl between the BHA and formation is greater. Increased friction increases torque which induced by the BHA to rotate opposite direction of rotation, where the collar inertia provides energy to make the BHA rotates backwards. This type of whirl could damage the drill string; the collar connections can be damaged and fatigued very fast. Resulting accelerating fatigue rate very rapidly, cracking, washout and possible twist off.

Chaotic Whirl

There are no size preferences of BHA contact to the formation. The torque is above the average along with lateral vibrations and shocks. Chaotic whirl may occur when changing RPM from forward or backward whirl. By drilling with a PDC bit in vertical wells, movements of the BHA would occur due to the aggressiveness of the bit by teeth interactions and none symmetric cutting displaces the bit and allows it to move chaotically.

2.2.4 Stick and slip

Pipe sticking

Some of the indicators of pipe sticking are an increase in torque and drag. Some preventions that should be done like to have lowest possible fluid loss of mud, control cuttings, swab and surge effects and to continue to rotate all the time if possible, to prevent most possible cuttings from falling to the bottom. One of the causes of mechanical sticking is the cutting from drilled formation. Instabilities in the borehole as hole caving or collapsing could cause a huge amount of cuttings that is challenging to control, especially in deviated wells. Also stopping pumping, mud causes accumulations of cuttings as illustrated in figure 9. [9]

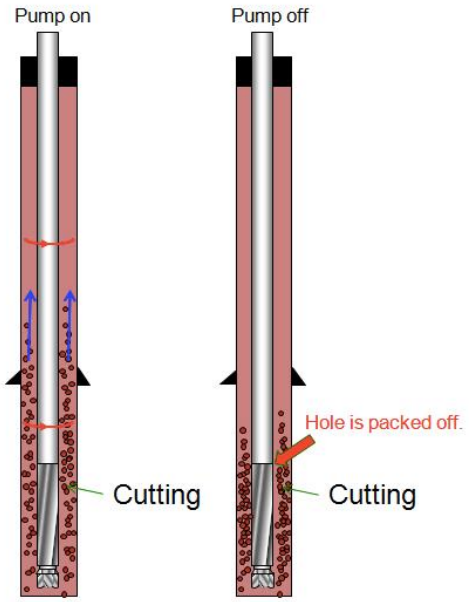

Figure 9: Cutting accumulation due to stop pumping and stop rotating [9].

Stick and slip

This phenomenon described as a non-uniform rotation of drill string, by slowing down and acceleration of the BHA. The BHA may stop or reverses its direction. As Illustrated in the curve in figure 10 below, the stick of the BHA stops at point A (stick point); that occurs because of friction effects where the BHA returns much slower than the pipe.

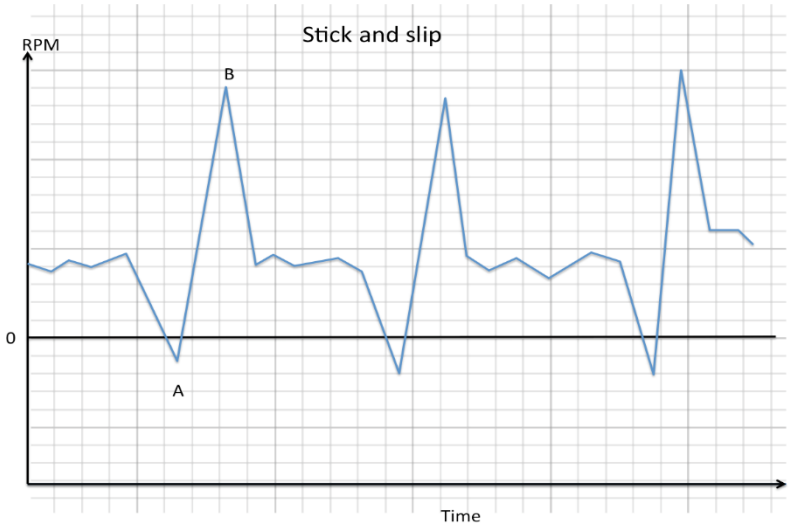

Figure 10: RPM behaviour during bit stick and slip.

Later, the stored energy in the string releases where the RPM increases drastically at point B (slip point).

Pipe sticking problems are mostly related to the stability of the borehole. For example, the use of low weight mud causing collapsing the borehole wall, which leads to sticking in next level. A pump system prepared in the design of Drillbotics that supplies from 9-13 liters/min to be able to transfer cuttings while drilling the cubic rock.

2.2.5 Buckling

Buckling is one of the issues that have most occurrence during drilling. There are two types of buckling sinusoidal and helical buckling as illustrated, figure 11. Sinusoidal is the first phase of buckling mode, the pipe buckles due to the axial compression force that exposed on the pipe due to the (WOB) during drilling. The Helical buckling is called the second phase of buckling by increasing the combined load and rotation on the pipe [10].

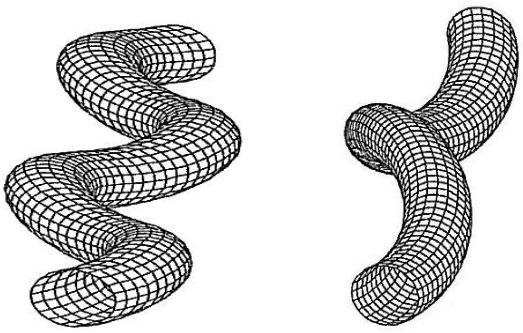

Figure 11: Sinusoidal (left)and helical (right)buckling [10].

Lockup

This phenomenon of a tubular in buckling situation when the pipe cannot push further. That means that when WOB applied the bit does not push, and this occurs because the axial force pushes the formed helix into the casing instead of pushing the bit as illustrated below

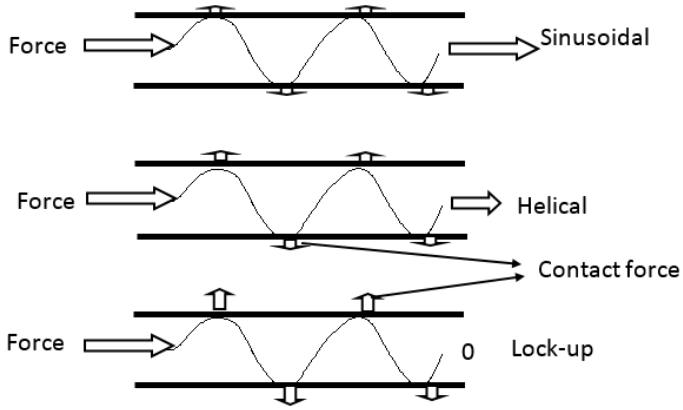

Figure 12: Lock up phenomenon [10].

2.2.6 Pack off

Pack off scenarios is plugging the wellbore around the drill string. Many reasons could be the cause behind that scenario like drilling with a high rate of penetration (ROP), collapsing the formation or due to weak cuttings transport or all three combined. During this scenario the circulation reduces or stops then followed by increasing pressure of the pump. So, if there are no remedial actions the pipe sticks in the hole [11].

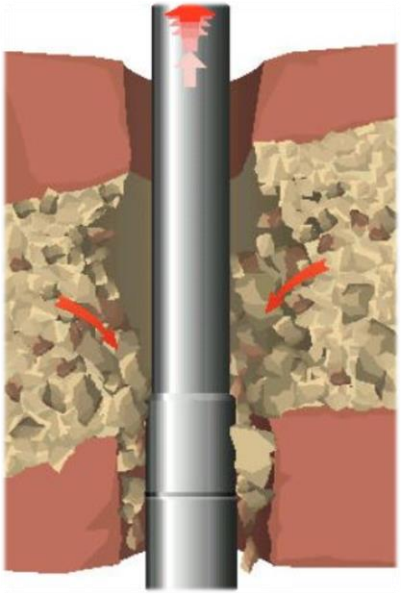

Figure 13: Collapsing causes pack off [11].

In our case, Drillbotics design, the real-time controller reacts to excessive pressure build up. It programmed in such way that when the pressure in the system builds up, the pressure sensor in the circulating system reads the pressure increase then command the pump to stop. The maximum pressure that the real-time controller operated with is 3.8 bar with 5% safety factor of the highest pressure of the pump 4 bars. Note that the pump has a built-in sensor that stops the pump if the pressure exceeds 4 bars.

2.2.7 washout

Leaks often discovered during drilling, but it is an advantage to discover leaks as early as possible. In our case, Drillbotics design, we use circulation pressure and flow rate measurements as a detection. Washout is pressure loss in the drilling system of the drill string, casing, and other equipment during drilling without changing any of the parameters as flow rate or mud type. Moreover, that pressure loss could be caused by leakage of drilling fluid somewhere in the system like for example leakages between connections of the drill string or in the drill pipe. So, Leakages causes pump pressure to drop, and the flow rate decreases [12].

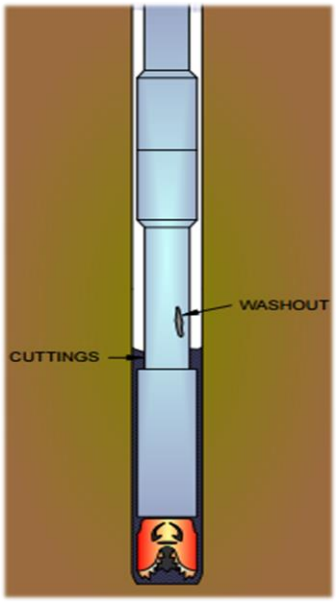

Figure 14: Drill pipe washout [12].

In our case, any leakages cause a risk for the rig and equipment because there are electric parts and workers in place. So If the pressure drops to 1.92 bars, the real-time controller reacts by stopping the pump immediately. The reason why 1.92 bar chose based on experiments where the most suitable pressure assumed to be 75% of pump pressure at the bit where the pressure at the bit averaged to 2.56 bar. That means if the leakage makes 25% pressure drop the pump stops.

2.2.8 Hole deviation

Hole deviation is a common problem that occurs very often. The deviation from the planned well path causes many problems during drilling. Drillers should be aware of such an issue that is very hard to avoid. The tendency to move from the path that planned could make problems like washouts and stick & slip. Moreover, this can cost much money. However, it is agreed on a combination of several reasons that could be accountable for deviation [13].

- Formation rock types
- WOB
- Inclination
- ROP
- RPM
- Hole size

- ❖ Stabilizers
- ❖ Hydraulics

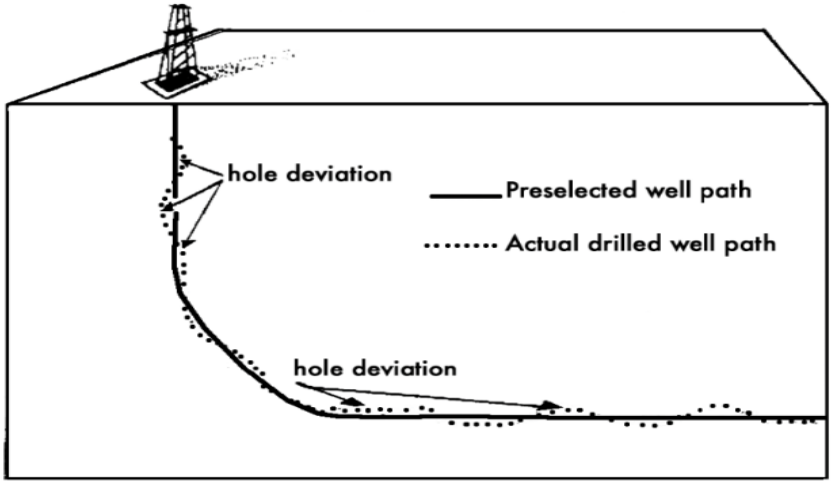

Figure 15: Typical places where hole deviation takes place [13].

There is a side force that acts on the drill bit that makes it deviate; it is kind of a complex force to describe, but it controlled by the BHA, Bit-rock interaction and some other parameters like drilling hydraulics. This force is related to the BHA as the placement of stabilisers and reamers plays a major role in controlling this force that makes the drill bit deviating from its planned path [13].

The compression load applied by increasing the WOB can cause buckling the drill pipe and the BHA, and that makes problems with controlling the side force of the drill bit. To minimise buckling of the drill string, controlling the WOB and stabilisers is required. The compressive strength of formation rocks also has a significant role in controlling the deviation of the drill bit during the bit-rock interaction. In the design of Drillbotics, a riser of a length of 30cm fixed at the bottom of the frame that is attached connected to an XY-beam actuator, figure 66 B. Eight load cells support the riser from the outside, those load cells measures the side forces on the riser due to the movements of the BHA. The XY-beam actuators react to the side forces and push the riser to correct the direction of the BHA. Later on, a full design of the riser is described in Chapter 4.

2.2.9 Hole cleaning

Failures of transferring the cuttings lead to many problems like stuck pipe, hole pack-off, slow ROP and loss of circulation. So many parameters control cleaning of the hole like flow rate, pumping cleaning pills, and rotation of string.

Hole cleaning has been a problem for inclined wells that are above 35^{o}. Because of cutting bed on the lower wall of the borehole. Mudflow rate should be sufficient enough to carry the cuttings to avoid cuttings fall that would cause problems like sticking and high torque. It proved that rotating the drill pipe all the time will help to prevent fall of cuttings and give a significant hole cleaning [13]. Cutting cleaning depends on the viscosity of mud in vertical wells and rotation speed in inclined wells [13]. A sufficient circulation system is necessary to give a good flow velocity to give a properly clean to the hole thereby minimising problems downhole like sticking, friction, and so forth.

In the other hand cuttings characteristics such the shape, size and weight affect the behaviour of the cuttings in the well. Laboratory tests on real samples of drilled wells help a lot to know which flow rate or mud type is used to carry such type of cuttings. The cutting size, also, depends on the bit-rock interaction. In the design of the competition, a water pump is connected to the drill string and pumps water up to 13 l/min at atmospheric pressure to be able to transport cuttings outside the wellbore.

2.3 Challenges related to drilling pipe

Drill pipe is the weakest element during drilling because it is long and thin in compare to the other parts of the drilling system. Many types of loads drill pipe exposed onto as tension, compression, and torque that can easily break the pipe. Optimising drilling parameter is an important concept that is not easy to fully control. Every drill pipe made of specific materials and those materials have different tolerance to various types of loads. If loads exceed the tolerance of the drill pipe, then the pipe would fail at that point. In other words, if the induced loads exceed the pipe material ultimate stress the failure would occur at the weakest point of the pipe. In the case of pipe sticking, the tensile and torque loads will increase and at a given moment the drill pipe will fail.

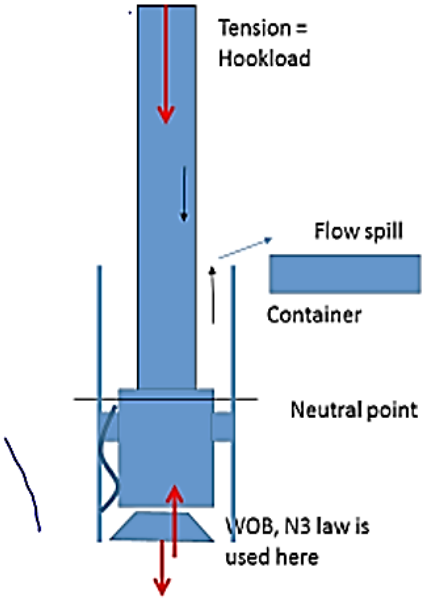

Figure 16: Some of the loads that drill pipe exposed to [5].

As illustrated in figure 16, there are tension loads at the top of the pipe while compression loads find a place at the bottom, and the neutral point in-between where the sum of tension and compression is zero [5]. In the case of sudden pipe sticking the torque increases and it might lead to failures as a result of twist off when the induced shear stress due to torque exceeds the ultimate shearing stress of the material of the pipe.

All materials become weaker after a long time of use, the variation of repeated vibrations and stress result in the weakening of the material of the pipe since it is the most part that is in movement. That phenomenon is called material fatigue; it forms micro-cracks that develop into macro-cracks due to repeated exposure to stress. Every material has a limit of repeated cyclic that will never fail, and that limit is studied to decide the maximum fatigue failure load that the material would not fail whatever how much. The biggest issue that we are concerned about in our design is the twist off. Issues like environment, burst and collapse would not be a problem in our case because drilling is not taking a long time and the pressure does not exceed 4-5 bars.

Chapter 3 Theory and design calculations of Drillbotics

The drill string is the main part of the drilling system because the heaviest load exposed to it where the formation drilled by drill string components. Therefore, it is imperative to make sure that the drill pipe is stable and able to drill through the different formation types, that is why simulations before drilling always help to avoid such problems.

Knowing what type of materials is important because every material has a specific tolerance according to tension, compression and bending before deformation. Different types of stresses are acting on the material such axial, radial and tangential stresses, which could deform the drill pipe [13]. As a result of continues loading on the material, the material structure deforms either elastically or plastically. The deformation caused by different loads Elastic deformation means that the deformation is reversible but plastically implies that the deformation is permanent [10].

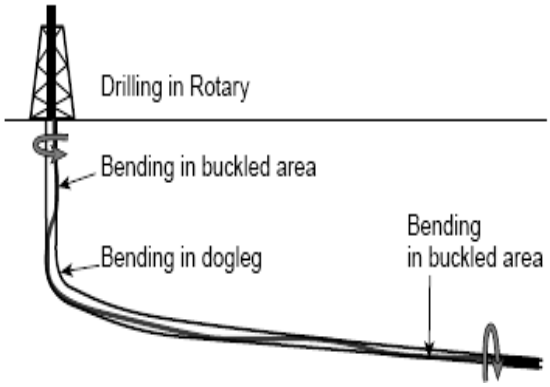

Figure 17: Different failures in different places in the wellbore [13].

3.1 Stress and strain

The analysis of stress and strain is quite important to deal with drill pipe mechanics to avoid failures. Its concepts are used to determine the stress and strain of axially loads and torsional loads of thin-walled cylinders, beams, and columns, to get information about how much the physical body of the material tolerates during drilling operations. Stress is the force per unit area. The stress on a plane is divided into two components, one perpendicular to the plane face, known as normal stress (σ), and the other parallel to plane, called shear stress (τxy**)** [10]**.**

Axially loaded members are the simplest to analyse, given the load and cross-sectional area, the axial stress and strain can be determined.

3.1.1 Axial stress

The two types of normal stress due to axial loading are tensile and compressive stress as illustrated in figure 18 and 19. The sign convention is:

- Tensile Stress: Positive (+)
- Compressive Stress: Negative (-)

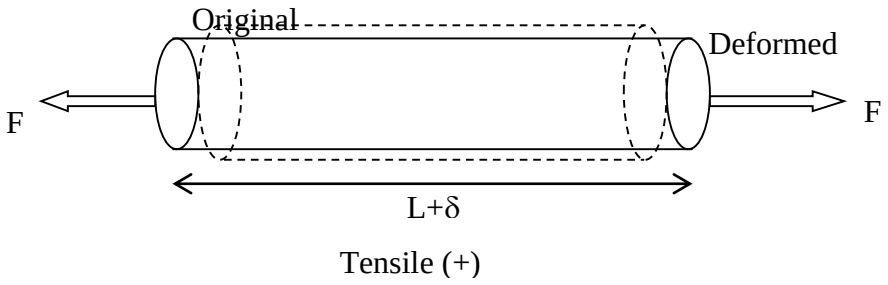

Figure 18: Tensile force on a cylinder (+) [10].

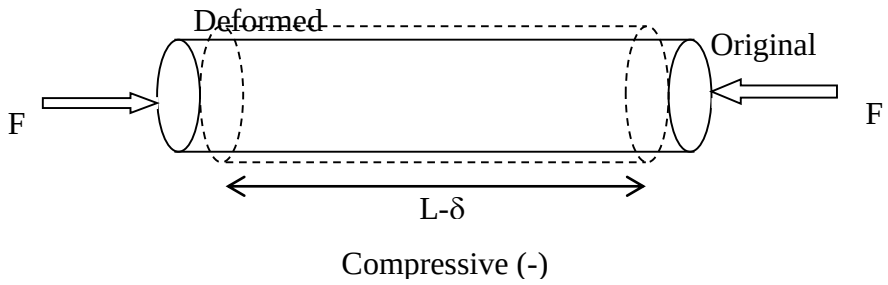

Figure 19: Compressive force on a cylinder (-) [10].

Normal stress, σ, is the ratio of the force to the normal area of the cylinder:

$$\sigma = F/A \qquad (1)$$

Where: F is the force. A is the cross-sectional area of the tube.

Compatibility relation: Normal strain, ε, is the change of length with respect to the original length of the loading cylinder [10]:

$$\varepsilon = \Delta L / L_0 \qquad (2)$$

Where ΔL is the change in length and L_0 is the original cylinder length.

Constitutive relation: Hooke's law

$$\sigma = E * \varepsilon \qquad (3)$$

By combining Eq. 1, 2 and 3, one can derive the load-deformation relation as:

$$\Delta L = \frac{F * L_0}{E * A} \qquad (4)$$

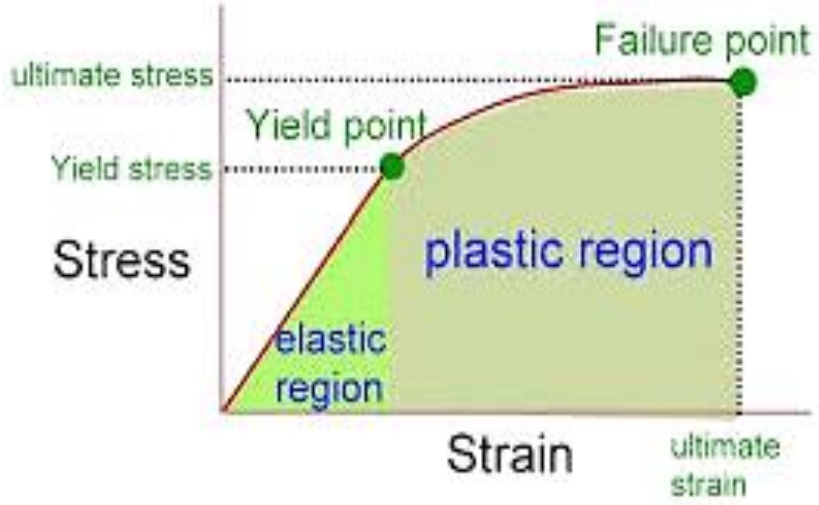

Figure 20: Stress/strain diagram [10].

Engineers use stress-strain diagrams to define the properties of materials that are significant in a safe design of a statically loaded cylinder. The following stress-strain curve shows typical steel that shows a transition between linear elastic to plastic. From the curve above, the yield stress and ultimate stress can be read where there are two regions, an elastic region that is reversible and a plastic region that is irreversible.

Stress-strain curve at figure 20 and 21 illustrated, where the following stress points that cause deformation of material [10]:

- **Point A (**Elastic limit): If the element exposed to a load F and followed by a removal of the load F, the strain in the bar returns to zero as the load F goes to zero. In other words, the material has been strained within an elastic limit (Figure: OA Part). The stress at point A is called proportionality limit σ_{pl} (it is the upper limit of perfectly elastic /elastic limit).

- **Point B** (Permanent Strain**)**: The increment of stress σ that exceeds the elastic limit. The elastic strain disappears upon unloading (LB'). A permanent strain (OL) remains, is called plastic strain at point B.

Yield Strength: The value of stress-strain associated with point B is known as the yield strength σ_y. The unloading curve is assumed to occur along the straight line BL, with a slope equal to that of the straight line OA. OL is called offset strain (usually, 0.2% is taken if the material doesn't show yield point, for some alloy materials).

- **Point C** (Ultimate yield strength): It defined as the maximum stress attained in the stress-strain diagram. As the material loaded beyond its yield stress (BC), the material maintains an increase in strain with an increase in stress. This response is called strain hardening.

From point C to F, the specimen reduces its areas and results a weakening effect. The area reduction has a softening (strength loss) effect. The response is called strain softening.

- **Point F** (Rapture) The specimen fails when the stress reaches the point F (fracture point).

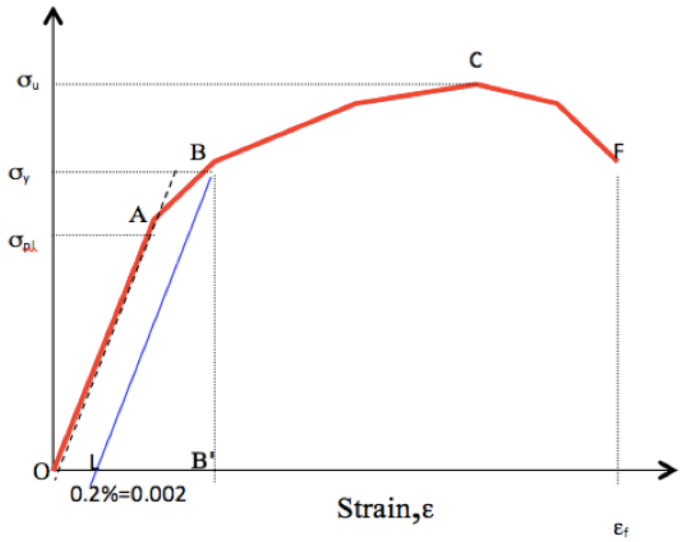

Figure 21: Stress vs. strain curve, determining the yield point [10].

3.1.2 Shear stress

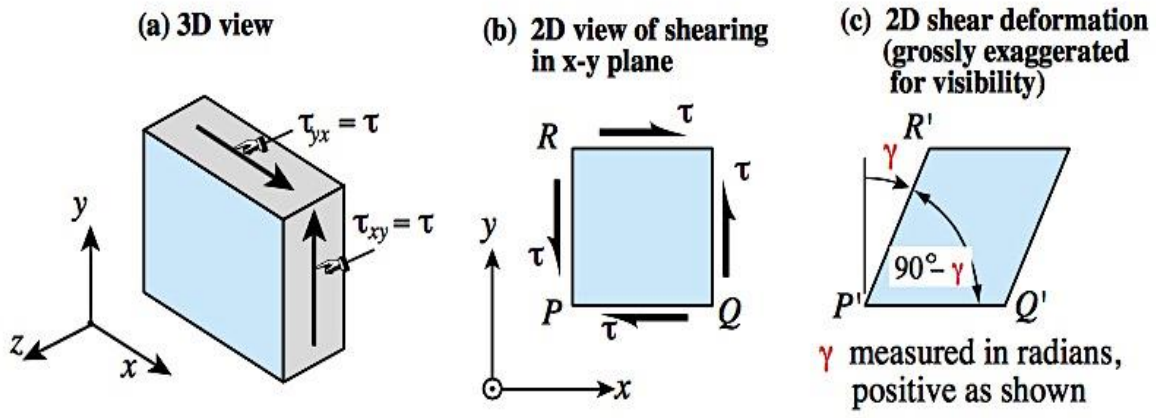

Figure 22: An illustration of shear stress [14].

Shear stress is a stress condition where the load is parallel to the face of the material. It has the same curve as the axial stress, but it is a measure of the angle change of the material due to torque forces.

Figure 22 illustrates the direction of the shear load on the material as the shear occurs due to the applied moment along the face of the element. It also has an elastic deformation or plastic deformation [14].

3.1.3 Typical failure criteria for yielding

The most of the books include Tresca and Von Mises theories when it comes to failure criteria and strength estimations where they are the two most important criteria that used. There are some differences between the two theories as one considers more parameters than the other. The Tresca formula was considered to be the more fundamental of the two, but the Mises from what revealed as an appealing, mathematically convenient approximation to it. Nowadays, both are usually stated side by side with little or no preference [15].

Tresca Criterion

This type of criteria takes into account the maximum and minimum stresses, where Tresca´s yield shear stress is equal to the average between the maximum and minimum shear stresses respectively.

This failure criterion based on that the yielding shear stress equals the maximum shear stress of the material.

$$\boldsymbol{\tau}_{max} = \boldsymbol{\tau}_{y} \tag{5}$$

Where

$$\boldsymbol{\tau}_{max} = \frac{\sigma_{max} - \sigma_{\min}}{2} \tag{6}$$

Where $\sigma_{\max}$ and $\sigma_{\min}$ are the maximum and minimum principle stresses respectively [16].

Von Mises

The Von Mises yield condition is commonly used to describe the yielding of steel under combined states of stress. Unlike others, Von Mises theory takes the intermediate stress into considerations. For instance, for a cylindrical structure, the initial yield limit is based on the combination of the three stresses (axial stress, radial stress, and hoop stress) and the shear stress caused by torque. Yielding stress as a function of the combined three stresses is given by [10]:

$$\sigma_{\text{VME}} = \sqrt{\frac{1}{2}\left\{\left(\sigma_{\theta} - \sigma_{\text{r}}\right)^2 + \left(\sigma_{\text{r}} - \sigma_{\text{a}}\right)^2 + \left(\sigma_{\text{a}} - \sigma_{\theta}\right)^2\right\} + 3\tau^2} \tag{7}$$

Note that if there is no torque, the shear stress term drops out of the equation. The yield limits for tubing calculated by setting the von Mises stress, σ_{vme} to the yield stress, σ_y, for the material.

3.1.3.1 The relationship between tensile stress and shear stress

If the maximum shear stress theory used on only ductile materials, the shear yield stress is the half of the tensile yield stress where $\tau_y = 0.50*\sigma_y$ according to Tresca. And another theory by Von Mises called the distortion energy theory for ductile materials gives the other comparison where $\tau_y = 0.577*\sigma_y$ [10].

So the relationship varies from 0.5 to 0.577 for yielding stress whether Tresca or Von Mises theories are used to determine the shear stress of the material in moderate temperatures. In the design of Drillbotics, 0.55 factor is used to convert the axial yield stress to shear yield stress and 0.65 to convert the ultimate axial stress to shear ultimate stress.

Case study

Determination of the maximum torque of drill pipe

To determine the maximum torque on the drill pipe that used in the competition, the following relationship between the tensile and shear stresses utilised. An aluminium drill pipe with an OD of 9.95mm/0.391in and an ID of 7.747mm/0.305in and a wall thickness of 2.2mm/0.086in used. Finding the maximum torque that the drill pipe could withstand is an important issue because the drill pipe is the weakest element of our drilling system and needs to explore to choose the right rotational speed and the WOB applied.

The ultimate strength of a plain aluminium is approximately σ_{max} =110 MPa [17]. Assuming a factor of 0.65 as the ultimate shear strength $\sigma_{shearmax} = 0.65 * 110 = 71.5MPa$. Then the ultimate torque that is needed to twist the pipe $\tau_{max} = \frac{\sigma_{shearmax}}{r}\frac{\pi}{32}(d_o^4 - d_i^4) = 8.79\ Nm.$

The tensile yield strength is approximated by $\sigma_{yield} = 95MPa$ [17]. Assuming a factor 0f 0.55 to determine the yield shear stress as $\sigma_{yieldshear} = 0.55\sigma_{yield} = 52MPa$ where the yield torque is defined as the following: $\tau_{yield} = \frac{\sigma_{Shearyield}}{r}\frac{\pi}{32}(d_o^4 - d_i^4) = 6.39\ Nm$. Where r is the radius of the drill pipe.

3.2 Friction

Friction is a quite complex to determine; the system needs to run and calibrated to find friction coefficients that are required to calculate the induced friction forces. There is friction in the system since the system contains many components like motor, BHA, Drill bit, and so forth. There are many types of friction in the design as static friction and kinetic friction. Friction types that are expected in the design as:

3.2.1 Coulomb friction (mechanical)

This kind of frictional force is corresponding to the axial normal force between two surfaces that are in contact with each other while the frictional force will be the tangential force between the two surfaces. This type of friction force always satisfies [18]:

$$Fc = \mu * N \tag{8}$$

Where μ is friction coefficient. This type of friction takes place between the bearings and between the drill string and riser and the weight of the drill string.

3.2.2 Lubricated friction

This type of friction occurs when there is liquid between two solids like grease (lubricant liquid). Bearings that lubricated with grease have a high frictional force because of the viscosity of the lubricant liquid. As experienced rotating the rotary swivel at figure 70 in chapter 4, the viscous friction is greater when the movement is slow comparing to faster movement. Lubricant liquid needs to be used to reduce wear between two solids during operations. Lubricated friction satisfies: $Fv = f * N$ Where f represents viscous coefficient. Bearings, motor, rotary swivel and slip ring will have viscous friction in our system [19].

3.2.3 Combined friction

In the case of a mixed environment, mechanical bodies and viscous fluid, the friction coefficient μ decreases because the fluid absorbs a big amount of the load and the area of the friction reduces as well. It is called hydrodynamic lubrication and defined by Stribeck curve as illustrated below. So the fluid is bearing the load and the friction coefficient increases with speed of movement.

Stribeck friction is a combined friction that originates at low sliding velocities. That type of friction happens due to the lubricated friction in a combined solid/hydrodynamic regime. Moreover, the load is represented partially by the solid surfaces, and partially by the viscous pressure. In other words, Stribeck friction is a continuous variation of movement between mechanical and viscous friction [20].

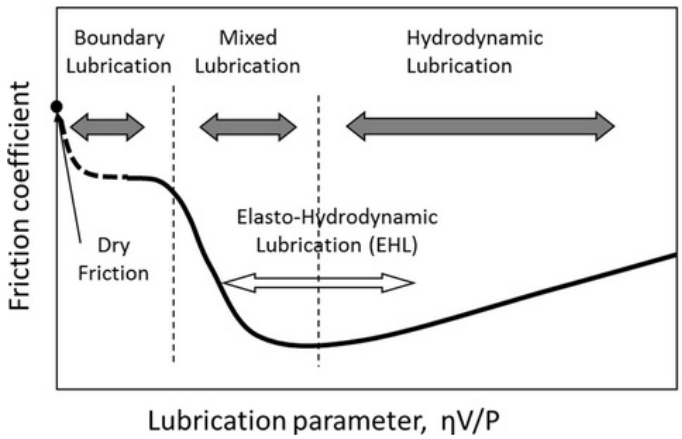

Figure 23: Stribeck friction curve [20].

The total friction that will affect the design will be coulomb friction, viscous friction, and Stribeck friction:

$$Ft = Fc + Fv + Fs \tag{9}$$

Where the total friction torque $\tau(fric) = Ft * r$ where r is the average radius of system components that are related to that friction [18].

3.3 Torsion

Formation rocks formed in different layers of sediments, they vary from soft to hard. When meeting hard formation rock the chance of twisting is greater. The weakest element in our system is the drill pipe, where drilling speed ROP and the angular speed has a huge role to get the drill pipe twisted. In addition to some incidents like sticking, which cause the drill bit to stop rotating while the top drive still rotating what leads to increase the twist angle of the drill string. If the difference between the external and internal pressure enhances the chance of collapsing or bursting the drill pipe increases.

3.3.1 Theory of torsion

If a cylindrical bar with one end twisted as shown in figure 24 below, the twisting moment is resisted by the shear stress τ of the cylinder. The shear stress is zero at the center of the bar, and it increases linearly with its radius and reaches its maximum value at the surface of the bar. Assumed that a point on a given cross-section remains on the outer wall of the cylinder after twisting the cylinder, and the torque applied at one end is axially, and the twist angle is small. The material is linearly elastic and obeys Hook´s law [21].

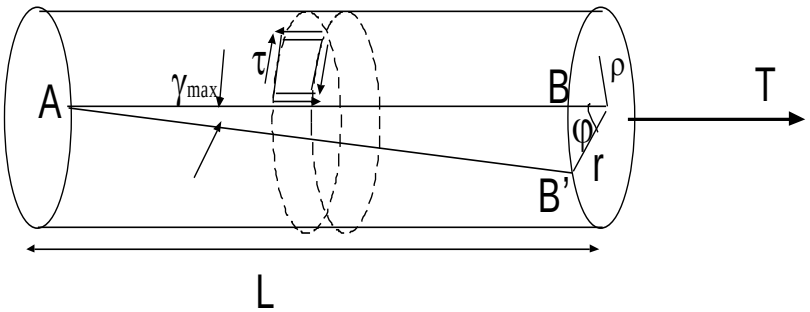

Figure 24: Twist angle γ in a cylinder [21].

3.3.1.1 Mechanics of Materials

Using Equilibrium condition, compatibility relation, and Hooke's law, one can derive the shear stress (maximum) at the outer side of the pipe [21]:

$$\sigma_{shear} = \frac{\tau * r}{J_z} \quad (10)$$

From the geometry and for small angle deflection one obtains shear strain (□) at a point on the surface:

$$\gamma = \frac{r\varphi}{L} = \frac{\tau}{G} \quad (11)$$

Rotation (twist angle) obtained from Eq.1 and 2 as:

$$\tau_{twist} = \frac{J_z}{l} G\theta \quad (12)$$

Where:

- τ = torque (Nm).
- G = Shear modulus (N/m^2).
- J_z= Moment of area, (m^4).
- θ = Twist angle (rad).

3.3.2 Over-torque

When drilling takes place, the driller needs to know where and how deep it expected to drill, where one of the main reasons is that the torque becomes greater, the deeper drilling goes. The drilling path has to be determined and planned to manage to drill without problems like over-torque of drill pipe. Drill pipes made of different materials, to determine which drill pipe used depends on the type of the well.

For example, the torsion that applied should not exceed 70% of the maximum torsion capacity of the pipe as most theories are mentioning. However, the problem here is where we do not

know really how the environment of the well is. Big amount of cuttings that collapses in the wellbore cause over-torque which is a typical drilling scenario of over-torque. In addition to friction factor, that plays a prominent role in over-torque.

3.3.3 Case study

Determination of expected twist angle in case of sudden stop

As mentioned earlier in chapter 3.1.4 the shear yield torque and the ultimate shear torque for the drill pipe that used for the job is 6.39 Nm and 8.79 Nm. According to previous calculations the following Eq. 12 for elastic torque is used to determine the expected twist angle for our aluminium drill pipe, where: OD 9.950mm and ID 7.747mm:

$$\tau_{twist} = \frac{J_z}{l} G\theta$$

That means that the top drive should not provide more than 6.39 Nm of torque to avoid yielding the pipe. If the torque that exposed on the drill pipe exceeds 8.79 Nm, then the drill pipe fails by twisting. According to the considered shear modulus of aluminium G= 24GPa and the second moment of area is $J_z = \frac{\pi}{64}(d_o^4 - d_i^4)$. Where the twist torque that is generated on the drill pipe is defined by $\tau_{twist} = \frac{J_z}{l} G\theta$.

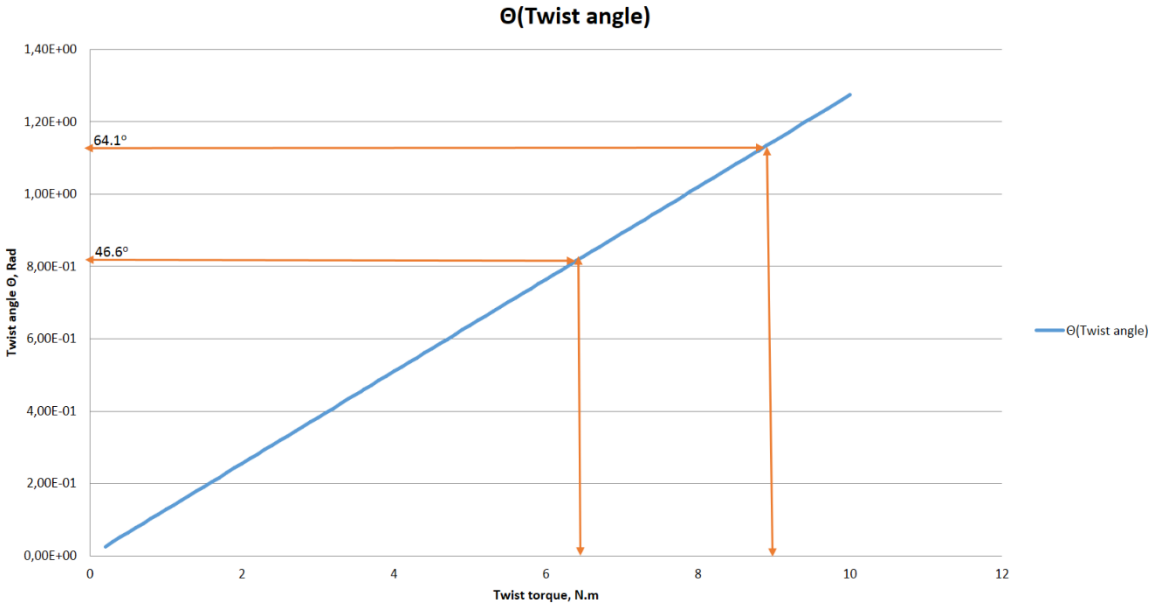

Figure 25: Twist angle at the yield and ultimate shear torque.

As illustrated on in figure 25, the maximum allowable twist angle to reach ultimate shear stress is 1.12 rad (64.1 ^{o}) and for yielding is 0.812 rad (46.6^{o}). That means that the drill pipe should not be twisted more than 0.812 rad to avoid shear yielding.

3.4 Optimisation of drilling parameters

The rotational speed RPM and WOB that applied are necessary parameters to control the ROP. Where higher ROP obtained by increasing the RPM and WOB as illustrated in figure 26, but higher ROP is not always positive where it could cause a big amount of cuttings and pack off problems. Experiments and simulations needed to be able to optimise drilling parameter procedure. The operational parameters are necessary to manage to drill safely without any failures because one single failure in drilling might cause a significant danger for the crew and environment.

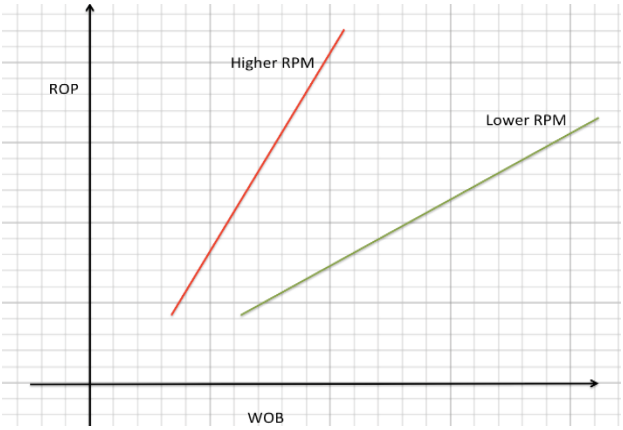

Figure 26: Higher rpm gives higher ROP.

To look at the previous failures, those happened before and knowing the effect of each drilling parameter is beneficial to get a better understanding. This case reported where a drill string failure occurred on average one of seven drilling operations, and that costs more than $100,000 each, as drilling parameters were not sufficient enough where that caused unnecessary non-productive time and the cost of the equipment [22]. Increasing understanding of drilling performance shall minimise costs for any drilling operation.

3.4.1 Relation between bit torque and WOB

Knowing the type of drill bit that used in our job, and the expected formation gives us a better overview about controlling the WOB and the RPM. When drillers apply more WOB, the interaction of drill bit teeth will be pushed deeper into formation rock. However, the type of formation rocks plays a major role in deciding the rate of penetration ROP.

It is important to predict the kind of the formation to choose the type of equipment materials that are most suitable for the job. The strength and variation of rock types is an important issue that considers where it needs more WOB to drill through the hard formation, while it does not need that much WOB to drilling through the soft formation, see figure 27. The design of the bit is one of the major factors that affects drilling rate in different types of formation. The ROP changes substantially with changes of bit type, the number of nozzles, cutters and the size and angle of the cutters shall affect the ROP. So it is quite important to understand which effect different types of drill bit have in addition to drilling parameters due to the huge effect on the rate of penetration during the drilling operation.

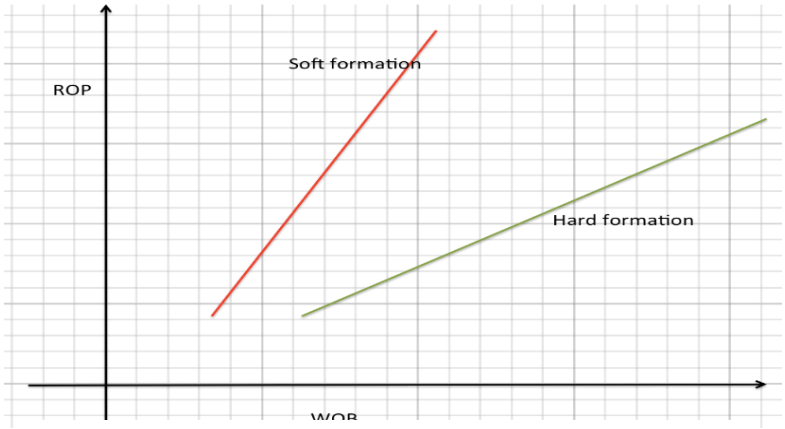

Figure 27: Higher ROP in soft formation than in hard formation.

An increase of the ROP is not always positive; it could lead to a huge amount of cuttings that would be hard to handle so higher ROP should require high pump rate to carry the cuttings not to get stuck.

CCS and UCS:

Unconfined compressive strength (UCS) defined as the maximum axial strength to crush the material rock under the unconfined condition like atmospheric pressure and temperature. Confined compressive strength (CCS) is the maximum axial strength to crush material rock under confined conditions.

One of the keys to optimising drill bit performance is to know the strength of the formation rocks that drilled. In our design case, the UCS of the rock formation used to maximise the drill bit performance at the atmospheric conditions since we are not drilling that deep. In other words, the bit performance is based on UCS of the rock formation to determine the mechanical specific energy (MSE).

In our case, the pressure in the borehole is almost equal the atmospheric pressure so we assume that CCS=UCS, Where the friction coefficient is $\mu = 0.9402e^{-1.16e-9\,CCS}$ [23].

Friction coefficient μ and formation strength CCS

(Passier & Fear, 1992) presented a model that includes the torque on bit T and the WOB in a formula that takes the friction coefficient into considerations and this coefficient will be reliable on the specific energy values, this formula converted to SI-units [23].

$$T = \frac{\mu * WOB * Da}{3} \tag{13}$$

Where:

WOB= kg

T= Bit-torque (Nm)

μ= Bit coefficient (no dimensions)

The model relates the bit torque to the WOB utilising a coefficient of friction μ for our design, where it´s expressed with respect to formation strength is approximated by converting to CCS into pascal:

$$\mu = 0.9402e^{-1.16e-9\,CCS} \tag{14}$$

The environment that we are drilling with is approximately equal to atmosphere conditions where CCS is assumed to be equal to UCS in our case. According to the simulations of Passier and Fear, the friction coefficient is none-proportional to the strength of the formation where a value of UCS= 10MPa gives μ = 0.93 and UCS=40MPa gives μ=0.90 as illustrated on the curve on figure 28.

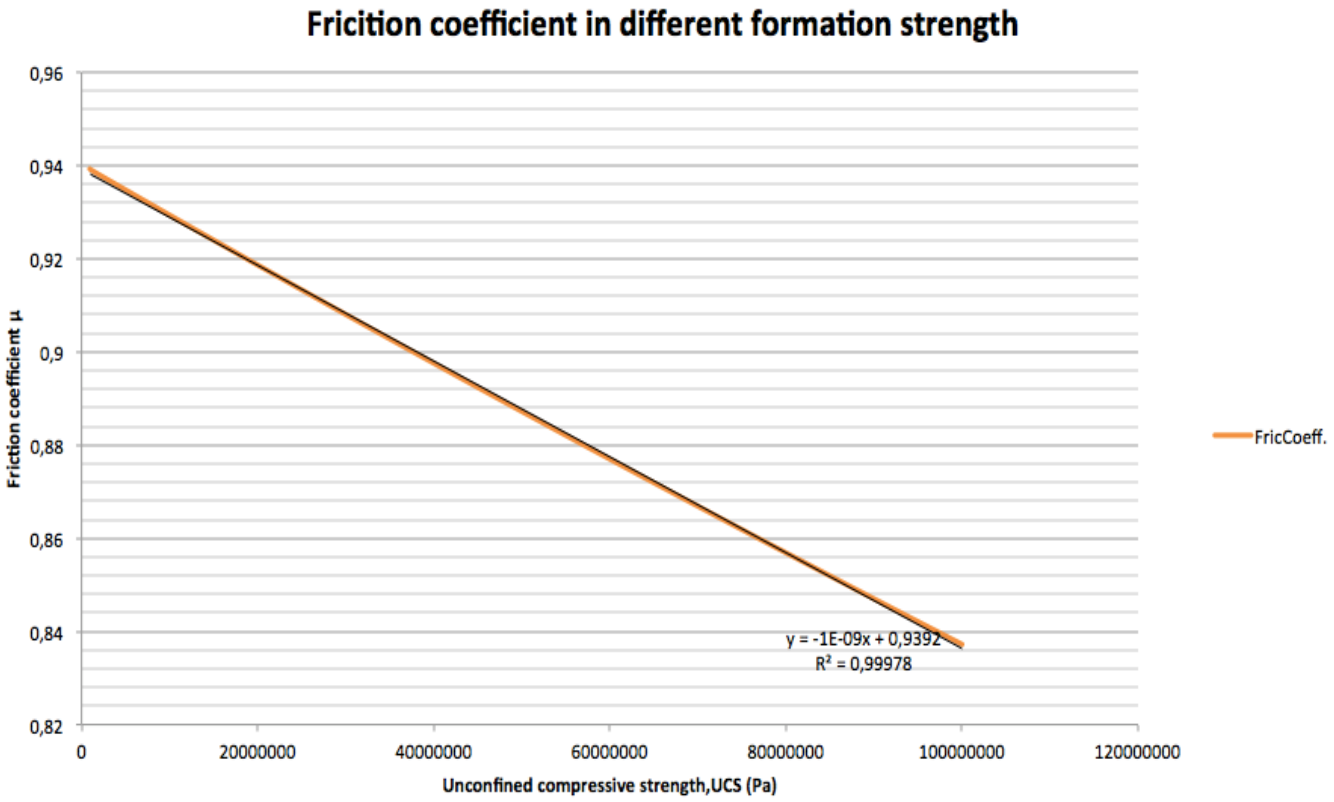

Figure 28: Friction coefficient decreases when meeting stronger formation.

3.4.2 Determination of the reaction time in case of sticking

During drilling through the cubic rock, 30x30x30cm where it includes many different layers, that could cause sticking problems. However, in the case of sticking the drill string will stop rotating where the system is connecting to a real-time controller that reacts in the event of problems like sticking and stops the rotating. If the drill bit stops rotating the twist angle between the bit and the rest of the drill string will increase what can cause twisting the drill string. The drill pipe is the weakest element and expected that it will be twisted initially if the motor still rotating while the bit is stuck.

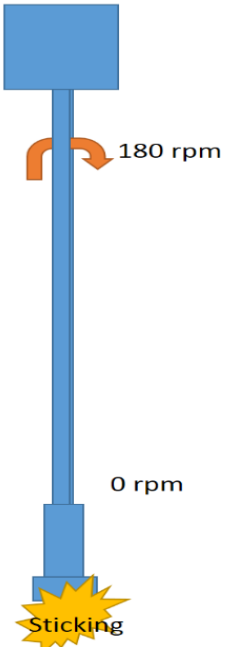

Figure 29: Twisting incident.

3.4.2.1 Calculations of Twist torque and maximum WOB in different time loops Δt

These calculations are calculated initially before testing and calibrations, where the moment of inertia right after stopping the motor and friction not taken into considerations. The motor is coupled to a PLC control loop to be able to monitor the speed of the motor and to stop the motor when needed.

Using the following formula from eq.12 for torque elasticity of the drill pipe $\tau_e = \frac{J_z}{l} G\dot{\omega}\Delta t$, where Δt is the time that real-time controller loop uses to react (stop) to bit sticking and $\dot{\omega}$ is the rotational speed RPM. The formula used to determine the maximum allowable torque that is applied in order to avoid twisting the drill pipe.

As illustrated in figure 30, twist torque increases with the loop duration. As mentioned short loop stop time shows lower twist torque values, and that would be safer to use short reaction time in loop control.

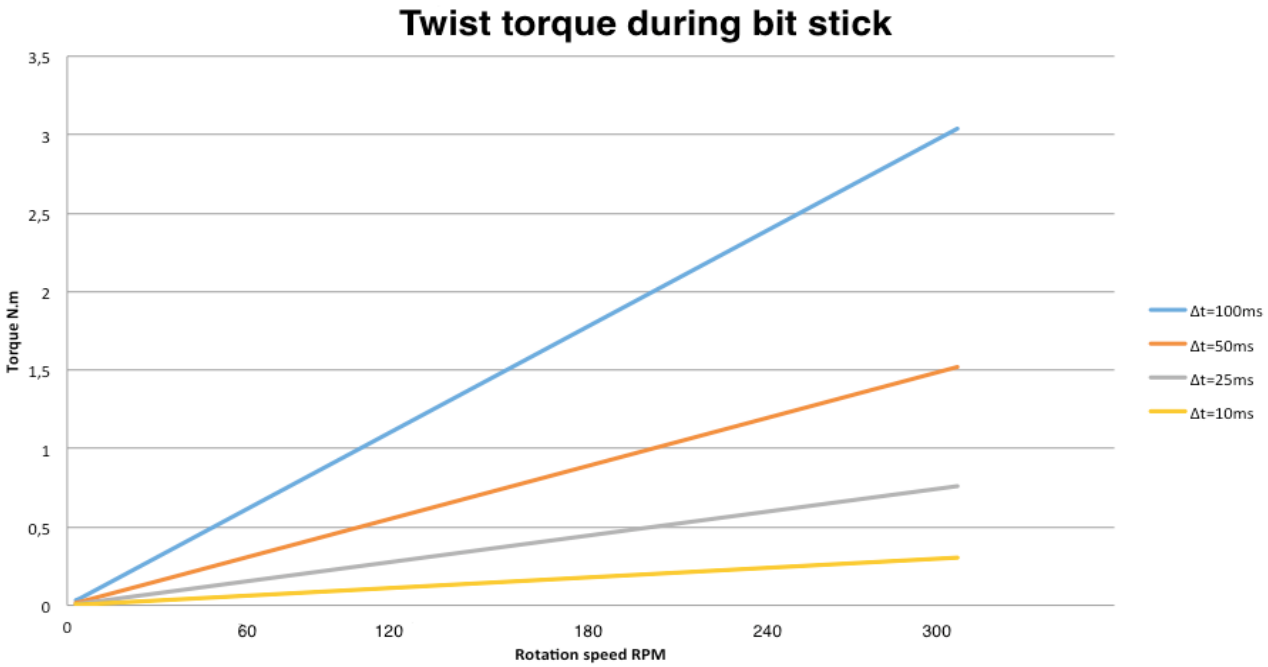

Figure 30: Elastic twist torque after sudden bit sticking at different reaction time steps 100ms, 50ms, 25ms and 10ms.

The maximum bit torque needs to be determined to get a better overview over the torque exposed during drilling. The maximum bit torque defined by subtracting the yield torque of

the pipe from twist torque values during bit stick that presented in figure 30. Below, figure 31 represents the yield torque minus the values in figure 30.

The maximum bit torque with different reaction time steps, where the maximum allowable torque before the pipe yields illustrated in figure 31. The maximum allowed bit torque is none-proportional to the rotational speed, so if the rotational speed higher, less torque required to twist the pipe. If the bit stops while it was rotating at 180 rpm with a reaction time of 10ms, the maximum allowable torque is 6.17Nm, and 5.90 Nm when the response time increases to 25ms. Where that estimation does not take the moment of inertia and friction into considerations.

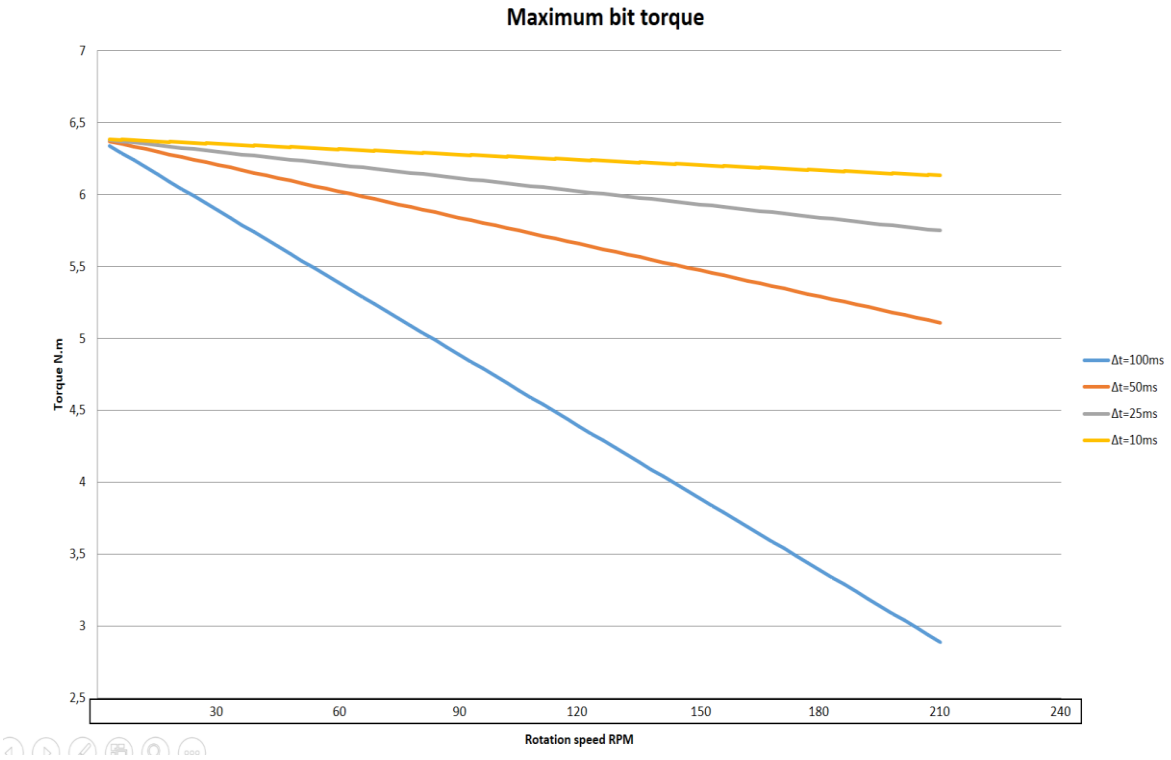

Figure 31: Maximum torque before yielding the pipe.

Passier and Fear 1992, has presented the following formula where $\tau = \frac{\mu * WOB * d_{bit}}{3}$ in order to convert from torque to WOB during drilling different types of formation rocks as illustrated in figure 32. μ is the friction coefficient $\mu = 0.9402e^{-1.16E-9 * CCS}$, where CCS assumed to be equal to UCS because of atmospheric conditions. According to the calculations on figure 32, the maximum WOB decreases with increasing the rotational speed. There is not

much difference of the maximum WOB in term of variation of formation strength from 10 to 40 MPa as illustrated, where the biggest difference is when different stop time loops Δt varies. For example, the values that obtained varies from 42 kg when rotating in 60 rpm to 40 kg when rotating in 180 rpm, based on stop time of 10 ms (yellow curve). The values of the WOB in this section does not take the friction and time of moment of inertia into considerations. Therefore, the values that obtained is only initial values to have an approximation about how it seems to be at the beginning of the work.

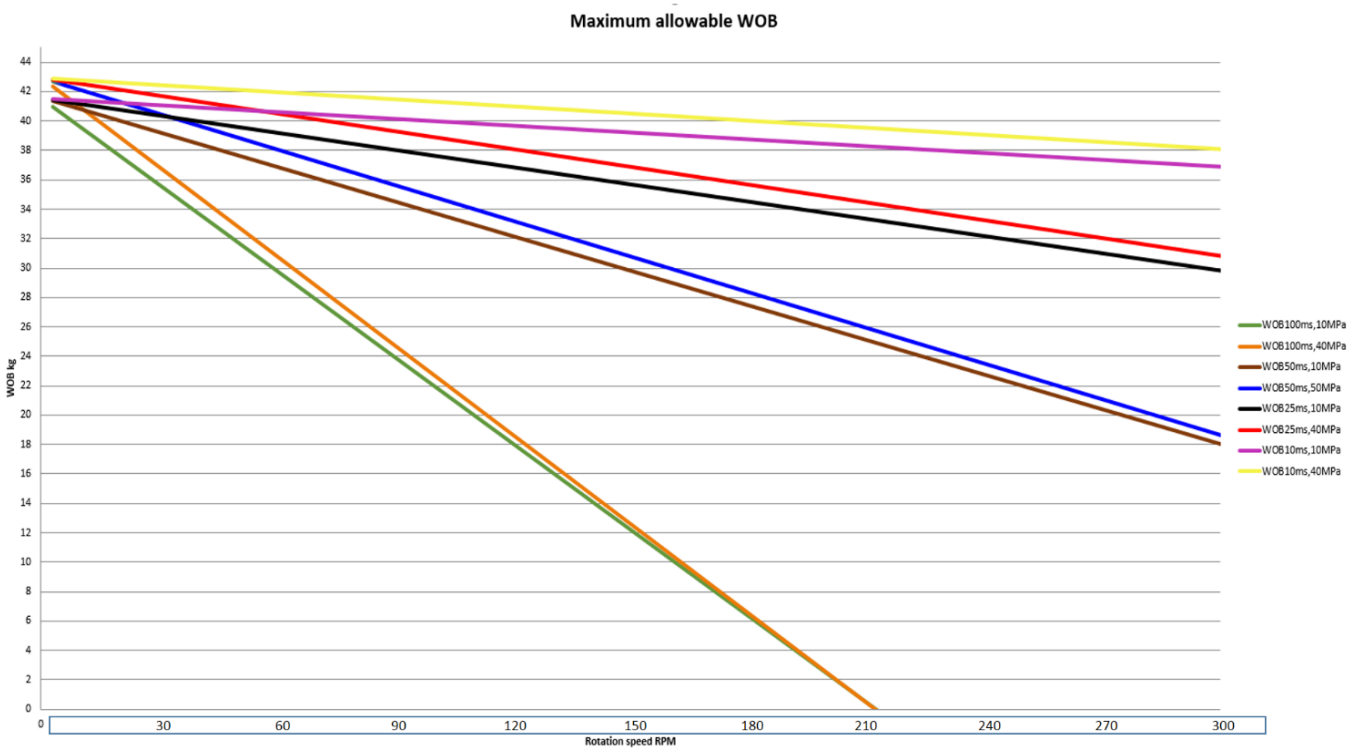

Figure 32: The maximum allowable weight on bit to avoid twisting drill pipe in two different formation types.

3.4.3 Final determinations of WOB and rotational speed

By using Newton´s second law, the following model determines twist angle and torque that applied in different cases presented in this section along the drill string. This model is taking the moment of inertia and friction into considerations by dividing the drill string into many components by discretising the whole drill string and determining torque and twist angle in different places and various time steps to make it easier to get the most accuracy out of it.

3.4.3.1 Modelling of power transmission

This model implemented into a software program that focuses on torsion of different parts of the drill string using Newton´s second law that calculates and converts different values of torque and twist angle in different time steps. Mechanical and viscous friction calculations included in the following model to give a better picture of what expected.

Using Newton's second law for moments that describes the relation between torque τ, moment of inertia I and the angular acceleration α:

$$\tau_{total} = \tau_{sys} - \tau_{fric} = I * \alpha \tag{15}$$

A general partial differential equation of Newton´s second law of moments as following [24]:

$$\frac{\partial}{\partial x}\left(GJ(x)\frac{\partial\theta(x,t)}{\partial x}\right) + f(x,t) = I(x)\frac{\partial^2\theta(x,t)}{\partial t^2} \tag{16}$$

Where:

$I(x) = \rho(x)J(x)$, ρ is the mass density,

J: The second moment of area which is presented by the following formula $J_i = \frac{\pi}{32}\left(d_{o_i}^4 - d_{i\ i}^4\right)$.

$f(x,t)$ Represents the external torques as static friction μ_{s_i}, kinetic friction μ_{k_i}, Stribeck coefficient c_{v_i} and viscous friction coefficient η_i such that the friction torque is $\tau_{f_i} = -\left(\mu_{k_i}F_{n_i}\frac{d_{o_i}}{2}sign(\dot{\theta}_i) + \left(\mu_{s_i}F_{n_i}\frac{d_{o_i}}{2} - \mu_{k_i}F_{n_i}\frac{d_{o_i}}{2}\right)e^{c_{v_i}|\dot{\theta}_i|}\right)sign(\dot{\theta}_i) - \eta_i\dot{\theta}_i$

This model consists of some material properties as (mass density ρ_i, shear modulus G, yield shear point σ_{syp_i}, ultimate shear strength σ_{su} and angular position θ_i).

The rotary system

The rotary system contains many components as mentioned earlier, which are:

- Motor rotor and bearings
- Upper shaft
- Rotary Union (Rotary swivel)

- Lower shaft
- Rotary ring
- Drill pipe
- Stabilizer
- Collar
- Bit

There are friction contacts at the bit, stabiliser, rotary union and the bearings supporting the motor rotor.

As illustrated in figure 33, the drill string is divided into components as shown and the system acts as a torsional pendulum. For more simplification, each element will be assumed to have an equivalent disc that has the same mass and the same moment of area as components are coupled to each other by a wire with zero moments of area having a torsional spring constant $k_i = \frac{G_i J_i}{l_i}$ [24].

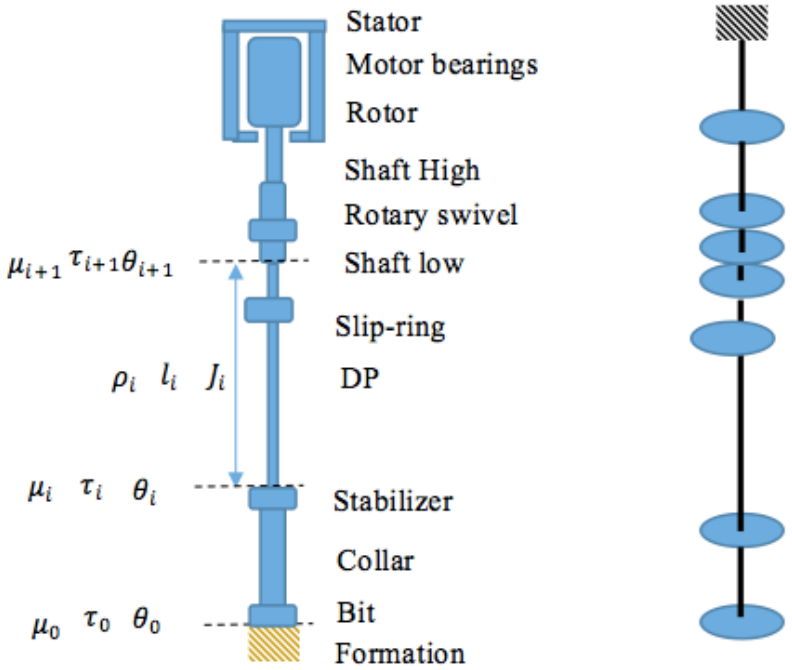

Figure 33: Discretising the drill string and assuming the components as disks [24].

Equilibrium of one element

The balance between an element i and another $i + 1$ is described by the discretised formula for Newton´s second law:

$$-\eta_i \frac{\partial \theta_i}{\partial t} + \tau_{f_i} - \frac{G_{i-1}J_{i-1}}{l_{i-1}}(\theta_i - \theta_{i-1}) + \frac{G_i J_i}{l_i}(\theta_{i+1} - \theta_i) = I_i l_i \frac{\partial^2 \theta_i}{\partial t^2} \quad (17)$$

Where

- i is the placement of the element along the drill string as $0, i, i+1$ ...
- $\frac{-G_{i-1}J_{i-1}}{l_{i-1}}(\theta_i - \theta_{i-1})$ And $\frac{G_i J_i}{l_i}(\theta_{i+1} - \theta_i)$ are the elastic torque between element i and the previous element $i-1$ that releases a negative effect.
- $-\eta_i \frac{\partial \theta_i}{\partial t}$ Describing the viscous friction.

Crank & Nicolson used the average of the sum of the moments between current time step and previous step of the same element, and that gives more stable solution like the following [24]:

$$I_i l_i \frac{\theta_{i,j+1} - 2\theta_{i,j} + \theta_{i,j-1}}{(\Delta t)^2} = \frac{1}{2}\left(-\eta_i \frac{\theta_{i,j} - \theta_{i,j-1}}{\Delta t} + \tau_{i,j} + \frac{G_i J_i}{l_i}\left(\theta_{i+1,j} - \theta_{i,j}\right) - \frac{G_{i-1}J_{i-1}}{l_{i-1}}\left(\theta_{i,j} - \theta_{i-1,j}\right) - \right.$$

$$\left. \eta_i \frac{\theta_{i,j+1} - \theta_{i,j}}{\Delta t} + \tau_{i,j+1} + \frac{G_i J_i}{l_i}\left(\theta_{i+1,j+1} - \theta_{i,j+1}\right) - \frac{G_{i-1}J_{i-1}}{l_{i-1}}\left(\theta_{i,j+1} - \theta_{i-1,j+1}\right)\right) \quad (18)$$

The following model implemented on a software simulator by Eric Cayeux (IRIS) to give an overview of the different parameters that is calculated and converted to twist angle along the string, angular velocity, and string torque when it comes to the influence that the torsional dynamic behaviour has on the drill string.

Table 2: Parameters of the simulator

Inputs	Outputs
Rotational speed	Gradient of the twist angle
Acceleration time	Angular velocity
Stop time	Torque along drill string

Case study

Determination of twist angle and necessary reaction stop time

The twist torque must not exceed the ultimate torque of the drill pipe. Otherwise, the drill pipe would fail due to twisting. In the case of sudden stop like sticking, the reaction time to stop rotation should be sufficient enough to avoid over-torqueing the pipe. The twist angle estimated using the software simulator of the previous transmission model.

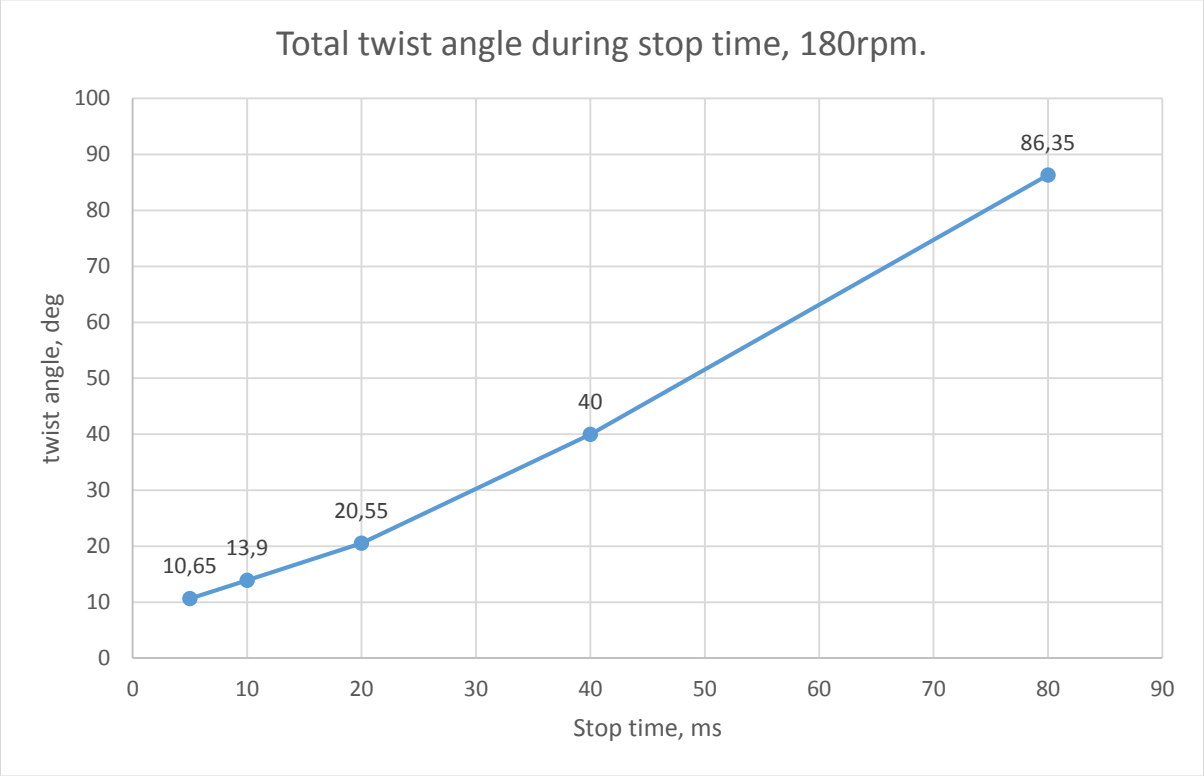

Figure 34: Twist angle (deg) vs. reaction stop time (ms).

After simulating using a rotational speed of 180 rpm, and varying the stop response time from 5ms to 80ms right after a sudden stop. As mentioned earlier, the drill pipe starts to yield after twisting it 46.6º, and it breaks after 64.1º of twisting. As illustrated in figure 34, a stop time of 40ms gives twist angle of 40º, and it seems to be safe. So in the case of sticking incidents a reaction time of 40ms is the maximum we can have to avoid twisting the drill pipe according to this model.

The maximum allowable twist angle is 46.6º before the pipe yields by twisting. The next step is to simulate the torque while varying the WOB to see how the combined effect of rotational

speed and WOB would affect the material of the drill pipe even more. Figure 35, illustrates the twisting torque using a rotational speed of 180 rpm constant input while varying the WOB. However, as shown the WOB is proportional to the twisting torque of the pipe. So a WOB of 24 kg yields the drill pipe where the torque of the pipe exceeds 6.39 Nm, which is the yield limit. Therefore, using WOB limit up to $24 * 0.85 = 20.4\ kg$ would be safer to avoid such twisting incidents in the case of bit sticking.

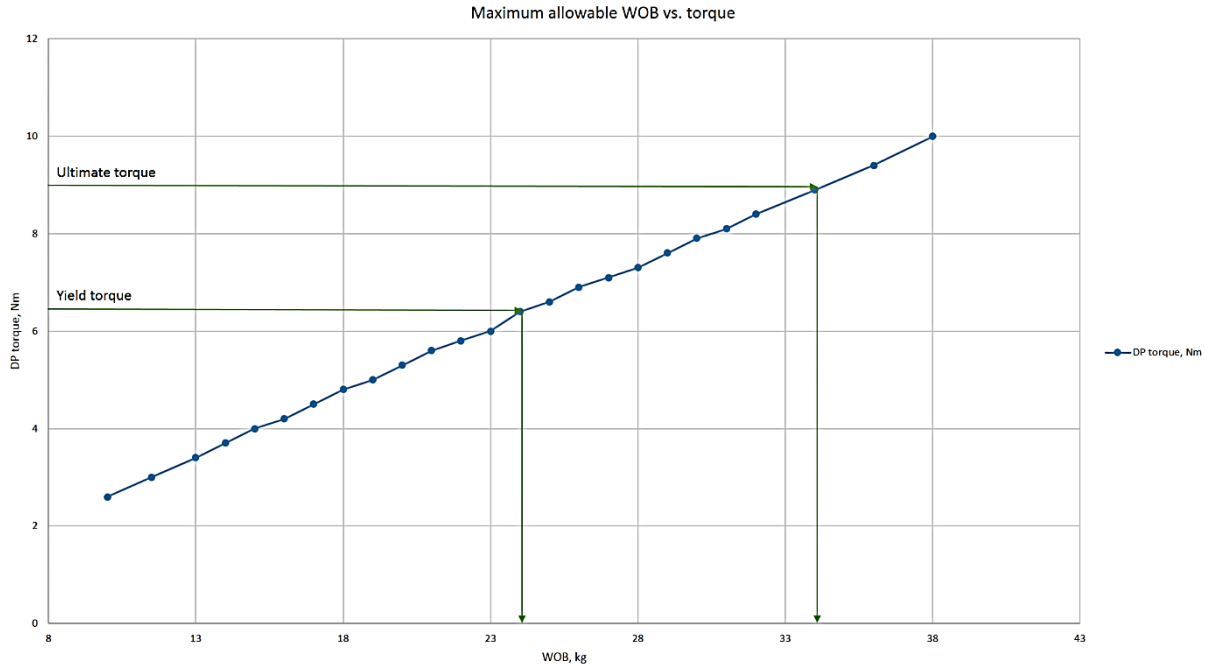

Figure 35: twist angle (deg) vs. weight on bit (kg).

As illustrated in the curve, figure 35, the maximum allowable WOB that fractures the drill pipe by twisting is 34 kg, when the rotational speed 180 rpm and sudden stop occurs. The rate of rotation that induces from the motor, the WOB and the reaction time are the major factors, which control the twisting torque exposed on a drill string in the case of sticking in such way that drilling is sufficient and safe.

Table 3: Results from simulations, for safe and sufficient parameters

Rotational speed	180 rpm
Weight on bit	20.4 kg
Reaction stops time	10 ms

The chosen values illustrated in Table 3. Being able to have efficient drilling is the goal of every driller, see figure 36. Staying below the founder point gives more drilling efficiency. This point is a found point to the highest allowable efficiency of drilling before drilling becomes inefficient. Note that high WOB and RPM gives much cuttings and makes sticking and twisting problems.

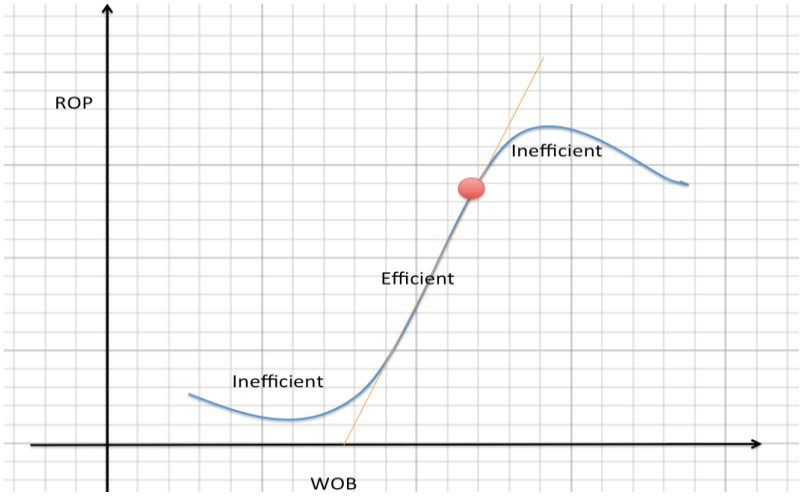

Figure 36: Depth of cut revolution vs. WOB.

3.5 Vibration, Modelling of accelerometers

An accelerometer is a small chip that placed in the BHA to measure the different vibrations and movements during rotation. The following model in a view giving an estimation about what type of movement to expect during rotating; there is placed a chip in the BHA parallel to the drill pipe.

The following model is used to determine the level and type of vibration that might meet the BHA. This model based on the rotational movement of the BHA. The base of the model is the various acceleration types that exposed on the BHA [25]:

- Centrifugal acceleration: $-\vec{\omega} \times (\vec{\omega} \times \vec{r})$
- Coriolis acceleration: $-2\vec{\omega} \times \vec{r}$
- Euler acceleration: $-\vec{\omega} \times \vec{r}$. Then the gravitation will be seen on the axis of the accelerometer.

Table 4: Parameters of vibration input and output. Appendix B

Input	**Output**
Motor step angle	Acceleration in X direction, m/s^2
Sensor distance to tube	Acceleration in Y direction, m/s^2
Hole diameter	Acceleration in Z direction, m/s^2
Hole inclination	
Lateral vibration speed (Whirl)	
Rotational speed of BHA	
Acceleration time	

The acceleration readings are the sum of the gravitation, axial acceleration, acceleration induced by the pipe rotation centreline and the one of the pipe centreline due to lateral movement. The acceleration in x, y and z- directions as following [25]:

$$\begin{cases} Acc.in\ x-direction: g\sin\beta\sin\varphi - r^{"}\dot{\theta}^{"2} + \left(\ddot{r}' - r'\dot{\theta}'^{2}\right)\cos\theta" + \left(r'\ddot{\theta}' + 2\dot{r}'\dot{\theta}'\right)\sin\theta" \\ Acc.in\ y-direction: g\sin\beta\cos\varphi + r^{"}\ddot{\theta}' - \left(\ddot{r}' - r'\dot{\theta}'^{2}\right)\sin\theta" + \left(r'\ddot{\theta}' + 2\dot{r}'\dot{\theta}'\right)\cos\theta" \\ Acc.in\ z-direction: g\cos\beta + \gamma_a \end{cases} \quad (19)$$

When there are no lateral and axial vibrations and for a steady rotation, the accelerometers will read [25]:

$$\begin{cases} g\sin\beta\sin\varphi - r^{"}\dot{\theta}^{"2} \\ g\sin\beta\cos\varphi \\ g\cos\beta \end{cases} \quad (20)$$

3.5.1 Case study

Determination of the maximum acceleration

By implementing the previous model into a simulator, Appendix B. Based on the type of whirl that expected where it is assumed that the whirl that we get is forward whirl. Values that are above 40 m/s^2 considered as a dangerously high where it equal to 3,9 G. The acceleration from the accelerometer based on the previous model [25], determined in different rotational speed 60, 80, 100, 120,140, 160 and 180rpm.

As illustrated in figure 39, the simulations show that the acceleration of the drill string is proportional to the rotational speed of the drill string, whirling in 120 rpm assumed in this case. The maximum acceleration is 17 m/s^2 in Y-direction as illustrated in figure 37, according to these values, the maximum acceleration is below 3.9 G, which is considered to be dangerous in our case design. So rotating at 180rpm would be safe in term of vibrations.

The values that extracted from the simulation can be accurate, but not precise. The values give an estimation about what expected in term of vibrations in different directions which seem to be quite high.

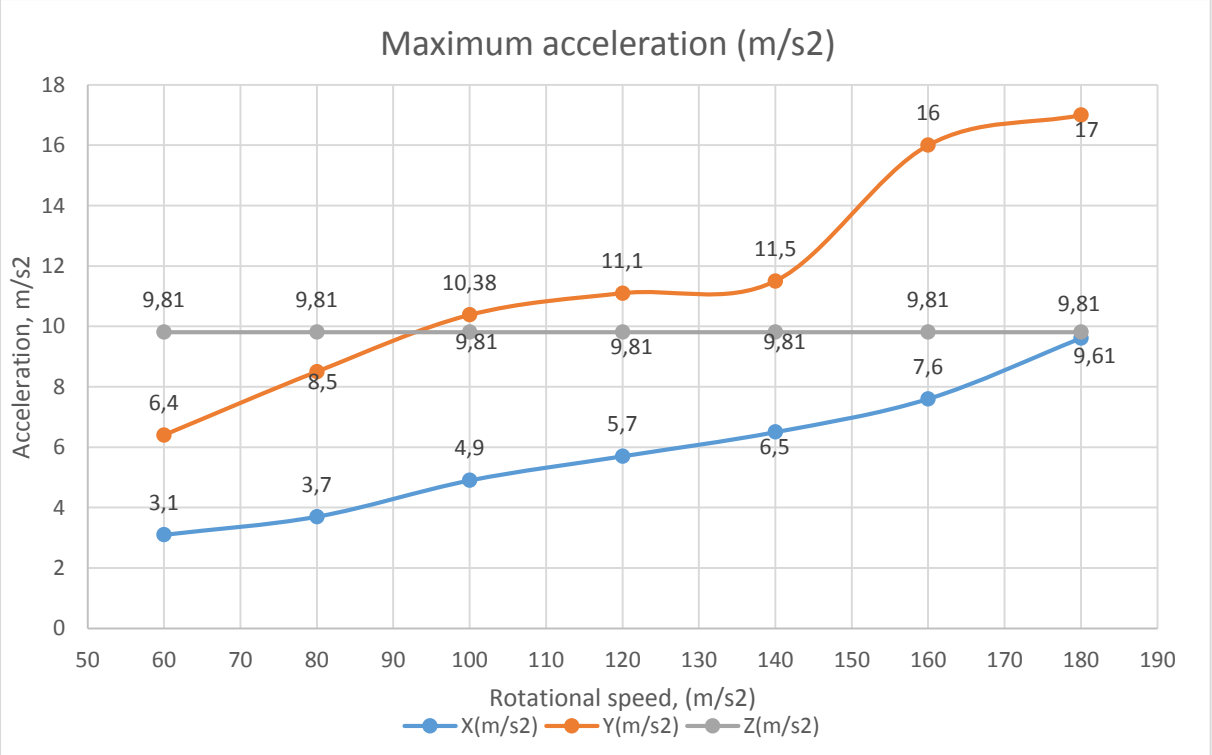

Figure 37: Acceleration in X, Y, and Z-directions.

3.6 Buckling

Buckling of drill pipe is an important issue that needs covering, and it expressed by a sudden sideways forces acting in the middle of an element due to a critical value of compressive loads. There are no 100% accurate models for buckling yet; there is a comparison between three buckling models: Euler, Pasley, and Rayleigh-Ritz.

Buckling occurs when the pipe is pinned on both ends then exposed to axial forces. If axial forces increase above the material limit of the drill pipe, then the pipe will buckle as a reaction to relief the axial forces that loaded on it. Controlling the WOB is an important issue to avoid buckling the drill pipe, in other words, maintain the neutral point at the BHA to secure drilling without buckling.

3.6.1 Neutral point for buckling

The neutral point (NP) is the point where there is a transition from tension to compression along the drill pipe in our case. In other words, it is the point where the sum of tension and compression is equal to zero. The neutral point is at the bottom of the bit while the drill bit hanging before it hits the ground, but when the bit hits the ground, then the neutral point moves upwards to a point where the sum of tension and compression are equal to zero as illustrated in figure 40.

Weight on bit and neutral point

Applied weight on bit causes the neutral point to move upwards to the drill pipe, and that needs to avoid. If the weight of the BHA is sufficient enough then the driller can apply more WOB. If the neutral point moves up to the drill pipe, then it causes drilling in compression which leads to bending the drill pipe after exceeding the buckling limits, see figure 38. A safety factor of 1.15 of the neutral point is chosen to ensure that the neutral point does not move up to the drill pipe as the following [26]:

$$\frac{W_{BHA}}{W\ applied} = 1.15 \qquad (21)$$

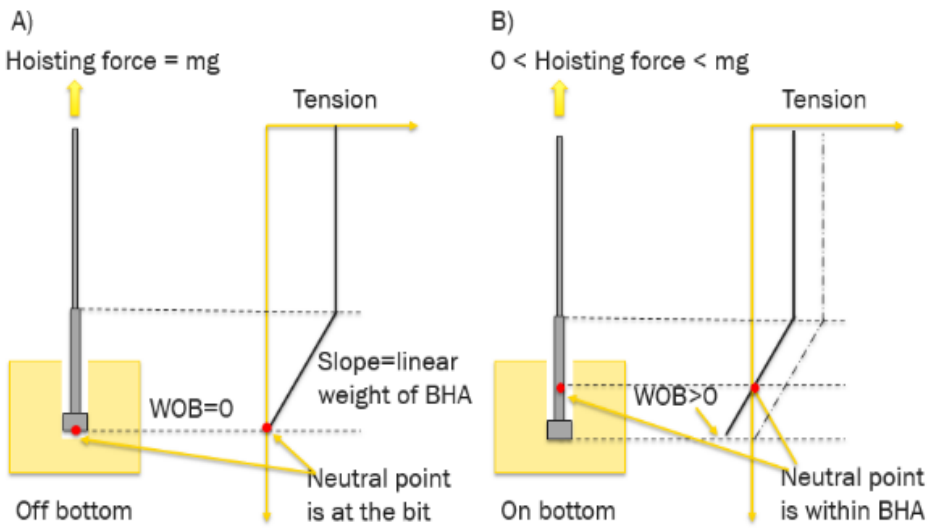

Figure 38: Neutral point transition where it moves upwards when WOB increases.

The weight of the drill string is around 1.0 kg so the weight on bit should not exceed the following:

$$W_{Applied} = \frac{W_{BHA}}{1.15} = 0.87kg$$

As calculated a weight on bit of 0.87 kg, is the maximum weight that can be applied unless the neutral point would move to the drill pipe.

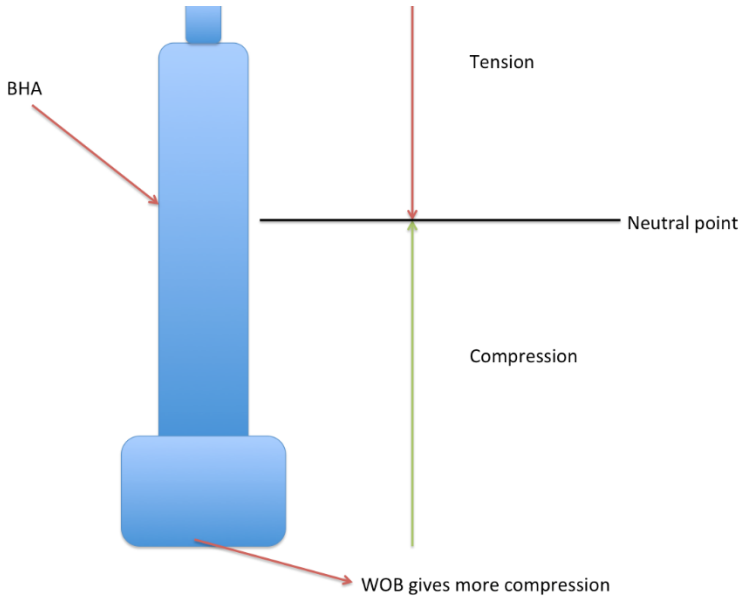

Figure 39: Too large WOB causes buckling the pipe where the neutral point should be in the BHA.

3.6.2 Buckling methods

Buckling methods are quite many and different, and they give different results based on the type of model and which parameters those models depending on. There is no accurate model for buckling yet; some models suit for some situations more than others. Three models are briefly reviewed in this chapter: Euler´s, Paslay´s and Rayleigh-Ritz models. Moreover, the results between the three models are compared to each other using the data from equipment that utilised in the design of drillbotics competition.

3.6.2.1 Euler´s buckling force

The mathematician Leonhard Euler derived the following equation to determine the minimum axial force needed to buckle a long and ideal column in room temperature and pressure; it is called the critical force to cause buckling. This formula derived without considerations for lateral forces [27]:

$$Fc = \frac{\pi^2 * E * I}{(KL)^2} \quad (22)$$

Where

Fc: The maximum axial force right before buckling

E: Modulus of elasticity of the element

I: Moment of inertia

K: Length factor that depends on factors like [27]:

- Both ends fixed, K=0.5
- Both ends pinned, K=1
- One end fixed, and other pinned, K=0.7
- One end fixed, and other end moves freely, K=2.

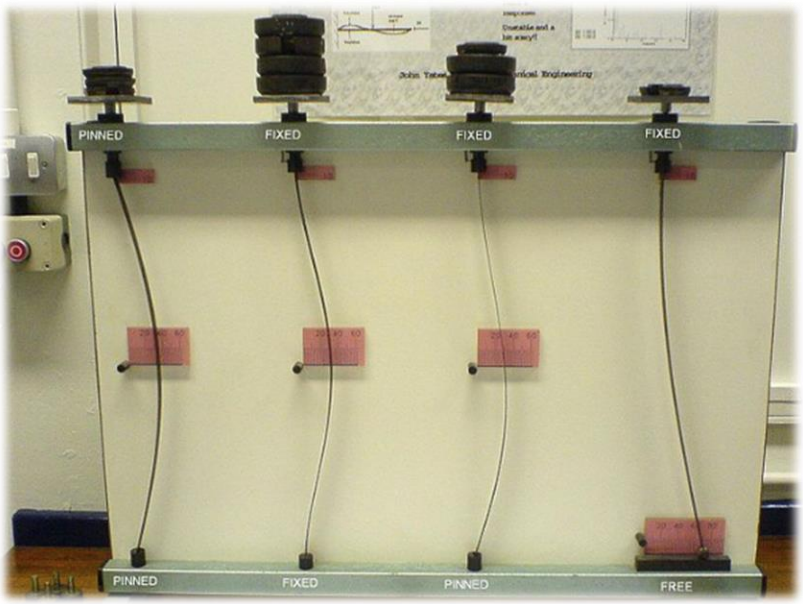

Figure 40: Different fixing models for buckling gives different value of K [27].

L: Length of the element

Figure 40, gives a demonstration that illustrates different models for buckling, and the fixed-free model would be the model that suits our design. The values of K vary from a situation that gives fixed/pinned ends where K=0.7 to another position where there are one fixed end and the other sways where K=2.0.

The curve below illustrates the minimum force that is needed to buckle an aluminum drill pipe with a thickness of only 0.0022m and a length of 1m when the values of K varies between 0.5 to 2.5. The calculations are illustrated in the curve below as depicted in the curve below:

A value of K=0.7 gives a critical buckling force of Fc= 315N, and a higher value of K=2.0 gives Fc=38N, by approximating to the maximum WOB the values located between 3.9 kg and 32.0 kg.

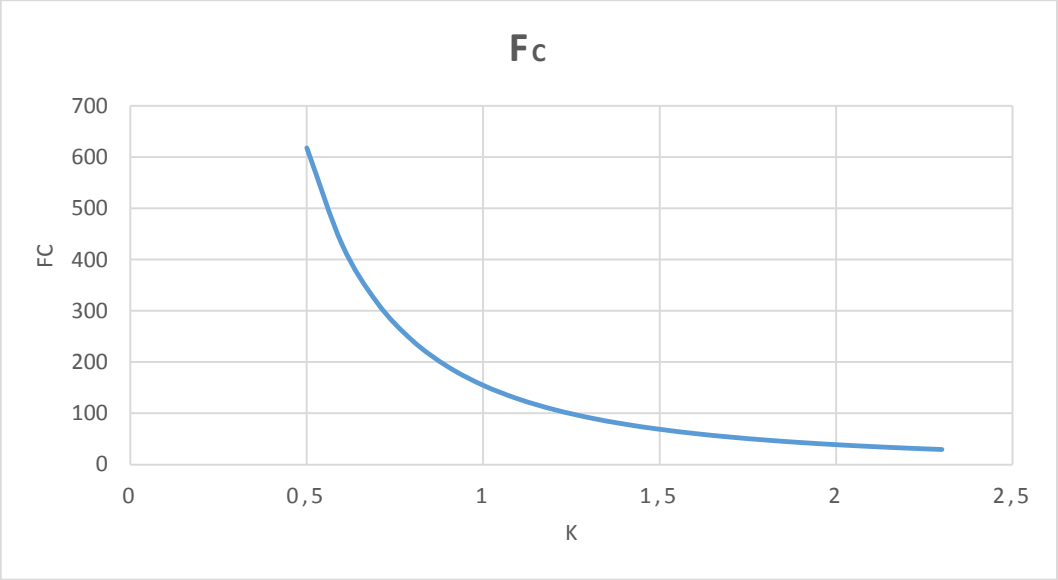

Figure 41: Buckling force with varying the length factor K.

3.6.2.2 Paslay´s buckling force

Buckling starts to occur when the buckling force F_b is greater than a threshold force Fp where Fp is the minimum force until buckling occurs [28]:

$$F_b = -F_a + pi * Ai - po * Ao \quad (23)$$

Where

F_a= axial force

pi & po= internal and external pressure

Ai & Ao= internal and external cross-sectional area

The following formula expresses Paslay's buckling force model as [28]:

$$Fp = \sqrt{\frac{E*I*wc}{r}} \tag{24}$$

Where

EI= bending stiffness of pipe

r= Radial annular clearance

wc= Casing contact load

$$wc = \sqrt{\left(we * \sin(ø) + Fb * \left(\frac{dø}{dz}\right)\right)^2 + \left(Fb * \sin(ø) * \left(\frac{\mathrm{do}}{\mathrm{dz}}\right)\right)^2} \tag{25}$$

ø= wellbore angle

o=wellbore azimuth angle

we= buoyed weight of casing, assumed to be drill pipe weight.

$\frac{dø}{dz}$ is assumed to be equal zero due to there is no inclination change.

$\frac{do}{dz}$ is assumed to be equal zero due to no azimuth change.

Then wc will be simplified by the following formula $wc = \sqrt{(we * \sin(ø))^2}$

Using the following equation as mentioned to find an estimation of the force that causes buckling:

$$Fp = \sqrt{\frac{E*I*wc}{r}}$$

The calculations illustrated in the curve, figure 42, and it shows that an inclination of 2.1° gives the highest values of the minimum buckling force of 1.83N that means that the drill pipe would easily buckle with a WOB, which is between 0.1-0.2 kg.

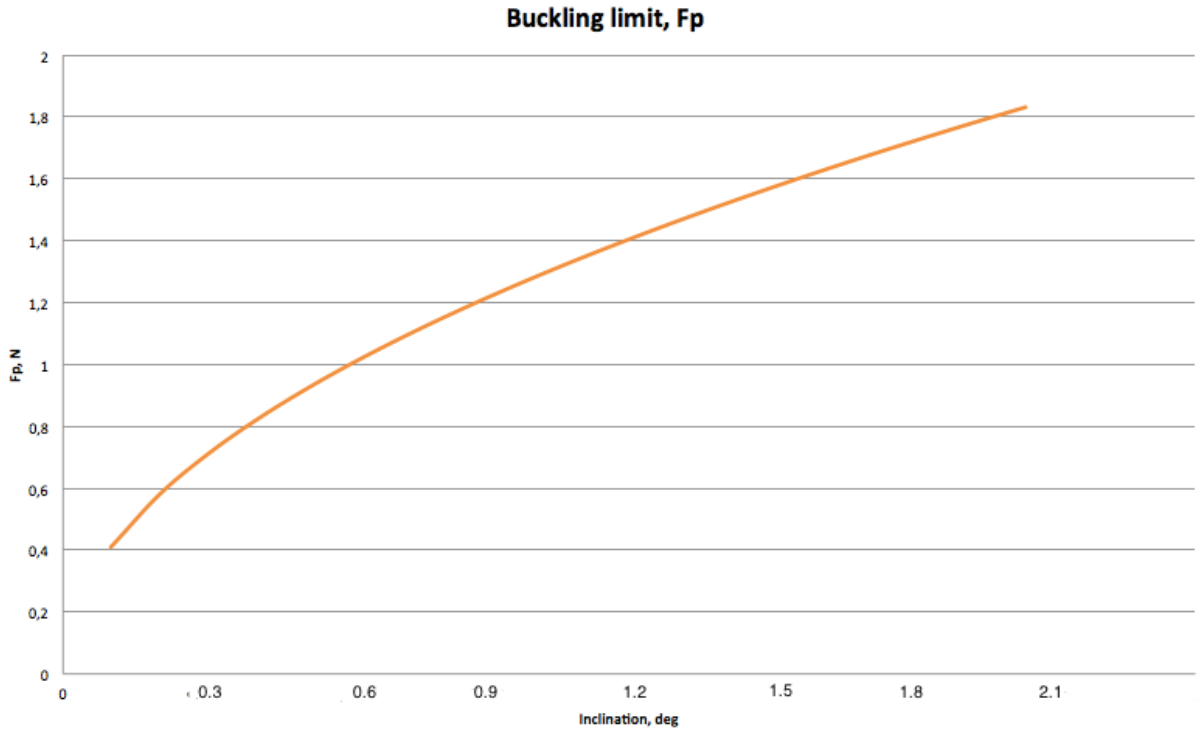

Figure 42: Allowable force to avoid buckling with respect to inclination.

Comparing the methods

The minimum buckling forces illustrated using both Euler's and Paslay`s methods. As shown previously the values that are obtained using both Euler´s and Paslay´s methods are different from each other, where Euler´s method showed higher values than Paslay´s, and the buckling force from Euler varied between 38N and 318N, but Paslay´s buckling limit values were between 0.4N and 2N. Euler´s method is more relied on the length factor K the way drill pipe

fixed, but Paslay´s method is more dependent on the inclination of the pipe. The parameters that used are different, and that might be the reason.

3.6.2.3 Rayleigh-Ritz method

This method takes much more parameters into consideration as this approach based on the principle of the minimal potential energy that applies to conservative systems. Based on that an approximation of the displacement of the element is detected by two-dimensional element. As mentioned this method builds on the principle of conservation of energy, as the following [29]:

$$U = \pi - W = \int \frac{EI}{2}\left(\frac{d^2y}{dX^2}\right)^2 dX - W \tag{26}$$

Where π represents the total strain energy of the element and W represents the total external work that are done on the element. The potential energy U of the system is formulated as $\pi - W$ and the displacement components are represented as [29]:

$$u(x) = \sum_{i=1}^{N} ci * y(x) \tag{27}$$

Where i = 1,2…N, are Rayleigh-Ritz coefficients. Where increasing the order N of approximation increases the accuracy of the Rayleigh-Ritz method to the truth.

The inputs are the parameters that we can control as the following:

- WOB
- Riser displacement
- Hole length
- Inclination

Moreover, the outputs are:

- Tilt angle
- Side force at bit
- Max deflection of drill string
- Side force at stabiliser to correct direction

This model used to determine the maximum allowable WOB to avoid buckling. In addition to that, the riser displacement is measured in order to determine the side force that would be applied to the stabilisers on the BHA to correct the direction of drilling in the case of deviations.

The derivation of the total potential energy of a system according to (Swaryn and Pattillo 2013) and (Walker 1973), including Lagrange multiplier contribution the total potential energy, where w(x) is the displacement [29]:

$$U = \int_0^L [\frac{1}{2} EI(x) * \left(\partial_x{}^2 w\right)^2 - \frac{1}{2} P(x)((\partial_x w)^2 - \frac{1}{2} q(x) cos\theta \int_0^x (\partial_{x'} w)^2 dx' - q(x)\, sin\theta\, w(x)]\, dx + \sum_{i=1}^{J} \lambda i\left[w\left(L_{s,i}\right) - \Delta ri\right].$$

(28)

(Walker 1978) and (Sawrayn 2012) were Approximating the true displacement function with trial functions and Ritz coefficients where w(x) is the deflection of the drill pipe at one point [29]:

$$w(x) = \sum_{n=0}^{\infty} Bn * \cos(xn * x) + \sum_{i=0}^{\infty} An * \sin(xn * x) \qquad (29)$$

Where Bn, An and xn are determined by the boundary conditions using the principle of the minimum potential energy.

The side force acting on the bit expressed on a small element of the assembly according to Sawaryn 2012 voiced by the following [29]:

$$F_0 = \sum_{n=0}^{N} \frac{A_n\left((2n+1)*\pi\right)}{2L} [EI(0) * \frac{(2n+1)^2 * \pi^2}{4L^2} - P_0] \qquad (30)$$

By implementing this method in software program. Having an input for the variation of the WOB and inclination to see when buckling occurs as illustrated in figure 43. The maximum WOB varies between 3.0 kg to 32.0 kg when the inclination varies between 0^o to 1^o as depicted. The maximum allowable WOB is proportional to the inclination of the drilling string according to the simulator of the Rayleigh-Ritz method to calculate buckling.

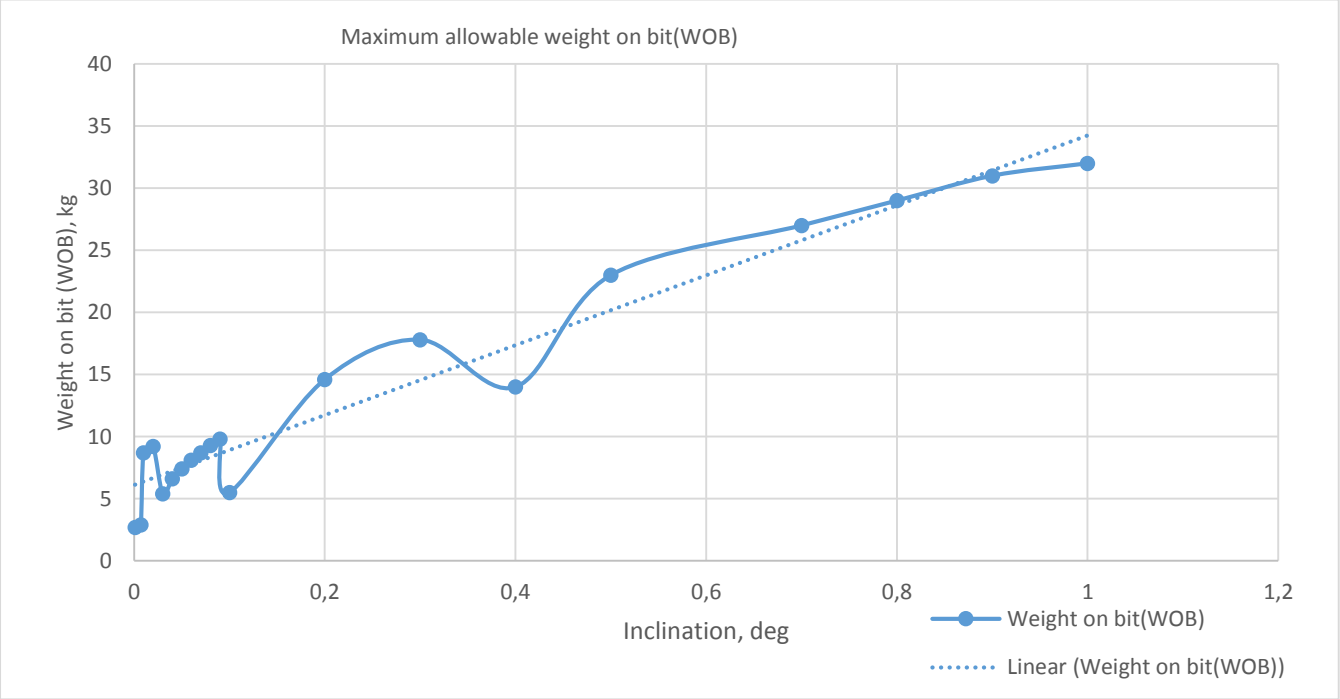

Figure 43: Maximum WOB allowed to avoid buckling in different inclination angles.

3.6.2.4 Case study

Determination of the maximum WOB

WOB/Method	***Euler***	***Pasley***	***Rayleigh-Ritz***
Min. WOB	3.9kg	0.04	3.0 kg
Max. WOB	32 kg	0.19 kg	32 kg

As illustrated in the table above, Euler and Rayleigh-Ritz methods give quite similar values on the maximum and minimum values WOB. According to Euler, the allowable WOB depends on how the pipe is fixed/pinned, and Rayleigh-Ritz`s and Pasley`s on the inclination.

Chapter 4 Design construction

Using aluminium buildings parts as a base for the whole structure. The structure consists of three parts. Two parts are moving while one part is fixed to a table. The middle part is the fixed part of the table, and the top part is sliding up and down on the fixed part to move the drill string up and down. The third part is sliding up and down to place the rock where drilling takes place. The design includes the following components:

- A 2.5-meter height frame that carries the drill string and its components.
- Motor 750W that delivers 2.4 Nm in average and 7 Nm in peak.
- 1m aluminium drill pipe, OD 9.95mm & ID 0.7747mm.
- BHA with a length of 42 cm. 1.0 kg, OD 22mm and ID 6.5mm.
- PDC bit with two teeth and one nozzle in the middle of the face.
- The whole design should be able to drill successfully through a cubic rock of 30x30x30cm that contains different layers.
- A water pump connected to the drill pipe by a hose attached to a rotary swivel.

Figure 44: The cubic rock that before drilling where the placement of layers in not to be seen.

The rock that drilled consists of different rock types with soft and medium/hard rocks that are sorted in various directions and cemented together to a big cubic sandwich with dimensions of 30x30x30 cm. A part of the challenge is that the layers of the rock are unseen due to the walls that are on the rock to be aware of drilling any rock without knowing the type of the next rock layer. This design has been made to ensure lower values of the moment of inertia in case of a

sudden stop due to stick situations that most expected during drilling. The design has a motor that is connected directly to the drill string.

Two hoisting systems equipped with the rig that splits the rig into three parts. The top part includes most of the top drill string equipment, and the bottom part includes BHA, drill bit, and riser, while the middle part fixed on a table. The middle part connects and supports the upper and lower parts together. Figure 47. Illustrates a 3D drawing of the rig and its components as the blue part is the fixed part, the green is the upper, and the yellow is the bottom part. Also, a drill string red coloured is illustrated with top drive components at the top and the BHA in the bottom.

Scheme of design system

The rig should have a power transmission system which consisting of a motor that is connected to the drill pipe to give a rotational speed to the drill bit. The C-beam actuator has a motor that is responsible for the elevation of the hoisting system and for applying weight on bit (WOB). There is also a water pump connected to the pipe by a swivel to pump water to the drill bit to make a circulation of water cleaning the borehole due to the cuttings produced during drilling.

A properly cleaning of the borehole could help against any sticking. Therefore, a use of a pump is required. Experiments will be done to give a better illustration of the parameters that utilised. A strategic decision controller takes control of these tasks by using the real-time controller, illustrated in figure 45.

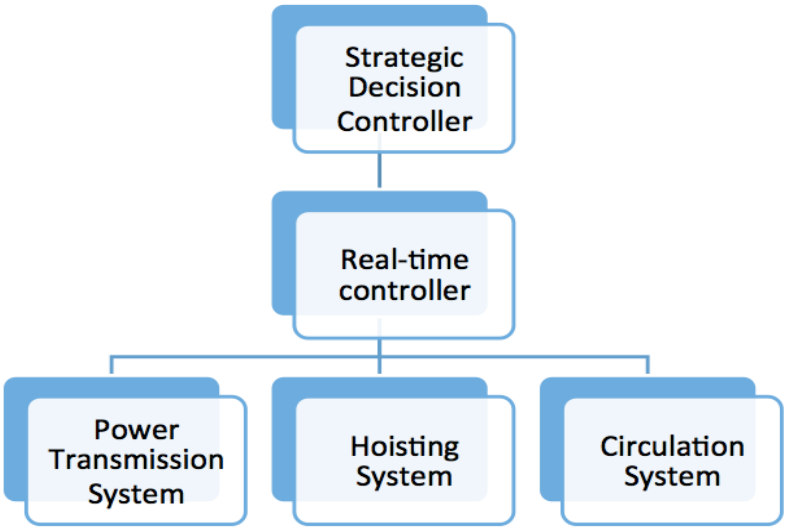

Figure 45: Scheme of design systems.

The illustration in figure 45, gives overall architecture as it gives the fastest and simplest control elements at the bottom (power transmission system, a hoisting system, and circulation system), at the top control loop working with variable reaction time (strategic decision controller).

Many problems stand against the design like the different strength of rocks where they are sorted 45º in every direction. Also, the thin drill pipe that has limited resistance against twisting. Therefore, that is required to optimise the most necessary drilling parameters in term of the speed of the motor, WOB and reaction time to be able to drill successfully. The required acceleration/deceleration points while changing the set point is to be controlled, and modifications of the set point are needed. This task applied by a real-time controller that is reacting slower than the speed and position of the hydro-mechanical system and the responding time controlled where the reaction time is to be determined based on the type of materials we are using to avoid failures. The challenges described as following:

- Rock layers 45º sorted, and the sequence and thickness are unknown.

- Building and design rig components.

- Testing and calibrating drilling components.

Rock sample

The task of the team is to make and build a rig design that can drill through a cubic rock 30x30x30cm. The cubic rock contains different rock types like sandstones, shale, and limestone then everything is cemented together to make it as a compact sandwich where the different layers are 45 deg. Sorted acting like a sandwich of different rock materials. The purpose of that sandwich block is to drill through the various types of rocks while dealing with sudden rock layer shift.

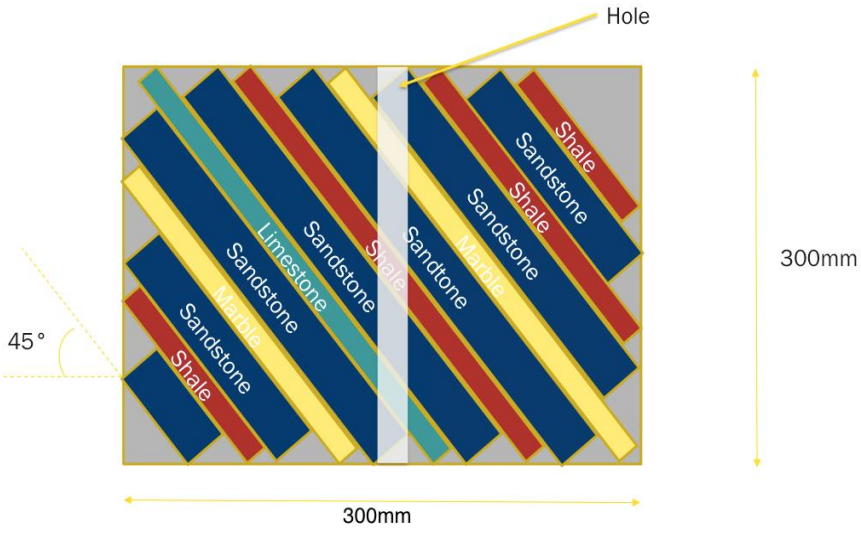

Figure 46: A sketch of rock layers.

4.1 Construction of the rig

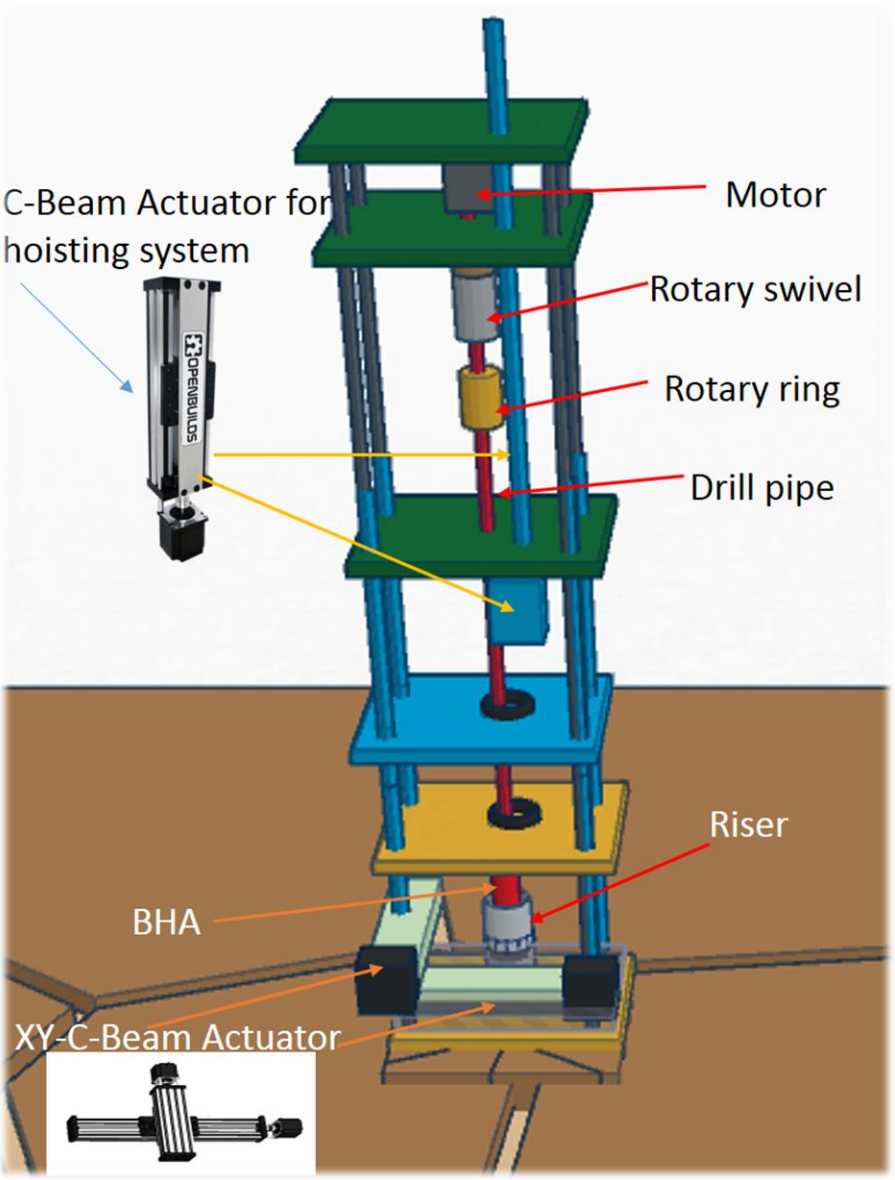

Figure 47: Simple illustration of the whole rig and its components.

As illustrated in figure 47, the green structure is the upper part that is moving up and down sliding on the fixed middle (blue) structure using small wheels. The whole upper structure is moving by a C-Beam linear actuator, which has a plate that fixed on the upper structure and the plate is moving by a motor that is following with the C-Beam actuator.

Top part

Figure 48 illustrates a vertical section of the rig. The top part of the structure is the green part and includes three floors, A, B and D. The drill string fixed on floor B and a C-Beam actuator on floor B to lift the top part up and down, which is called the hoisting system. Floor D is the base for the upper structure, which is sitting on the table.

Middle part

The middle part is the blue part, and it has three floors (floor C, E & G), where floor E is the table. The main purpose of the middle part is to make a base for the whole structure, and it connects the upper and lower parts by sliding wheels, and the bottom of the C-Beam actuator fixed on floor C as illustrated.

Lower part

The bottom part is the yellow part that includes the riser, BHA, and drill bit. This part consists of three floors (F, H and I), which is attached to the middle part sliding wheels. An XY C-Beam linear actuators installed on floor-H to provide force to support the riser against any abnormal movement. The purpose of using drilling riser is to be able to support and apply side force against the direction of deviation to drill as vertically as possible.

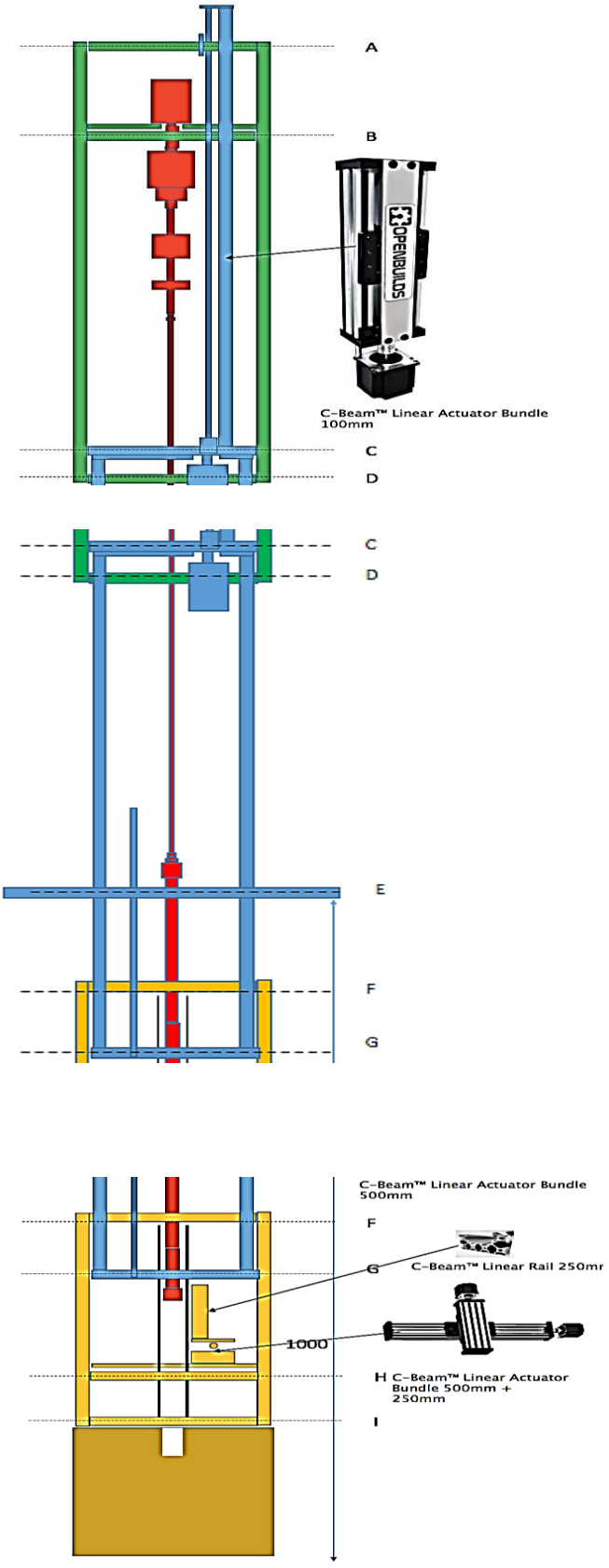

Figure 48: Vertical section of the rig.

4.2 drilling string

The drill string has a length of approximately 1.92m and includes the top drive components, drill pipe and bottom hole assembly (BHA). The top-drive and its components have a length of 0.5m. Then there is 1m drill pipe that made of aluminium has OD 9.95 mm and ID 7.75 mm.

The BHA consists of integral parallel stabilisers, BHA elongate and a bit with a total length of approximately 0.42m. The drill-bit has two cutters and one nozzle of a diameter of 4.7mm and to cutters.

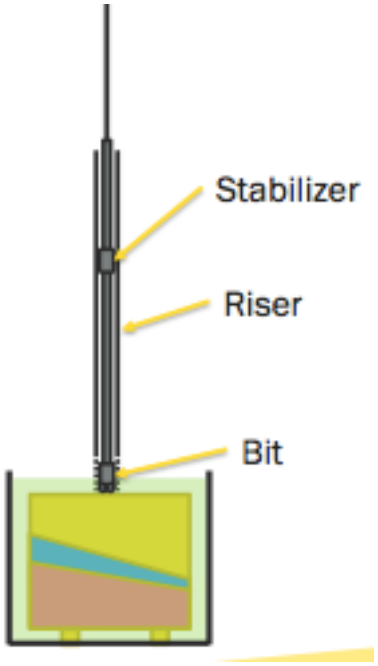

Figure 49: Lower part of the drill string.

4.2.1 Top Drive

The top drive is consisting of four plates, where plate #4 is the base of the top drive, and it has four load cells. The load cells are placed just under plate #2 as illustrated in figure 50, to measure the hook load of the drill string's components. One end of the load cells fixed on plate #4 with a thick washer and the second end that measures fixed on plate #2. The following plates #1, #2, #3 and the rest of the drill string are hanging on the load cells that are on plate #4, to measure the hook load from the four load cells.

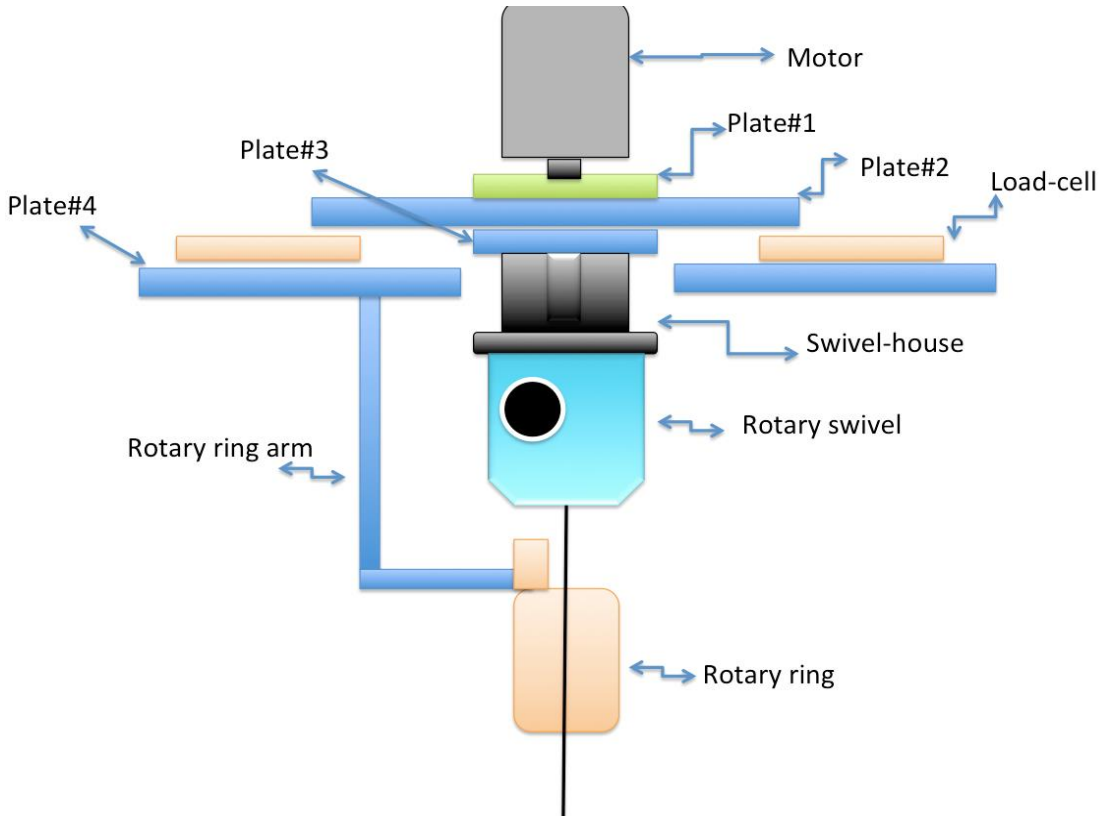

Figure 50: Sketch of top drive structure, four load cells on plate #4 to measure the hook load.

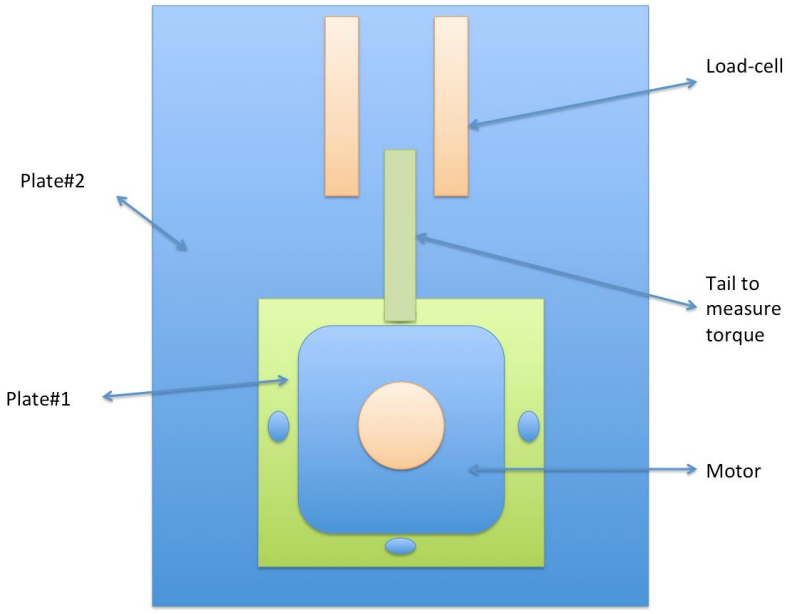

Figure 51: An illustration of the top part of the top drive.

As illustrated in figure 51, plate #1 is returnable and has a tail that touches the load cells when it rotates, to measure the torque that induced from the motor during drilling. Plate #1 and plate #3 are fixed together by a long 25mm screw that goes through plate #2, where plate #2 has a 10mm hole that the long screw goes through, to give a space allowing plate #1 to rotate some millimeters, to measure the torque. Plate #1 has a 4 cm tail that touches the two load cells on top of plate #2. The force that applied to the load cells is calculated by the motor torque times the length of the tail $r = 4cm$ in addition to the distance to the motor center $s = 5cm$, which gives a total arm of 9cm

$$F = \frac{\tau}{r} \qquad 1$$

The maximum torque is 7 Nm, which gives a force of 78N and weight of 7.9kg on the load cells. The load cells that amounted tolerates 10 kg of weight so rotating with the maximum torque will not damage the load cells.

4.2.1.1 Load cells

A load cell is a small 8-10 cm long device that creates an electrical signal that is directly proportional to the exposed force. The device fixed on one end and a strain gauge sensor in the middle to measure the load that subjected to on the other end. The principle of the load cell based on the stress that the strain gauges subjected to where the resistance of the electrical conductor changes when the length changes due to loads [30].

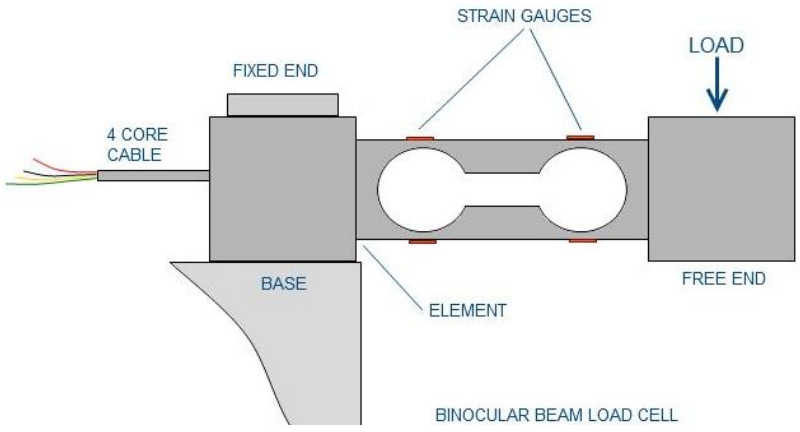

Figure 52: Simple illustration of the nature work of a load cell [30].

Each load cell in the system connected to an amplifier to convert the force that a load cell receives to achieve logical values because the value that a load cell receive is in Volt(V) and not well understandable.

4.2.2 Drill string components

4.2.2.1 Motor

The motor that used is a stepper-motor (R88M-G75030H/T (750 W)), figure 53. Stepper motors have discrete steps as they have multiple coils that organised in groups, see figure 53. This type of motors can be controlled by Programmed Logic Controller to give a precise positioning of every step, and that would be a perfect choice for our design.

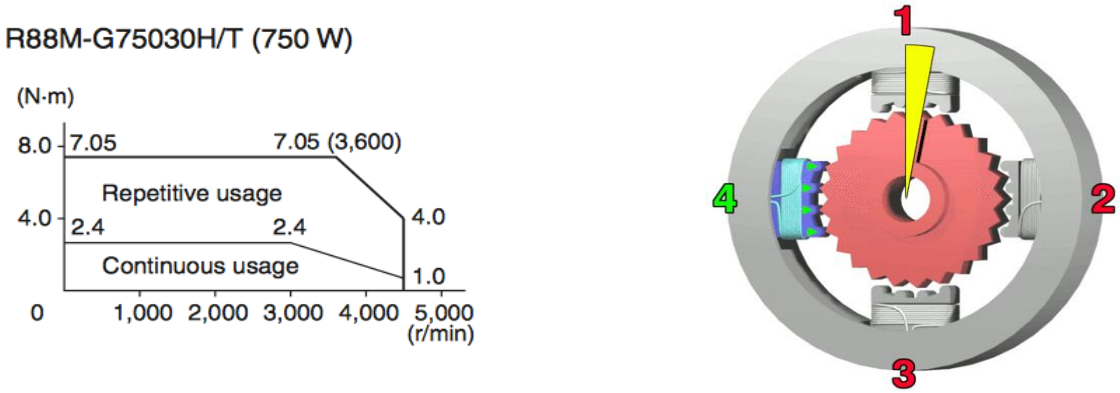

Figure 53: Torque of the motor at left. Stepper motor with four coils at the right [31], [32].

A DC motor could be used as well, but the problem with DC motors in our case is the extended period of the moment of inertia and precision that finds a place in stepper motors. The stepper motor is different from a normal DC-motor, a normal DC-motor has fast speed and high torque, but stepper-motor is slow and more precise that could give better positional control which is suited for such an automated design. That is why using a stepper motor gives a precise stop. Where it has a step angle of 1.8 degrees. Note that every motor step gives a twisting torque of 0.17 N.m. The motor is coupled to the rotary swivel using a beam coupling just to ensure rotating without misalignments.

4.2.2.2 Motor Coupling beam

The beam coupling is attached to the end of the motor shaft, also known as helical coupling. The reason why this beam is used to correct in case of misalignment between the motor and the next coupling to extend the life of the motor. Misalignment works against the motor and damages the motor. It has a spiral path that results in a flexible movement to allow misalignment without damaging the motor. [33]

Figure 54: Coupling beam between two shafts [33].

There are used four coupling beams in the whole rig. One coupling placed between the motor and rotary swivel, and one between the brake and c-beam actuator for the hoisting system. The last two couplings placed between the motor and c-beam actuator in the XY-C-beam actuator at the bottom part.

4.2.2.3 Rotary swivel

The rotary swivel is connected to the motor by a coupling beam, and to the drill pipe by a 20 cm long tube. The rotary swivel is used to secure drilling fluid to the drill pipe, where it converts a static condition above the swivel to a rotary movement below the swivel to the drill pipe. It has a stationary part on the outside to be fixed using a swivel house that is attached to plate #3, and the rotating part is at the inside center. A hose that supplies drilling fluid connected to the static part and the rest of the drilling string coupled to the rotating part.

Figure 55: Rotary swivel.

4.2.2.4 Slip ring

As shown in figure 56, this ring is slide into the 20 cm pipe between the rotary swivel and drill pipe and the reason why using this part is to separate the static movement from the rotary. It has a stationary outer part, and an inner rotary part where the rotating part is attached to the drill string, and it has wires and connections to the BHA and riser, and the stationary has wires that connected to the computer of the system. [34]

Figure 56: Rotary ring [34].

4.2.2.5 Drill pipe

A drill pipe of a length of 1m attached from top to a 20cm pipe that comes through the rotary ring and to the BHA from the bottom. As mentioned earlier, the aluminium drill pipe is the weakest element in the drill string, the specifications illustrated in Table 5.

Table 5: Drill pipe specifications.

Drill Pipe	
Material	Aluminium
Weight	0.07kg
Length	1m
OD	0.00995m
ID	0.007477m

4.2.2.6 BHA

The BHA has a total weight of 0.92 kg and an outer diameter of 22 mm and the inner diameter of 6.5 mm. The BHA in our case consisting of a drill collar designed as illustrated in figure 57 to:

- Provide significant WOB due to its heavy weight.
- Directional control by four integral blades at the top part (stabilisers).
- At the bottom part, there are installed accelerometers to measure accelerations and give more information about the process.

Stabilisers at the top have a diameter of 27 mm together with the collar, where they are some integral blades that have a direction parallel to the collar. In this case, stabilisers support the drill string to drill as vertically as possible. At the bottom of the collar, two rooms made to place two pieces of accelerometers to get information about the abnormal movements (vibrations). As illustrated in figure 57.

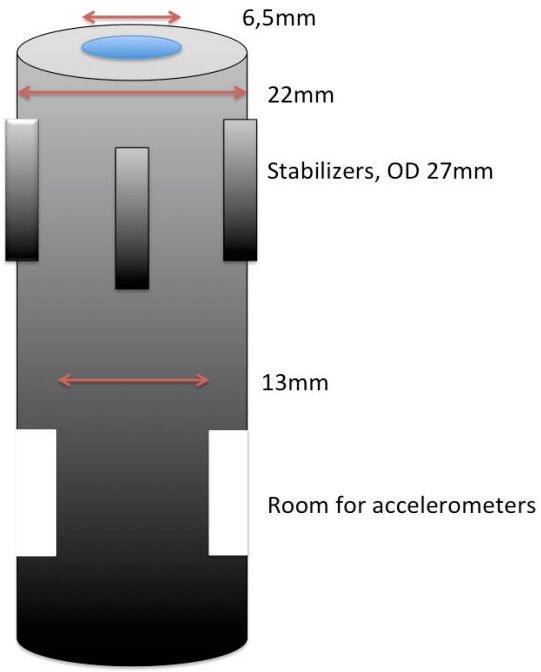

Figure 57: Schematic of the bottom hole assembly.

Accelerometers

The accelerometer is a small chip, has dimensions of 22x16mm fixed in the room of the BHA. It measures the acceleration motions in X, Y and Z directions to give a better picture of the vibrational movements of the BHA. Those forces can be constant forces like gravitational force or dynamical due to the rotation and friction between the BHA and the riser. The accelerometer is providing data during drilling, and this data could be useful for the operation to get more information about vibrations on the BHA.

To determine how deeply the room that accelerometers placed in, the following calculations are required to put the accelerometers into the drill collar without sticking out. The accelerometers shall be hiding inside the drill collar to avoid damages during drilling.

A cross section of the Drill collar illustrated in figure 58 below. This part is quite sensitive where the accelerometer should not stick out of the collar. Also, the accelerometers have a length of 22 mm and a width of 16 mm, and it screwed in the room that made, and the screws should not reach the inner diameter avoiding puncturing into the inside diameter while making screw holes. Therefore, the length of the screws that fixed on the accelerometer should be calculated.

The dimensions of the accelerometer are 16x22 mm, as mentioned earlier these dimensions shall fit into the room. Some assumptions and choices required; later the assumptions need verification.

The length of the room chosen E= 30mm, see figure 59. Moreover, the depth of the room that made is R= 4.5 mm as illustrated in figure 58, but when it comes to the width D, there will be a need to calculate it because the width is proportional to the depth of the room R.

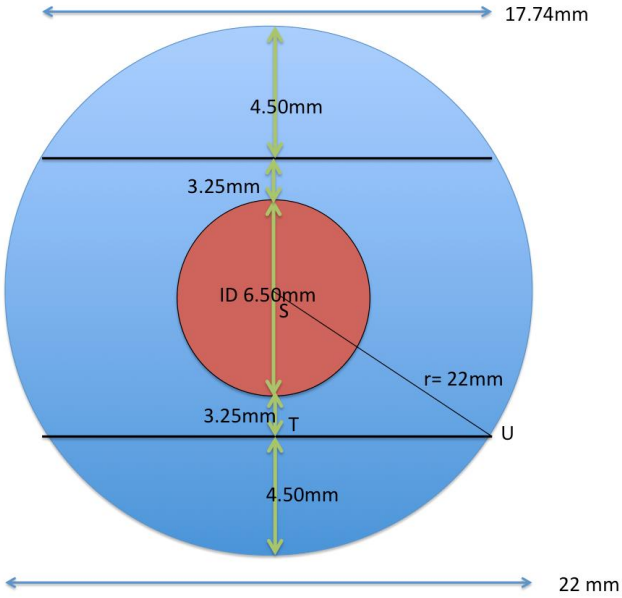

R=4.5mm

Figure 58: Cross section of the lower part of the drill collar.

It is determined that the depth of the chamber is 4.5mm into the lowest part of the drill collar, but it needs verification that the accelerometer would fit according to the width by solving the following triangle ΔSTU , in figure 60, Where $TS = 3.25 + 6.5 = 9.75mm$ and $SU = r = 22mm$, then $TU = \sqrt{SU^2 - TS^2} = 8.87mm$, where the width is $2 * TU = 17.74mm$.

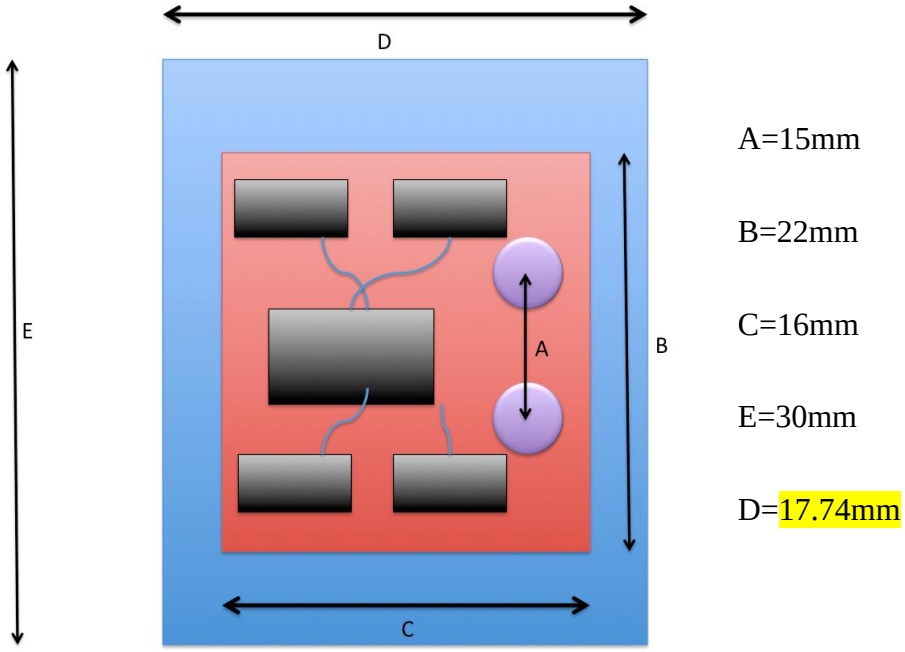

Figure 59: Blue square is the room of the accelerometer. Red is the accelerometer.

A width of 17.74mm is enough since the width of the accelerometer is 16mm. Moreover, a length of 30mm is sufficient for 22mm; then the result verifies a depth of room of 4.5mm. Figure 59 is a schematic of the room that made for the accelerometer, where the accelerometer placed in the middle with two screws; A is the distance between the two small bolts. The accelerometers connected to small wires that pass all the way to the rotary ring to the system computer.

BHA extender and drill bit

A BHA extender is necessary to give more weight to the BHA and to elongate the bit. Where the drill bit is about 5 cm long. An extender with a length of 15 cm screwed to the short bit to make it 15 cm longer.

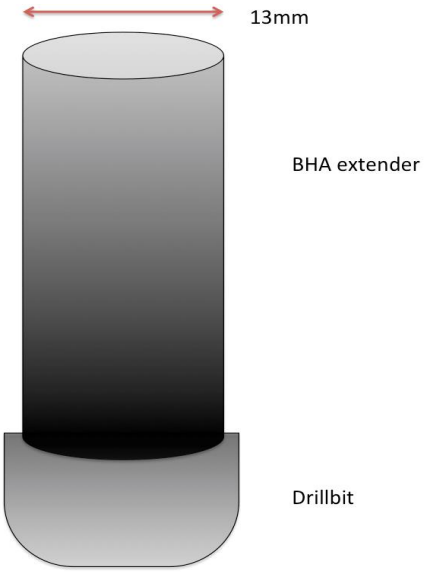

Figure 60: BHA extender and bit.

PDC drilling bit is used in Drillbotics design because it is one of the rules, and it is the easiest one to use according to availability to such small size bits that have two cutters, one nozzle and only an OD of 2.8 cm. See figure 61.

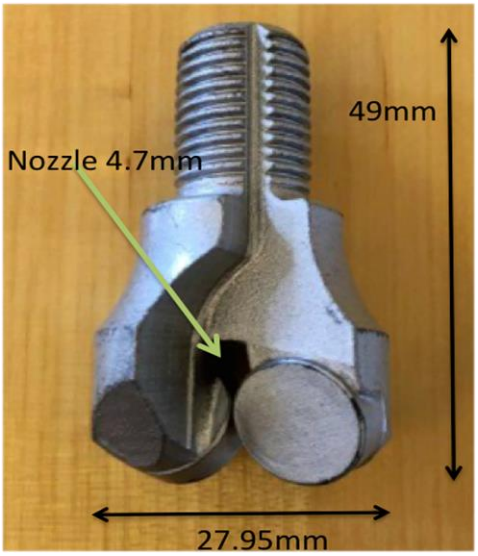

Figure 61: Drill bit, two cutters and one nozzle.

4.2.2.6 Riser (design)

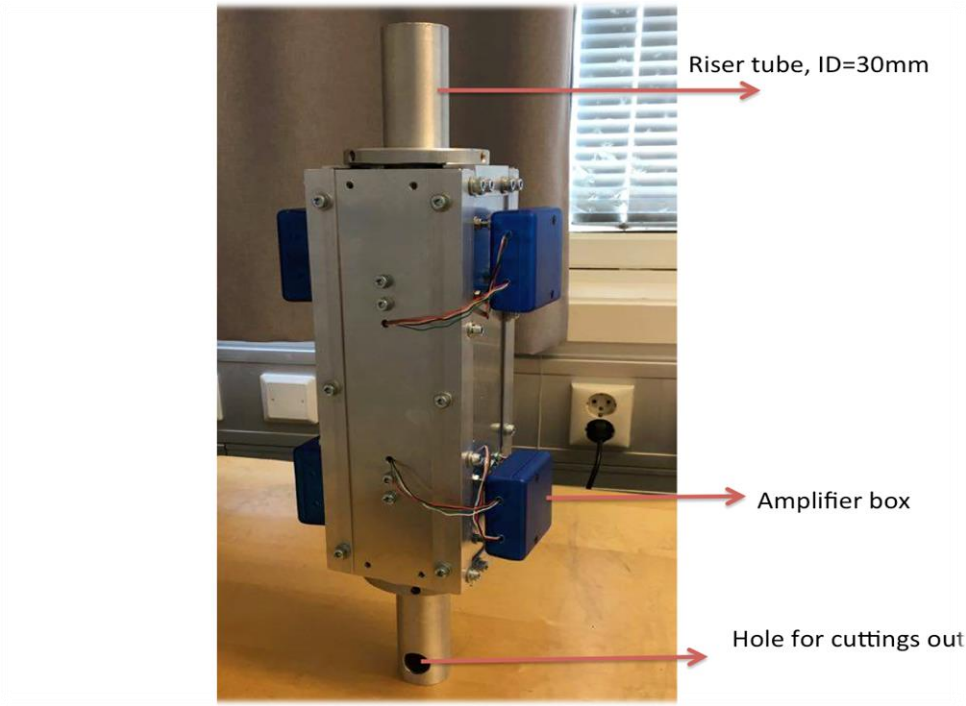

Figure 62: Riser and its components.

It is required to have a riser in our design where a riser would help to support the BHA to avoid deviations. Having a riser would help to maintain a vertical direction in our case. Note that fluids are not allowed to enter through the outer side of the riser due to the electronics that is installed outside of it, where there is a hole that is made at the end of the riser to make it possible that cuttings pass through.

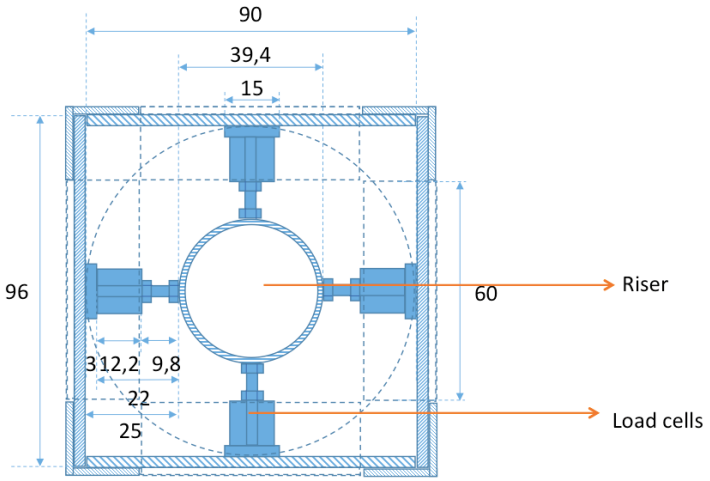

Figure 63: The riser including 8 load cells, 4 at the top and 4 at the bottom.

Eight load cells installed inside the aluminium box that illustrated in figure 62. Four load cells in the upper part and four others in the bottom part placed between the riser tube and the aluminium box connected to the amplifier at the outside. Horizontal section of the riser at figure 63.

4.3 C-Beam actuator

This device used as mentioned before in different places in our rig. We are using 3 C-beam actuators; the first one placed between the upper and the middle part of the rig for the hoisting system. Moreover, the two others are making an XY-C-beam actuator support the riser in the case of some deviations. As illustrated in figure 64.

The first linear actuator is placed to move the hoisting system to hold it up and to apply weight on bit (WOB) if necessary. It has a lead screw of a pitch of 2mm, and it controlled by a stepper motor with 0.18^{o} resolution each step. So every step gives a movement of 0.001 mm in position, so If the C-beam actuator that is responsible for hoisting moves 0.001 mm that would give 0.250 kg more in WOB.

The actuator that is in charge of hoisting and lowers the drilling string is attached to a break to be able to hold it in place in case of unwanted movement shown in figure 64A.

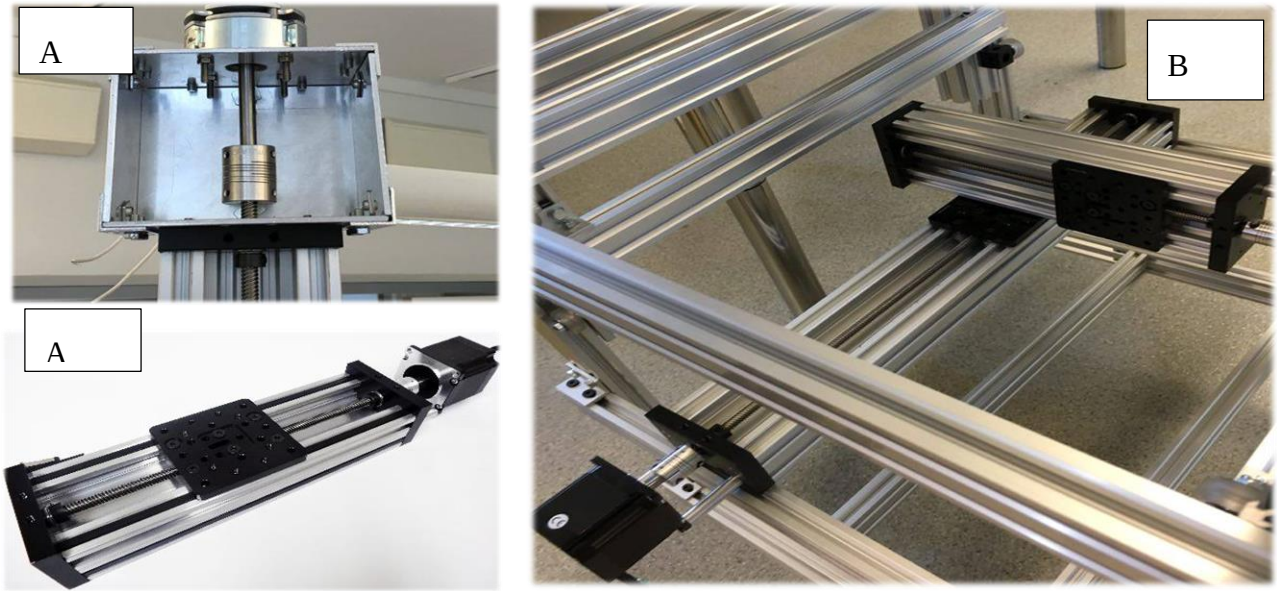

Figure 64: C-Beam actuators: A: C-beam actuator with a break. B: XY-C-beams to support the riser.

4.4 Pump

The design connected to a pump that delivers 3-4 bars to circulate the cuttings that induced during drilling. The pump is attached to a hose then directly to the rotary swivel where drilling fluid (water in our case) is going through the rotary swivel along the pipe into the bit.

The height of the rock is 0.30 meters, and the BHA is 0.42 meters; that means that the annulus that is between the BHA and the borehole, which counts, not the drill pipes outer diameter (OD).

It is recommended having the fluid velocity above 0.7 m/s to be able to get a sufficient cutting transport to clean the hole. The diameter of the hole has the same diameter as the bit approximately 0.028 meters. The flow velocity should be sufficient at the smallest outer diameter 20mm for the BHA extender. Where the flow rate approximated as:

$$Q = \pi \frac{v}{4}(d_{bit}^2 - d_o^2) = 2.11 * 10^{-4} \frac{m^3}{s} = 12.66 \frac{l}{min}$$

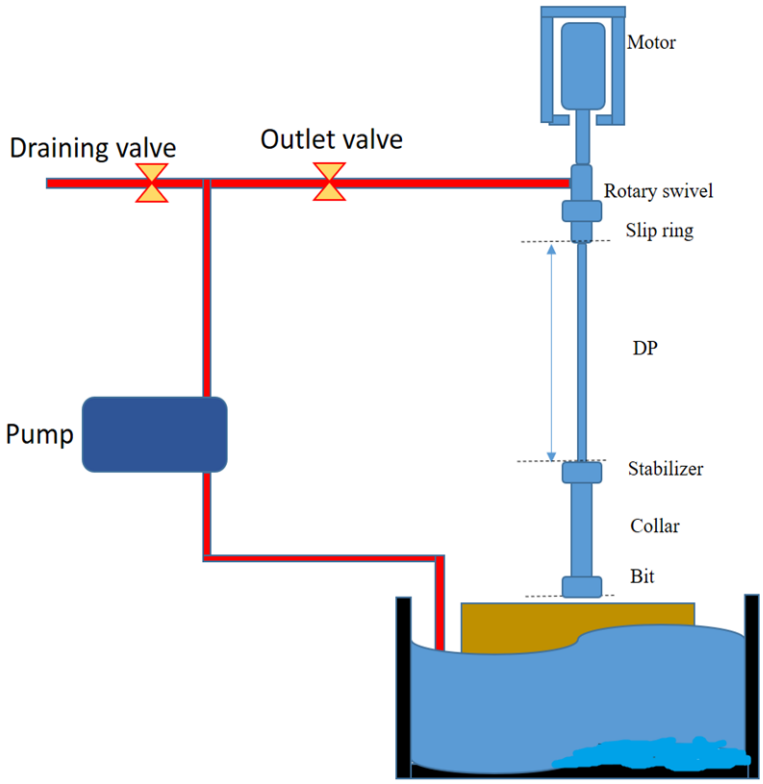

Figure 65: Circulation system of the rig.

The 30x30x30cm cubic rock placed in a bucket for water circulation issues as illustrated in figure 65. The bucket filled with water at a certain level, and a hose comes from the bucket to the pump. Drilling fluid (water) pumped to the rotary swivel then to the bit. Outlet valve placed right before the rotary swivel, and there is a draining valve to be able to drain drilling fluid if required and in the case of emergency.

Chapter 5: Drillbotics testing results

Testing system components is essential to make sure that everything works as expected to be able to perform the task that is required. Moreover, to ensure that the system handles different incidents. The following steps performed:

- Calibration of the load cells
- Pump testing
- Leakage and overpressure testing
- Over-torque, sticking scenario
- Correction for accelerometers

5.1 Load cell calibration

Every load cell that used in the design needs calibration to be able to understand the obtained signal. The load cells show a signal of voltage and this signal needs to be calibrated and converted to force value.

Load cells measuring torque

After mounting a load cell carefully, calibration required where it connected to an adapter and voltmeter to read the voltage. As depicted in figure 66, the load cell is loaded with 5 kg and observing the voltage value from the voltmeter. The value that obtained by a weight of 5 kg is 1.41 V. The same calibration is done for the second load cell. The distance from the force applied to the tail of plate #1 and the load cell is 6.2 cm which gives a torque of 3 Nm, which means that a torque of 3 Nm gives a reading of 1.41V. Where the wire weight is neglected.

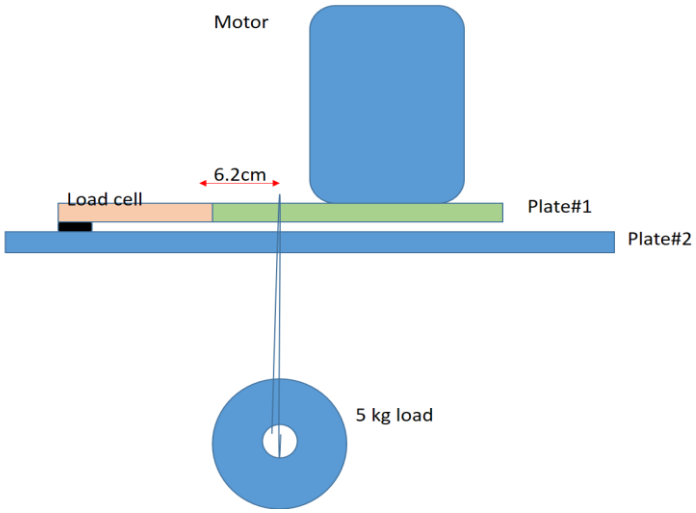

Figure 66: Calibrating the load cells at top.

Load cells measuring hook load

The top drive and the whole drill string is hanging on the four load cells at plate #4. The weight is approximated by 9.80 kg. The weight on each cell is 2.45kg where the load is divided into four since there are four load cells on plate #4 as illustrated previously in fig. 50. The maximum voltage that one load cell gives is around 3.30V. We consider a maximum voltage of 2.64 V, having a safety factor of 20% since the hook load can be higher in the case of bit sticking and hoisting at the same time, where Volt as mentioned is the measurement from voltmeter which refers to the force applied. The load cell is calibrated to give a reading of 2.64V when placing a weight of 2.45kg on it. In the end, we know that a load of 2.45 kg gives a reading of 2.64 V.

The rest of the load cells calibrated by the same way, where every single load cell in the system calibrated to provide a logical value of the exposed load.

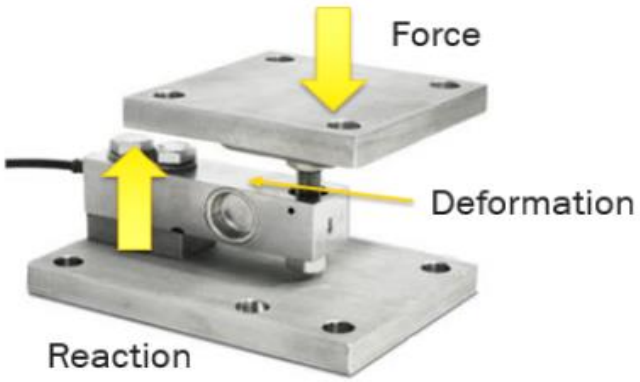

Figure 67: load cell measuring hook load.

5.2 Pump testing

After connecting pump components such hoses, sensor and other connections into each other, it needs to be tested. All connections screwed together using thread tape as showed in figure 68.

Figure 68: Thread taping to avoid leaking.

After fixing the couplings, the pump connected to an electric source and starting circulating water with various pressure to ensure that the sensor is working and no leakage between the different connections.

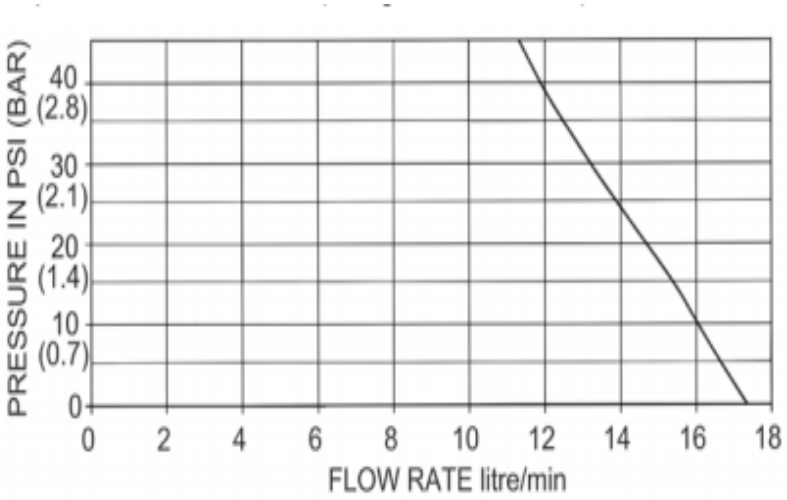

Figure 69: Pump characteristics from datasheet on left side and the pump on the right side.

As illustrated in figure 69, the pump characteristics show that the flow rate decreases when the pressure of the circulation system increases. Based on that the pump is tested to find out if the characteristics valid or not.

Afterwards, the flow rate and pressure measured at every point of the drill string. Starting to check the flow rate and pump pressure at the bit, then taking the bit apart and measure the pressure and flow rate at the BHA. Later, the BHA is taken apart and the flow rate and pressure measured, so the same measurements for drill string components until the rotary ring. Table 6 and figure 69 illustrate the measurement points at each element.

Table 6: Pressure and flow rate at various components in the drill string.

Element\measurement	Pressure(bara)	Flowrate(l/min)
Pump-outlet	1.00	14
Swivel	1.35	13,47
Slip ring	1.40	13,515
Pipe	1,75	12,465
BHA	1.87	11,865
Bit	2.56	9,9

The flow rate at different points of the drill string illustrated in figure 70, where the maximum flow rate is 13.51 $liter/min$ at the slip ring, and the minimum flow rate of 9.9 $liter/min$ at the drill bit. As illustrated the choice of the pump was based on the datasheet where the wanted flow rate was 12,66- 13 l/min, but the testing at the bit gives a flow rate of 9.9 l/min which is also acceptable, but below the wanted value. If we consider a drilled hole with a diameter of 0.03 m, the flow rate at the bit gives a flow velocity of 0.31 m/s at the bottom of the hole. As mentioned the pump pressure under drilling starts at 2.56 bar.

The reason why the values are below the values from the datasheet for pump might be because of the pressure loss from the inner wall of the tube and the height of the rig. The test performed five times on each component, and the average values presented.

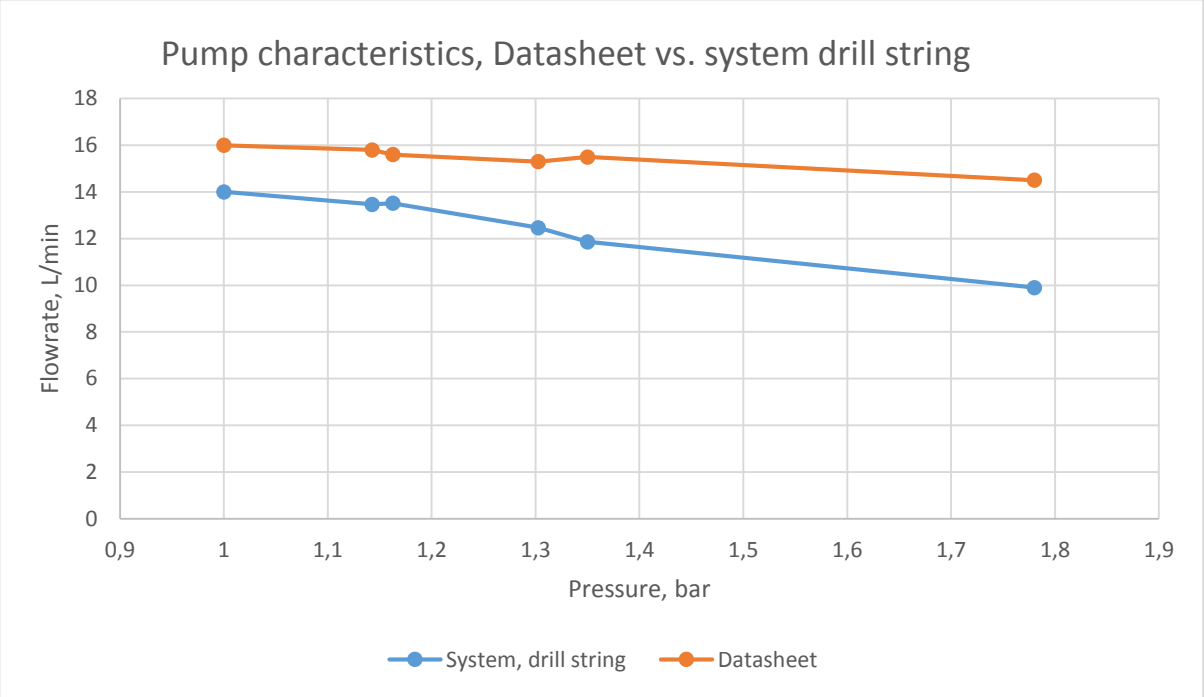

Figure 70: Pump characteristics datasheet vs. actual system drill string flow rate.

Figure 71 illustrates the pressure at every component at the drill string, starting with the pressure at the rotary ring 1.356 bars to pressure at the bit 2.562 bars.

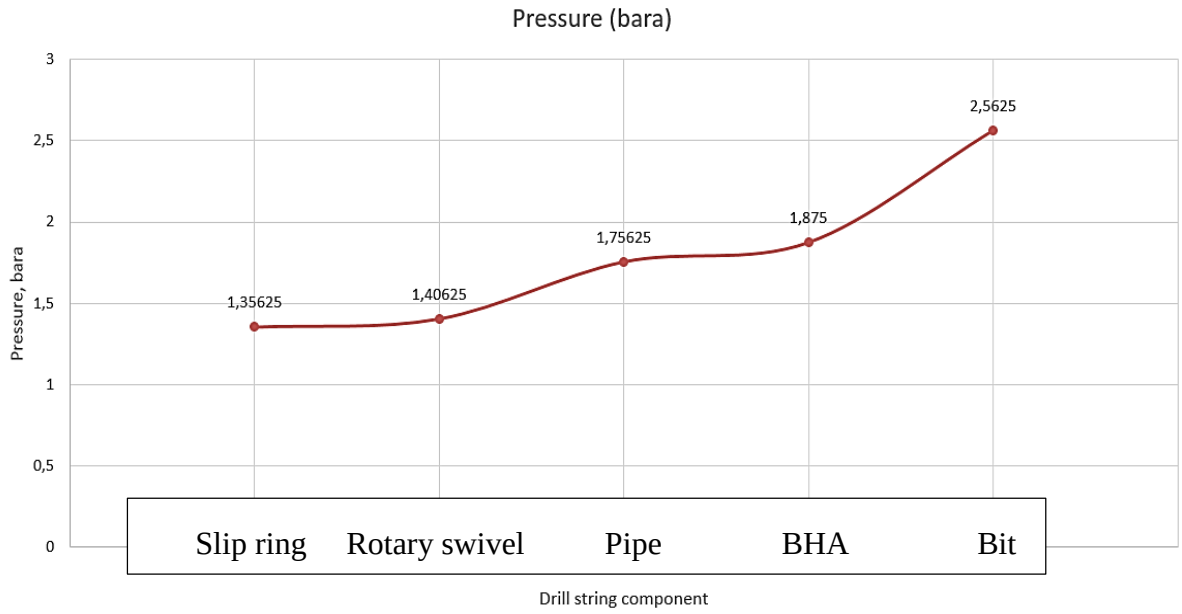

Figure 71: Pump pressure at every component.

5.3 Leakage and overpressure scenarios

The pump that placed has a maximum pressure of four bars. The real-time controller programmed to have pressure limits between 1.92 bars and 3.80 bars where the pump shuts off if the pressure passes these boundaries. If the pressure exceeds 3.80 bars, then there is an overpressure situation that explained by a reduction of the ability to circulate cuttings, and the pressure starts to build up. On the other side, if the pressure drops below 1.92 bars that means there is a leakage situation where drilling fluid spoiled out somewhere. The goal of this experiment is to make sure that the circulation system is working properly by pumping in the chosen limits and ensuring safety around the system, which is one of the top priorities.

The resources that are needed is a circulating system which includes the pump, connections, hoses and bucket full of water, where water used as a drilling fluid. During the testing, the pump is connected to the real time controller to measure and control in case of abnormal incidents.

Experiment

The test performed by using the two valves in the circulation system, draining valve and outlet valve. The two valves are used to demonstrate the two scenarios; leakage and overpressure.

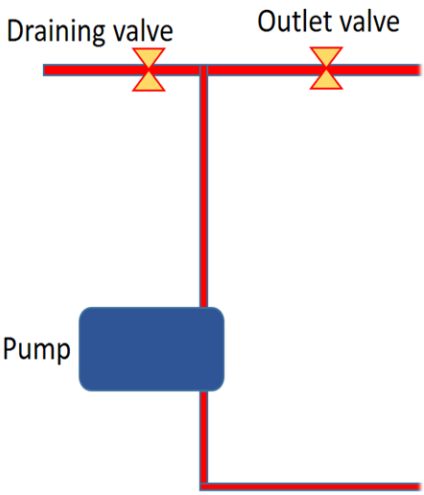

For leakage scenario:

- The outlet valve is open and draining valve is closed.
- Start pumping until the pressure stabilises at the bit.
- Afterwards opening the draining valve with a normal rotational speed approximated 22^{o}/s.

While opening the valve observing pressure drop until the pressure reaches the lower limit which is 1.92 bar, then the expected reaction from the pump is to stop pumping water.

For overpressure scenario:

- The draining valve is closed, and the outlet valve is open.
- Start pumping until the pressure stabilises at the bit.
- Afterwards, start closing the outlet valve in 22^{o}/s.

Then observing a rise of pump pressure until reaching the upper limit of 3.8 bars. Moreover, observing if the pump reacts to pressure boundaries in both cases leakage or overpressure scenarios.

Normal pressure

As illustrated in figure 72 below, the normal pump pressure of the system is 2.56-2.60 bar, and the normal flow rate is 9.9 l/min. The pressure boundaries determined (1.92-3.80) bar.

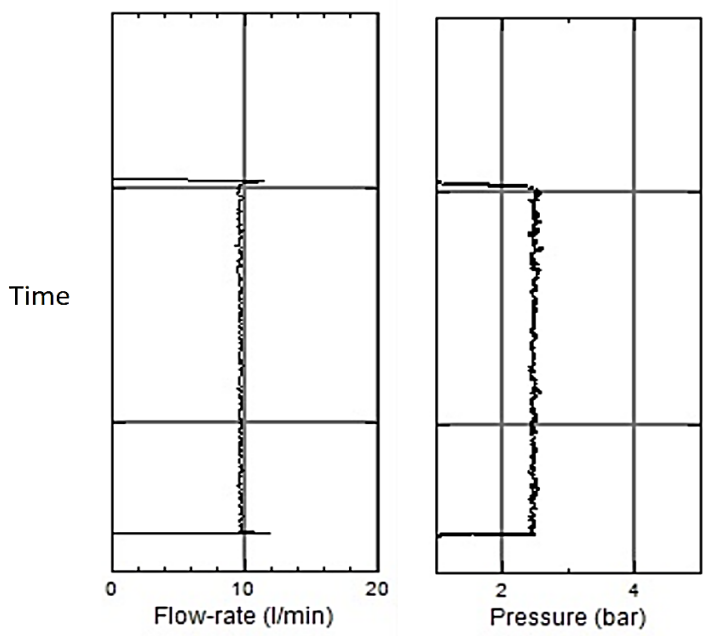

Figure 72: Logs from the real-time controller, normal pressure and normal flow rate.

Leakage

The pump pressure recorded at the stop point to estimate at which pressure point the pump reacts. This experiment performed five times to obtain more precise values for stop pressure in case of leakage scenarios. As illustrated in Table 7 below, the average stop pump pressure is 1.88 bars which is quite close to what the real-time controller programmed with 1.92 bars.

Another leakage experiment performed by opening the draining valve as fast as possible acting like a sudden pressure loss, and the pressure which the pump stopped at was 1.01; that means that the pump needs more time to respond to sudden leakages.

Table 7: Pump pressure during leakage scenario.

Experiment\Pressure	**Start pressure at bit(bara)**	**Stop pressure limit due to washout(bara)**
1	2,5625	1,8875
2	2,5625	1,9375
3	2,5625	1,88125
4	2,5625	1,86875
4	2,55625	1,8375
Average	**2,56125**	**1,8825**
Sudden pressure loss	**Stop pressure (bara)**	1,0125

When pump pressure decreases due to leakage, the flow rate increases. As illustrated in figure 73, several other experiments are done on the pump as:

- Making a leakage in normal speed as done earlier 22^{o}/s.
- Making faster leakage rate.
- Making a sudden leakage as quickly as possible.
- Starting the pump when there is already leakage.

As illustrated pump pressure is none-proportional to pump flow rate.

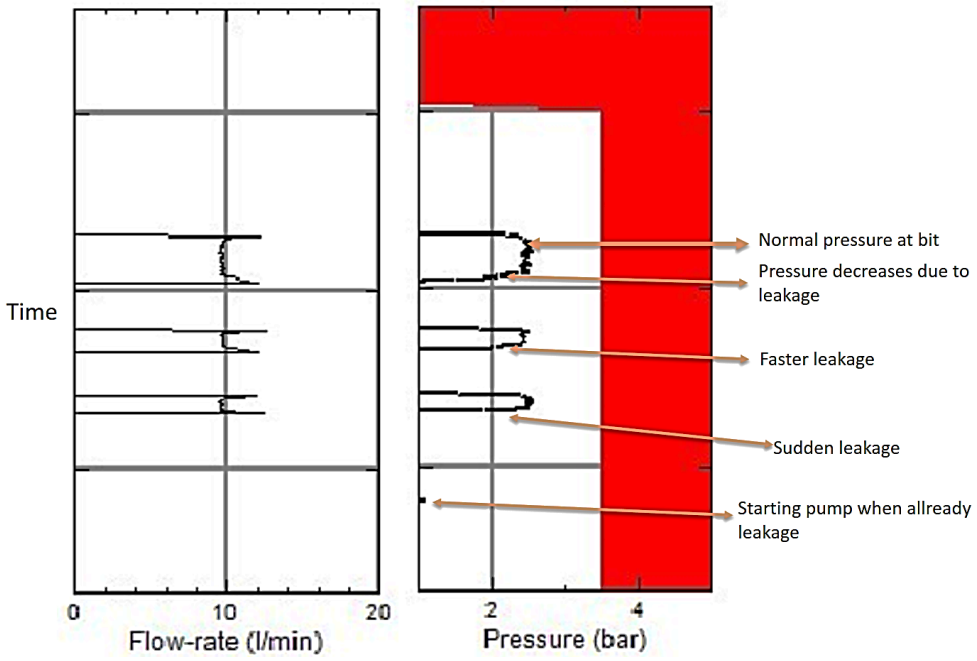

Figure 73: Logs from real-time controller while leakage testing different speeds of leakages.

Overpressure

This experiment based on closing the outlet valve with a normal speed 22°/s by increasing the pressure of the circulation system acting like an overpressure situation. The experiment performed five times, and the average pump stop pressure was 3.82 bar, which is quite close to the chosen pressure 3.8 bars as illustrated in Table 8. The next experiment is closing the valve as fast as possible, and the pump stop pressure was at 3.96 bars, the pump stop pressure was higher when there is a sudden pressure build-up. However, the pump has an inbuilt sensor that shuts the pump if the pressure exceeds 4 bars.

As illustrated in the logs figure 74 from the real-time controller, pump flow rate is none proportional to pump pressure. Several tests are done for overpressure as well, like the following:

- Normal pressure rise.
- Sudden plugged system while pumping.
- Already plugged system.

Table 8: Pump pressure during overpressure.

Experiment\Pressure	Start pressure at bit(bara)	Stop pressure limit due to pack off(bara)
1	2,55625	3,875
2	2,5875	3,81875
3	2,56875	3,80625
4	2,525	3,78125
4	2,525	3,85
Average	**2,5525**	**3,82625**
Sudden pressure builds up stop	**Stop pressure (bara)**	3.95

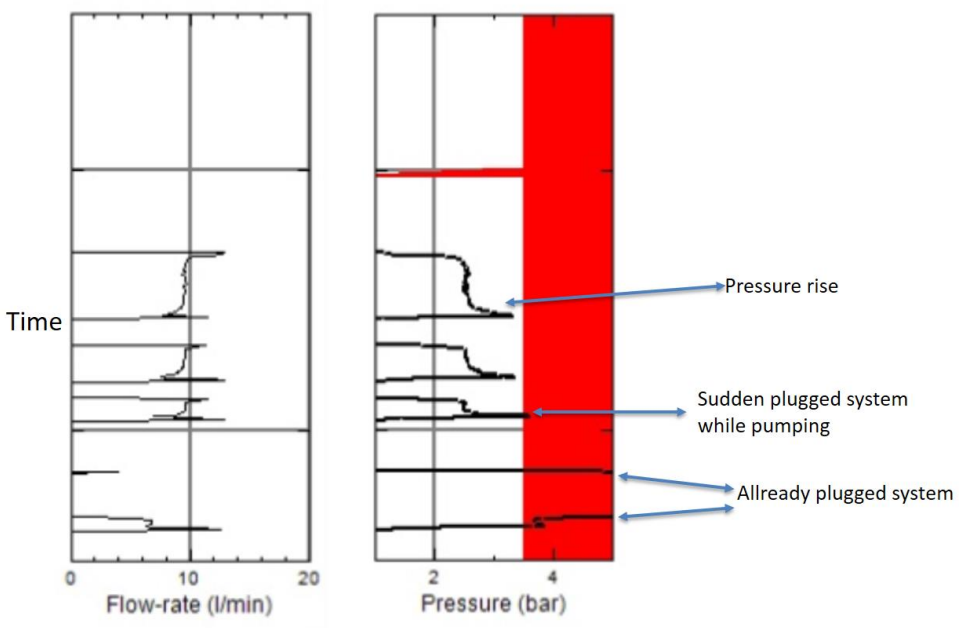

Figure 74: Logs from real-time controller, overpressure in different closing speeds.

Leakage and overpressure scenarios experimented by using the outlet and draining valve and the real-time controller reacts to the change of the pressure with an accuracy of 98% for leakage and 99% for overpressure which seems to be quite good for incidents that occur slowly, used

normal open/close rotational speed of 22°/s. However, if the incident occurs suddenly, the pump needs 2 seconds to stop.

The usual pressure at the bit is around 2.56 bar and having a flow rate of 9.9 l/min. The flow rate and pump pressure change when there is a leak or overpressure scenario. Where the flow rate increases when there is leakage and decreases when there is overpressure as shown in previous logs.

5.4 Over-torque

During drilling in different formation layers, bit sticking might occur. Bit sticking scenarios detected by a torque rise due to the rotation of the motor while the bit still stuck. So, if the torque exceeds certain limits the pipe twists off.

In other words, if the torque of the drill pipe exceeds the boundaries of the aluminium material, the pipe yields then breaks at the ultimate torque of the material. The motor of the top drive connected to the real-time controller where it measures the torque by the load cells that placed on the plate of the top drive. However, the real-time controller should react and stop immediately when the torque of the motor increases above a certain limit. The limit that determined is 2.7 Nm; this limit is only assumed to test the response of the real-time controller. The torque measured by the load cells next to the motor. When the drill string rotates freely, the torque is almost equal to zero. While drilling, the torque increases, so if the torque exceeds 2.7 Nm, the motor should stop.

The major concept of this experiment is to observe the reaction of the real-time controller, where the motor should stop when the torque goes beyond the limit. Note that the torque increases during drilling and even more in the case of sudden sticking.

Experiment

The test begins with rotating the drill string at a constant rpm (60, 90, 120, 150 and 180) each experiment. Afterwards start to apply counterforce on the BHA then observing the torque that the real-time controller responds at. The average stop torque is illustrated in Table 9; the real-time controller is quite precise, but not 100% accurate where the motor stops a small value above the set limit, 2.70 Nm. Note that each experiment performed three times.

Table 9: Stop torque measurements while rotating at different speeds.

Torque\rotational speed	60rpm	90rpm	120rpm	150rpm	180rpm
Stop torque, Nm	2.90	2.75	2.73	2.77	2.80
	2.88	2.84	2.72	2.75	2.82
	2.93	2.71	2.77	2.80	2.78
Average	**2.90**	**2.77**	**2.74**	**2.77**	**2.80**

As illustrated in Table 10, the accuracy of stop torque illustrated compared to the torque limit that set when rotating at different speeds. The real-time controller has an accuracy of 96% when rotating in 180rpm for a stop limit of 2.70 Nm.

Table 10: Accuracy of stop torque

Torque\rotational speed	60rpm	90rpm	120rpm	150rpm	180rpm
Accuracy of reaction	93%	97%	98%	97%	96%

As shown in figure 75, two logs from the real-time controller show the reaction of the rotational speed when the torque of the drill string increases above the set limit (Red area). The blue curve is the set point of the rotational speed, and the black curve is the rotational rate of the drill string. As shown the speed of the drill string is a bit higher than the set point due to programming issues. This experiment demonstrates a sticking scenario where the torque increases when we have stuck pipe. The motor gives a peak torque of 7 Nm, so the pipe will not twist because the ultimate torque to twist the pipe is 8.79 Nm. As a conclusion, the pipe did not twist after a sudden stop while rotating in 180 rpm.

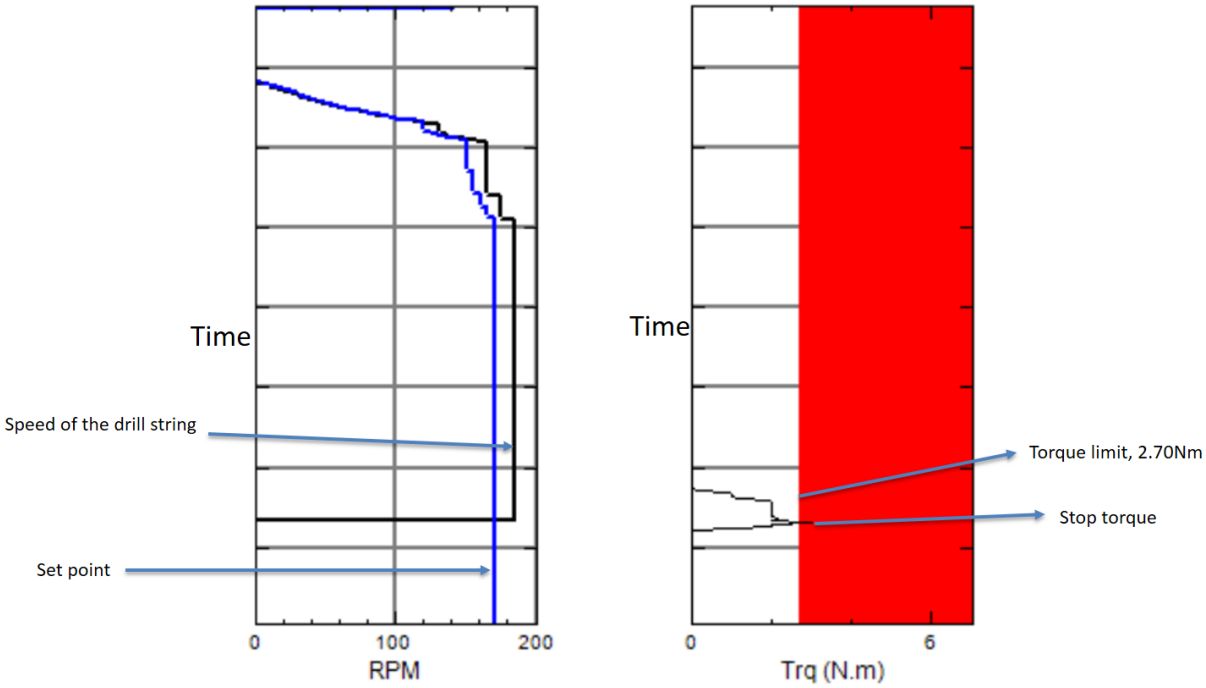

Figure 75: Logs from the real-time controller, Rotational speed and Torque.

5.5 Buckling

The neutral point passes the BHA after the WOB exceeds 0.87 kg, that means that we are drilling in compression. Several tests performed on drill pipe to find the maximum allowable weight before the pipe buckles, starting with applying 10 kg of weight then increasing the weight until reaching the weight that makes the pipe buckle. Table 11 shows the results, where applying 20 kg bends the pipe 2-3 centimeters, but the buckling does not occur. When increasing the weight applied to 25 kg, the pipe bends with a deflection of 9 cm. That gives the WOB a limit of $(25\ kg * 0.80) = 20\ kg$, a safety factor of 0.80 assumed to be in the safe window.

The top drive and the whole drill string weights together less than 10 kg what means that if we apply more than 10 kg, the load cells that placed to measure the hook load will work in tension where the load cells are not designed to resist tension. That means that the maximum WOB should not exceed 10 kg, or the load cells will be damaged.

Table 11: Testing the buckling point of drill pipe.

Weight applied, kg	Buckling
10 kg	No
15 kg	No
20 kg	No, start to bend
25 kg	Yes, 9 cm deflection

5.6 Accelerometers

The accelerometers are fixed to the lower side of the BHA as illustrated in the previous chapter. The accelerometers glued into the BHA; they are supposed to be perfectly in line with the pipe, that means that the z-axis is perfectly parallel to the pipe axis. However, when we glued the accelerometers, we realised that it is very hard to get it exactly in line with the drill pipe. Because of that parallax error, the accelerometer measurements are different from the model that presented in Chapter 3.5.

There is some sinusoidal variation in the z-acceleration. The parallax error illustrated in figure 76. The first error angle is (a) when the facing axis is the x-axis, and the second error angle is (b) when facing the y-axis. The readings we get from the accelerometers are $x`$, $y`$ and $z`$, but the actually readings that are needed is x, y and z.

The acceleration reading values from the control panel of the real-time controller for accelerometers in stationary state gives the following:

$$x' = 1.2\ \frac{m}{s^2}\ \ y' = -1.6\ \frac{m}{s^2}\ and\ z' = 9.6\ \frac{m}{s^2}$$

Those values seem to be a bit wrong where x and y in the stationary state should show 0 m/s^2, and z should show 9.81 m/s^2, gravity direction.

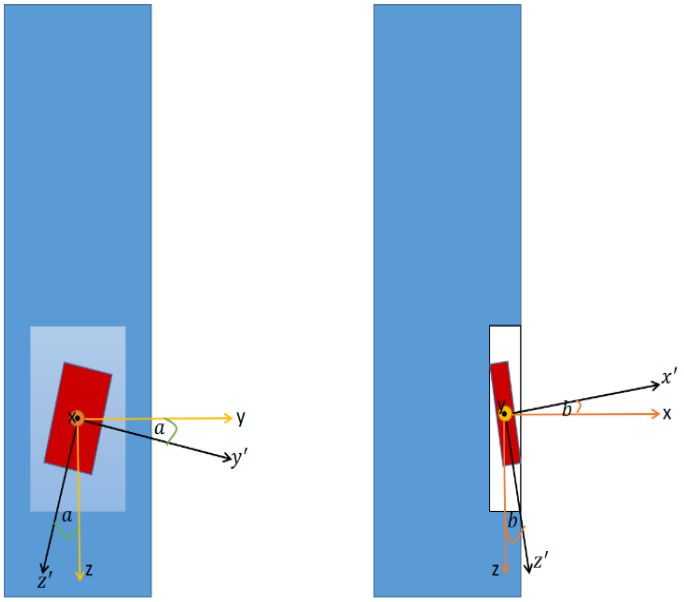

Figure 76: Placement of the accelerometer where it is not parallel to the drill pipe

To solve that problem, the deviation of 3D elementary rotation matrices theory used.

- **General 2D rotation XY-plane**

By using the rotating XY-plane of the Cartesian coordinate system. For 2D rotation the (x, y) coordinates in term of (x`, y`) [35]:

$$x = x`cos\theta - y`sin\theta$$

$$y = x`sin\theta + y`cos\theta$$

Where the matrix form gives the following:

$$\begin{bmatrix} x \\ y \end{bmatrix} = \begin{bmatrix} x` \\ y` \end{bmatrix} \begin{bmatrix} cos\theta & -sin\theta \\ sin\theta & cos\theta \end{bmatrix}$$

By rotating the matrix

$$\begin{bmatrix} x` \\ y` \end{bmatrix} = \begin{bmatrix} x \\ y \end{bmatrix} \begin{bmatrix} cos\theta & sin\theta \\ -sin\theta & cos\theta \end{bmatrix} \quad (1)$$

- **3D rotation around X-axis**

By extending the 2D rotation into 3D by constructing elementary 3D rotation matrix. Where the X-axis is the one that is rotating:

$$\begin{bmatrix} x` \\ y` \\ z` \end{bmatrix} = \begin{bmatrix} 1 & 0 & 0 \\ 0 & cosa & sina \\ 0 & -sina & cosa \end{bmatrix} \begin{bmatrix} x \\ y \\ z \end{bmatrix} = S_x \begin{bmatrix} x \\ y \\ z \end{bmatrix} \quad (2)$$

- **3D rotation around Y-axis**

By doing the same, but this time around the Y-axis, getting the following:

$$\begin{bmatrix} x` \\ y` \\ z` \end{bmatrix} = \begin{bmatrix} cosb & 0 & -sinb \\ 0 & 1 & 0 \\ sinb & 0 & cosb \end{bmatrix} \begin{bmatrix} x \\ y \\ z \end{bmatrix} = S_y \begin{bmatrix} x \\ y \\ z \end{bmatrix} \quad (3)$$

The rotation error of the accelerometer observed around the X- and Y-axis, not the Z-axis, that is why we have two rotation angles a and b. Now, these two elementary matrices are combined to make any 3D rotation correction by the following:

$$S = S_x S_y$$

Then the correction matrix for the 3D rotation is:

$$S = \begin{bmatrix} cosb & 0 & -sinb \\ sina\ sinb & cosa & sina\ cosb \\ cosa\ sinb & -sina & cosa\ cosb \end{bmatrix}$$

Then $$\begin{bmatrix} x` \\ y` \\ z` \end{bmatrix} = \begin{bmatrix} cosb & 0 & -sinb \\ sina\ sinb & cosa & sina\ cosb \\ cosa\ sinb & -sina & cosa\ cosb \end{bmatrix} \begin{bmatrix} x \\ y \\ z \end{bmatrix} \quad (4)$$

The two angles of error are calculated using the matrix above:

$a = 9.5\ degrees$ and $b = 7.0\ degrees$.

The actual values from the accelerometer are for acceleration in x, y and z directions:

$$\begin{bmatrix} x \\ y \\ z \end{bmatrix} = \begin{bmatrix} cosb & 0 & -sinb \\ sina\ sinb & cosa & sina\ cosb \\ cosa\ sinb & -sina & cosa\ cosb \end{bmatrix}^{-1} \begin{bmatrix} x` \\ y` \\ z` \end{bmatrix} \quad (5)$$

Corrected | Correction | Reading

Chapter 6: Discussion and conclusions

6.1 Discussion

Initially, basic calculations on the material properties were made to gain knowledge of the boundaries of the yield and ultimate torque of the drill pipe. The results were 6.39 Nm and 8.79 Nm respectively. Based on drill pipe materials tolerance a proper choice of the basic drilling parameters including weight on bit and rotational speed could be made to maintain drilling without incidents like twisting, buckling, and vibrations.

While working to obtain a suitable layout, several hoisting systems were considered, either using hydraulic cylinders to connect the moveable parts or using small wheels. Sliding wheels were used to allow smaller friction in contrast to standard hydraulic cylinders, with its high viscous forces and moment of inertia. The following hoisting system is attached to a C-Beam actuator, which has a motor that controls mobilisation in the vertical direction, this design is chosen specifically for its rigidity and precision.

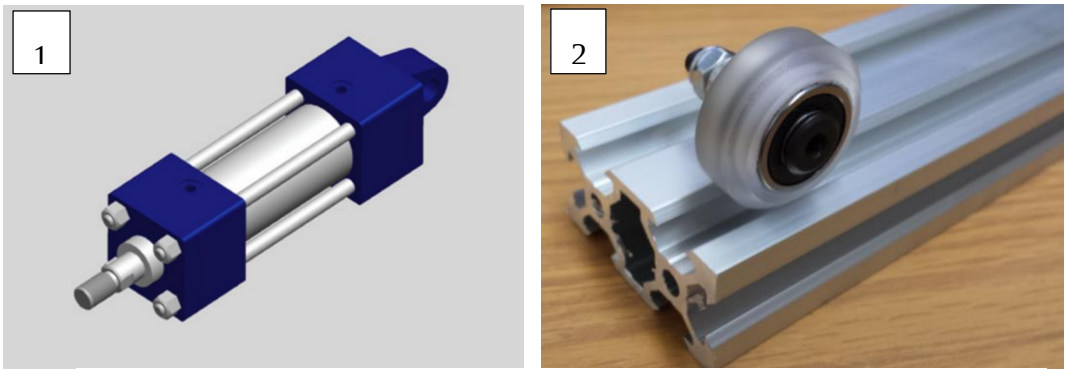

Figure 77: Hydraulic cylinder. 2: Sliding wheels between beams.

The stepper motor on the C-Beam actuator has the advantage of rotating in 1.8^{o} per step and can provide an accurate reading of WOB. The accuracy of such motors is in the range of 0.001mm at each step, where one addition step provides an increase of 0.250 kg in WOB, which at the scope of the design is significantly high.

While working on the design, a 750W stepper motor used in the top drive which delivers torque between 2.8 Nm and 7 Nm. Such motor was chosen in order to give a sufficient torque to the

drill string. Also, the rotary swivel in the drill string is quite heavy, and it has high viscous friction which needs a powerful motor that applies sufficient torque to set it in rotational motion. To avoid twisting of pipe, programming of the motor was made in such way that torque exposure on the drill pipe did not exceed the yield limit.

The pump that used in the system has a pressure capacity between 1-4 bar in order to supply a sufficient flow velocity. The velocity that obtained is around 0.31 m/s in a hole of an OD of 30cm and the pump pressure was 2.56 bar at the bit, which was acceptable to transfer the cuttings at that small scale. The minimum limit of the real-time controller to shut off the pump is 1.92 bar, this value chosen as an assumption of 75% of pump pressure at the bit.

The maximum limit is 3.80 bar which is just below the maximum pump pressure 4.0 bar. This value determined because we needed as much flow rate as possible in case of cuttings accumulation. The real-time controller reacted very well to the slow pressure change in the circulation system where the pump stopped at an average pressure of 1.88 bars and 3.82 bars, which gave a reaction accuracy of 98 and 99% respectively. The pump cannot react very well to sudden pressure change where it takes 2-3 seconds to stop pumping.

In the case of sticking scenarios, a maximum torque limit of 2.70 Nm is implemented in the real-time controller. This value assumed to test the reaction of the real-time controller. The real-time controller responded very well to over-torque. The accuracy to react to the set point was between 93-98% where the motor stopped rotation when the bit torque exceeded the set point while rotating between 60 to 180 rpm.

The maximum allowable WOB estimated based on a rotational speed of 180 rpm and a stop time of 10ms in the case of sudden stoppage. The power transmission model [24] estimates a maximum WOB of 20.4 kg to avoid twisting the pipe. This method takes the friction and moment of inertia into considerations. Therefore, it seems reasonable to depend on this approach to estimate the WOB. However, by applying 20.4 kg of WOB then meeting sudden stop, the twist angle that generated is 38.7 ^{o}, which is below the yield twist angle 46.6^{o}.

By using Rayleigh-Ritz method, the maximum allowable WOB to avoid buckling was between 3.0 kg to 32.0 kg, almost the same values obtained using Euler`s method as well. The testing showed that the pipe buckles at 25.0 kg with a deflection of 9.0 cm. The buckling

results from experiment seem to be reasonable, and it is between the calculated values according to Euler and Rayleigh-Ritz methods.

After rotating the motor, small vertical misalignments in the connection of drill string components observed. Such misalignments cause huge vibrations that might accelerate damaging the drill string very easily. We had difficulties of manually preparing a drill string that is 100% vertical, the prime cause is related to the complexity at the four connection points, and additionally three of them would require glueing procedures. Lack of stability in structure design is also an important contribution to the undesired vibrations observed. Improvements to stability was made through the table the rig was fixed on, by utilising plate stabilisers that hold the legs together.

Other factors that affect the process such friction forces that are between every component in the drill string. The rotary swivel was filled with grease to give a smooth rotation what caused noticeable viscous friction. Friction could affect the rotation negatively, the rotational speed that delivered to the bit at the lower part was less in compare to the top part.

Protecting against any flying objects and water splashing is essential, therefore a barrier of a plexiglass protection with two sides placed around the rig frame as a protection wall in the case of any failures during drilling.

Changing of Drillbotics rules

One of the essential rules of Drillbotics 2016 competition is that the thickness of the drill pipe should not be more than 0.41 mm. The whole design that we have built based on that ultra-thin drill pipe. At the end of March, the Drillbotics committee changed the drill pipe specifications where the thickness of the pipe changed from 0.41 mm to approximately 2.20 mm. The yield torque of the pipe changed from 0.47 Nm to 6.39 Nm. That was the reason why many components of the top drive changed including the motor, where the motor delivers a maximum torque of 7 Nm so the pipe will not twist because the ultimate torque is around 8.79 Nm, see Table 12.

The highest weight for buckling was 8.0 kg then it changed to 25.0 kg. The whole drill string and top drive weights less than 10 kg; that means that the maximum WOB cannot be more

than 10 kg. The load cells designed to work in compression, so if the WOB exceeds 10 kg, the load cells will work in tension (negative hook load), and tension damages the load cells.

As explained changing the drill pipe thickness changed the whole concept of the design we have made. The design that we have done focuses on the 0.42 mm thin drill pipe, where the design could be much simpler with the new pipe of 2.20 mm, but that could not help us when we knew the new rules at the beginning of April. Therefore, we needed more time to start drilling properly.

Table 12: Comparing the change of drill pipe specifications.

	Old drill pipe	**New drill pipe**
Thickness	0.41 mm	2.20 mm
Yield torque	0.47 Nm	6.39 Nm
Ultimate torque	1.28 Nm	8.79 Nm
Buckling force	8 kg	25 kg

6.2 Conclusions

By optimising the rate of rotation, WOB and the response time of the real-time controller in case of sticking, drill pipe failures reduces and makes drilling more safe and sufficient. The concept is to analyse the weakest element in the drill string; drill pipe. The analyse started with determining the how much drill pipe material tolerates. The maximum and most sufficient WOB and rotational speed are determined based on the specifications of the material of the drill pipe.

Furthermore, leakage and overpressure experiments are done to determine at what point the real-time controller reacts to variations in circulation pressure. Moreover, the real-time controller reacted very well to pressure change. However, it needed more time to respond to changes that occurred suddenly, as mentioned before; the rate of leakage or sealing is controlled by the speed of opening/closing the draining/inlet valve.

Later, an over-torque experiment performed as an example of sticking having an over-torque limit of 2.70 Nm. The real-time controller reacted very well when the torque increased while rotating at different speeds between 60-180 rpm. It had an accuracy between 93-98% above the set limit, 2.70 Nm, which was acceptable.

The theoretical analysis showed that the drill pipe would not twist after a sudden stoppage while rotating at 180 rpm, the over-torque experiment verified that the pipe did not twist. The experiments also verified that the drill pipe would buckle after applying 25 kg WOB, where the simulations showed values between 3 kg to 32 kg based on Rayleigh-Ritz method. So the actual buckling force located within the boundaries of Rayleigh-Ritz.

On the other hand, the accelerometers were not reading correctly because of the noise due to the whirl of the BHA on the riser. There were vibrations on the drill string even though the length is only around 2.0 m. Based on the work on the design and observations, some small misalignments between connections that might have made some unbalances that caused additional vibrations.

During rotation, the rotary swivel had quite high viscous friction due to the grease that is inside of it, which caused decreasing the speed of the drill pipe in compare of the rotational speed at the top.

The rig was not finished, so we were not able to drill, but some experiments of the incidents that might occur are performed as mentioned because the rig includes quite many components what needed more time to be finished with. In the end, careful planning and good analysis give protection to avoid drilling incidents because they are dangerous in real life drilling and may reduce the age of the drill string and its components.

Benefits

We were three students that were working on the design and for a degree of petroleum engineering at the same time. Two of us are petroleum's engineering including me and one software engineering. The time was not much, and the design needed more time and people to finish properly, because of the amount of the programming and electrical connections. Such

big design was impossible to finish in five months in addition to writing thesis report. However, this experience developed me as a person and taught me how to is it like to be a designer in such projects.

What I have learned is:

- HSE, as every part of the design, has a safety limit where every element would stop in case of emergency, for example, the pump, which stops when the pressure decreases or increases a certain limit. Moreover, if the torque exceeds the limits, the motor stops.
- Working in a team, we had to work together to perform the design where we needed each other's results and calculations to carry on working the design.
- We have learned more about constructing, building, screwing together and testing.
- The importance and quality of each component in the design.

Recommendation to future work

- The drill string connections must be perfectly vertical, and use another type of table that is easier to make it balance to reduce vibrations that occur due to rotations which also improves the readings of the accelerometers.
- Testing the Rotary swivel before mounting it, because it is possible that it leaks during pumping.
- Using the workshop to design some parts of the design is expensive, carefully designing and planning would spare a lot.
- Start studying the theories and planning the layout at the same time from day one. That gives a better overview of what needs to be done as early as possible.
- This design is promising and something that should be a carried on for the next years because such projects are necessary for future work in oil and gas industries. Also, it gives more picture about the reality of the work as an engineer for a student.
- We started this design work from scratch so that project can be a base for the next year students where they can learn from the failures that we have done. So they can participate in the next year competition.

References

[1] The Drilling Systems Automation Technical Section, “Drillbotics,” 2015. [Online]. Available: www.Drillbotics.com.

[2] R. Sweet, “Case History of Drillstem Failures Offshore West Africa,” in *paper SPE 18653-PA*, New Orleans, Louisiana, 1989 IADC/SPE drilling conferance, 28. Feb to Mar 03..

[3] T. Hill, Drill stem Design and Operation, Third edition, Jan. 2004.

[4] Pegasus vertex, Inc.-Blog, “Drilling software training in snow,” pvisoftware, 13 August 2013. [Online]. Available: http://www.pvisoftware.com/blog/tag/sinusoidal-buckling/.

[5] PET505, “Lecture 2,” Directional drilling. [Online].

[6] *Deepwater Horizon Blowout Animation.* [Film]. youtube.com, 2014.

[7] Silvertip Fishing Tools, “SOME OF YOUR FISHING OPERATIONS,” [Online]. Available: http://www.silvertiprentals.com/id9.html.

[8] Schlumberger, “Drillstring vibrations and vibration modeling,” Schlumberger, [Online]. Available: https://www.slb.com/~/media/Files/drilling/brochures/drilling_opt/drillstring_vib_br.pdf.

[9] DrillingFormulas, “Cutting Settling in Deviated Wells Cause Stuck Pipe,” [Online]. Available: http://www.drillingformulas.com/2011/07/. [Accessed 28 July 2011].

[10] PET525, “Well engineering chapter 2,” [Online]. [Accessed 2015].

[11] H. S. Effendi, “Petroleum support,” [Online]. Available: http://petroleumsupport.com/unconsolidated-formations-pack-off-reason/. [Accessed 8 august 2015].

[12] B. a. d. Matanović Davorin. [Online]. Available: http://rgn.hr/~dmatan/nids_dmatanovic/_private/KRAKOW_INSTRUMENTATION/15_drilling_instrumentation.pdf.

[13] U. o. T. By J.J. Azar, “Drilling Problems and solutions,” pp. Pgs. 433-454, 2006.

[14] S. Lecture 4, “www.colorado.edu/,” [Online]. Available: http://www.colorado.edu/engineering/CAS/courses.d/Structures.d/IAST.Lect04.d/IAST.Lect04.pdf.

[15] H. D. M. a. T. F. In, “failurecriteria,” [Online]. Available: http://www.failurecriteria.com/misescriteriontr.html. [Accessed 11 Jan 2016].

[16] F. c. f. y. Dr. Andri Andriyana. [Online]. Available: https://andriandriyana.files.wordpress.com/2008/03/yield_criteria.pdf. [Accessed spring 2008].

[17] M. o. E. o. Y. M. -. a. T. M. f. c. Materials, “Engineeringtoolbox,” [Online]. Available: http://www.engineeringtoolbox.com/young-modulus-d_417.html.

[18] D. f. Wikipedia. [Online]. Available: https://en.wikipedia.org/wiki/Friction#Dry_friction. [Accessed May 2016].

[19] L. F. Wikipedia. [Online]. Available: https://en.wikipedia.org/wiki/Friction. [Accessed 31 May 2016].

[20] J.-i. Kadokawa., "Tribological Properties of Ionic Liquids," [Online]. Available: http://www.intechopen.com/books/ionic-liquids-new-aspects-for-the-future/tribological-properties-of-ionic-liquids. [Accessed Jan 2013].

[21] Aadnøy, Mechanics of Drilling, 2006.

[22] "Drill String Failure, Cases and Prevention," , Changent Systems, [Online]. Available: http ://www. changent.ispeedway. com/.

[23] W. M. C. a. R. T. E. Hector U. Caicedo, "Unique ROP Predictor Using Bit-specific Coefficient of Sliding Friction and Mechanical Efficiency as a Function of Confined Compressive Strength Impacts Drilling," in *SPE/IADC Drilling Conference*, Amsterdam, The Netherlands, Drilling Conference, 2005.

[24] E. Cayeux, "Modelling of power transmission, Internal note Appendix A," Stavanger, 2016.

[25] E. Cayeux, "modelling of accelerometer, internal note. Appendix B," 2016.

[26] S. p. 2. Drill string and drill collars rotary drilling, "slideshare," [Online]. Available: http://www.slideshare.net/Almenra/drill-string-and-drill-collars-rotary-drilling.

[27] Buckling, "Wikipedia," [Online]. Available: https://en.wikipedia.org/wiki/Buckling. [Accessed 2016].

[28] SPE, "Petrowiki," [Online]. Available: http://petrowiki.org/Casing_and_tubing_buckling. [Accessed 25 June 2015].

[29] H. S. S. K. B. D. Eric Cayeux, “Drillwell, drilling and well for improved recovery.,” Drillwell.no, Jan. 2015.

[30] t. a. a. d. Load cell working, “Instrumentation Engineering,” [Online]. Available: http://www.instrumentationengineers.org/2013/07/load-cell-working-types-advantages-and.html. [Accessed July 2013].

[31] c. Bill Earl, “Adafruit,” [Online]. Available: https://learn.adafruit.com/assets/16204.

[32] Motorsheet750W. [Online]. Available: http://www.limasoft.cz/omron/pdf/G-Series%20Motors(I107E-EN-01A)Datasheet[1].pdf.

[33] H. C. 2008, “Datasheet, coupling flexi joint,” [Online]. Available: http://www.olympus-controls.com/Documents/HelicalCatalog2008.pdf.

[34] alibaba.com. [Online]. Available: http://moflon.en.alibaba.com/product/1898747156-221834828/MT038_series_through_bore_slip_ring_from_Moflon.html?spm=a2700.7724838.0.0.RxeK5b.

[35] Rotation matrix, “Wikipedia,” 2016. [Online]. Available: https://en.wikipedia.org/wiki/Rotation_matrix.

Appendix

A Power transmission modelling Drillbotics 2016

Modelling:

General equation:

The angular movement of an elastic system is described by the following general partial differential equation (Newton's second law for moments):

$$\frac{\partial}{\partial x}\left(GJ(x)\frac{\partial\theta(x,t)}{\partial x}\right)+f(x,t)=I(x)\frac{\partial^2\theta(x,t)}{\partial t^2}$$

with $I(x)=\rho(x)J(x)$, ρ is the mass density, J is the second moment of area, $f(x,t)$ the external torques, and G is the shear modulus.

Decomposition of the system:

The power transmission chain is composed of different elements. Each element is characterized by:

- geometrical dimensions (length l_i, OD d_{o_i}, ID d_{i_i} which corresponds to a second moment of area $J_i=\frac{\pi}{32}\left(d_{o_i}^4-d_{i_i}^4\right)$),
- material properties (mass density ρ_i, shear modulus G_i, shear yield point σ_{syp_i} and ultimate shear strength σ_{su_i}),
- an angular position θ_i,
- a contact friction (static friction μ_{s_i}, kinetic friction μ_{k_i}, Stribeck coefficient c_{v_i} and viscous friction coefficient η_i such that the friction torque is $\tau_{f_i}=-\left(\mu_{k_i}F_{n_i}\frac{d_{oi}}{2}sign(\dot{\theta}_i)+\left(\mu_{s_i}F_{n_i}\frac{d_{oi}}{2}-\mu_{k_i}F_{n_i}\frac{d_{oi}}{2}\right)e^{c_{vi}|\dot{\theta}_i|}\right)sign(\dot{\theta}_i)-\eta_i\dot{\theta}_i$
- a torque τ_i

For instance, the UiS Drillbotics 2016 rotating system can be decomposed in:

- bit
- collar
- stabilizer
- aluminum drill-pipe

- lower shaft
- rotary union
- upper shaft
- motor rotor with bearings

There are friction contacts at the bit, stabilizer, rotary union and the bearings supporting the motor rotor.

Simplification:

A simplification consists in lumping each element in an equivalent disk having the same mass and the same second moment of area than the element itself and to connect each of the lumped disk to each other with a massless spring wire with a zero second moment of area but having a spring torsional constant $k_i = \frac{G_i J_i}{l_i}$.

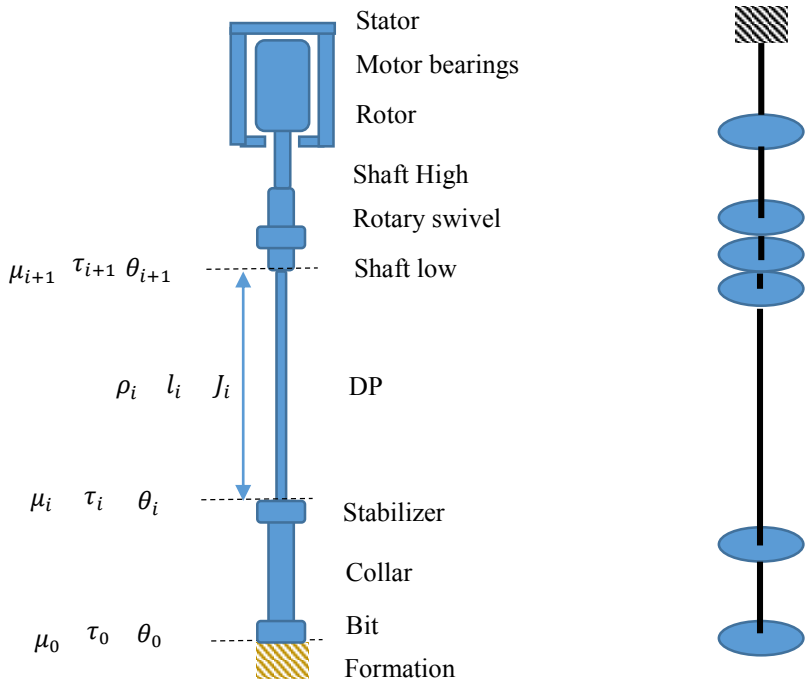

Equilibrium of one element

Considering a friction torque τ_{f_i}, between element i and element $i+1$, i.e. any elements that is neither the bit nor the rotor, the equilibrium is described by:

$$-\eta_i \frac{\partial \theta_i}{\partial t} + \tau_{f_i} - \frac{G_{i-1}J_{i-1}}{l_{i-1}}(\theta_i - \theta_{i-1}) + \frac{G_i J_i}{l_i}(\theta_{i+1} - \theta_i) = I_i l_i \frac{\partial^2 \theta_i}{\partial t^2}$$

We will now linearize in time, by considering discrete time instants (indexed j) separated by a short time interval Δt. The Taylor expansion of the second derivative of the angle θ_i is:

$$\frac{\partial^2 \theta_i}{\partial t^2} \approx \frac{\theta_{i,j+1} - 2\theta_{i,j} + \theta_{i,j-1}}{(\Delta t)^2}$$

And the Taylor expansion of the first derivative is:

$$\frac{\partial \theta_i}{\partial t} \approx \frac{\theta_{i,j+1} - \theta_{i,j}}{\Delta t}$$

It is then possible to rewrite the equilibrium of each elements as a linear function of the $\theta_{i,j+1}$, $\theta_{i,j}$ and $\theta_{i,j-1}$. At a given time step all the $\theta_{i,j}$ and $\theta_{i,j-1}$ are known (they are in the past) and therefore we can easily calculate all the $\theta_{i,j+1}$. However, this explicit method tends to require very small time steps and can easily diverge due to numerical accuracy. It is much more stable to use a semi-implicit formulation as the one of Crank-Nicolson where the average of the sum of the moments between the current time step and the previous one is used as the second member:

$$\begin{aligned} I_i l_i \frac{\theta_{i,j+1} - 2\theta_{i,j} + \theta_{i,j-1}}{(\Delta t)^2} \\ = \frac{1}{2}\Bigg(-\eta_i \frac{\theta_{i,j} - \theta_{i,j-1}}{\Delta t} + \tau_{i,j} + \frac{G_i J_i}{l_i}(\theta_{i+1,j} - \theta_{i,j}) - \frac{G_{i-1}J_{i-1}}{l_{i-1}}(\theta_{i,j} - \theta_{i-1,j}) \\ - \eta_i \frac{\theta_{i,j+1} - \theta_{i,j}}{\Delta t} + \tau_{i,j+1} + \frac{G_i J_i}{l_i}(\theta_{i+1,j+1} - \theta_{i,j+1}) \\ - \frac{G_{i-1}J_{i-1}}{l_{i-1}}(\theta_{i,j+1} - \theta_{i-1,j+1}) \Bigg) \end{aligned}$$

Which gives after regrouping:

$$-\left(\frac{G_{i-1}J_{i-1}}{2l_{i-1}}\right)\theta_{i-1,j+1}+\left(\frac{I_i l_i}{(\Delta t)^2}+\frac{G_i J_i}{2l_i}+\frac{G_{i-1}J_{i-1}}{2l_{i-1}}+\frac{\eta_i}{2\Delta t}\right)\theta_{i,j+1}-\left(\frac{G_i J_i}{2l_i}\right)\theta_{i+1,j+1}$$
$$=\frac{1}{2}\left(\eta_i\frac{\theta_{i,j-1}}{\Delta t}+\tau_{i,j}+\tau_{i,j+1}+\frac{G_i J_i}{l_i}(\theta_{i+1,j}-\theta_{i,j})-\frac{G_{i-1}J_{i-1}}{l_{i-1}}(\theta_{i,j}-\theta_{i-1,j})\right)$$
$$-\frac{I_i l_i}{(\Delta t)^2}(-2\theta_{i,j}+\theta_{i,j-1})$$

For the bit, the equilibrium is defined by:

$$I_0 l_0\frac{\theta_{0,j+1}-2\theta_{0,j}+\theta_{0,j-1}}{(\Delta t)^2}$$
$$=\frac{1}{2}\left(-\eta_0\frac{\theta_{0,j}-\theta_{0,j-1}}{\Delta t}+\tau_{0,j}+\frac{G_0 J_0}{l_0}(\theta_{1,j}-\theta_{0,j})-\eta_0\frac{\theta_{0,j+1}-\theta_{0,j}}{\Delta t}+\tau_{0,j+1}\right.$$
$$\left.+\frac{G_0 J_0}{l_0}(\theta_{1,j+1}-\theta_{0,j+1})\right)$$

where $\tau_{0,j}$ is the torque on bit. If the boundary condition is the torque at the bit, then this equation can be rearranged as a function of $\theta_{0,j+1}$ and $\theta_{1,j+1}$:

$$\left(\frac{I_0 l_0}{(\Delta t)^2}+\frac{G_0 J_0}{2l_0}+\frac{\eta_0}{2\Delta t}\right)\theta_{0,j+1}-\left(\frac{G_0 J_0}{2l_0}\right)\theta_{1,j+1}$$
$$=\frac{1}{2}\left(\eta_0\frac{\theta_{0,j-1}}{\Delta t}+\tau_{0,j}+\tau_{0,j+1}+\frac{G_0 J_0}{l_0}(\theta_{1,j}-\theta_{0,j})\right)-\frac{I_0 l_0}{(\Delta t)^2}(-2\theta_{0,j}+\theta_{0,j-1})$$

However, if the boundary condition is the bit angle, then this equation can be rearranged as a function of $\tau_{0,j+1}$ and $\theta_{1,j+1}$:

$$-\frac{1}{2}\tau_{0,j+1}-\frac{1}{2}\frac{G_0 J_0}{l_0}\theta_{1,j+1}$$
$$=\frac{1}{2}\left(-\frac{\eta_0}{\Delta t}(\theta_{0,j+1}-\theta_{0,j-1})+\tau_{0,j}+\frac{G_0 J_0}{l_0}(\theta_{1,j}-\theta_{0,j}-\theta_{0,j+1})\right)$$
$$-I_0 l_0\frac{\theta_{0,j+1}-2\theta_{0,j}+\theta_{0,j-1}}{(\Delta t)^2}$$

The equilibrium of the next element is defined by:

$$I_1 l_1 \frac{\theta_{1,j+1} - 2\theta_{1,j} + \theta_{1,j-1}}{(\Delta t)^2}$$
$$= \frac{1}{2}\left(-\eta_1 \frac{\theta_{1,j} - \theta_{1,j-1}}{\Delta t} + \tau_{1,j} - \frac{G_0 J_0}{l_0}(\theta_{1,j} - \theta_{0,j}) + \frac{G_1 J_1}{l_1}(\theta_{2,j} - \theta_{1,j}) \right.$$
$$\left. - \eta_1 \frac{\theta_{1,j+1} - \theta_{1,j}}{\Delta t} + \tau_{1,j+1} - \frac{G_0 J_0}{l_0}(\theta_{1,j+1} - \theta_{0,j+1}) + \frac{G_1 J_1}{l_1}(\theta_{2,j+1} - \theta_{1,j+1}) \right)$$

Which can be rearranged as:

$$\left(\frac{I_1 l_1}{(\Delta t)^2} + \frac{\eta_1}{2\Delta t} + \frac{G_0 J_0}{2 l_0} + \frac{G_1 J_1}{2 l_1} \right) \theta_{1,j+1} - \frac{G_1 J_1}{2 l_1} \theta_{2,j+1}$$
$$= \frac{1}{2}\left(\frac{\eta_1}{\Delta t}\theta_{1,j-1} + \tau_{1,j} + \tau_{1,j+1} - \frac{G_0 J_0}{l_0}(\theta_{1,j} - \theta_{0,j} - \theta_{0,j+1}) + \frac{G_1 J_1}{l_1}(\theta_{2,j} - \theta_{1,j}) \right)$$
$$- \frac{I_1 l_1}{(\Delta t)^2}(-2\theta_{1,j} + \theta_{1,j-1})$$

The equilibrium of the bottom part of the element just below the rotor is:

$$I_n l_n \frac{\theta_{n,j+1} - 2\theta_{n,j} + \theta_{n,j-1}}{(\Delta t)^2}$$
$$= \frac{1}{2}\left(\eta_n \frac{\theta_{n,j} - \theta_{n,j-1}}{\Delta t} + \tau_{n,j} + \frac{G_n J_n}{l_n}(\theta_{n+1,j} - \theta_{n,j}) - \frac{G_{n-1} J_{n-1}}{l_{n-1}}(\theta_{n,j} - \theta_{n-1,j}) \right.$$
$$+ \eta_n \frac{\theta_{n,j+1} - \theta_{n,j}}{\Delta t} + \tau_{n,j+1} + \frac{G_n J_n}{l_n}(\theta_{n+1,j+1} - \theta_{n,j+1})$$
$$\left. - \frac{G_{n-1} J_{n-1}}{l_{n-1}}(\theta_{n,j+1} - \theta_{n-1,j+1}) \right)$$

But $\theta_{n+1,j+1}$ is known as it is imposed by the motor speed controller. The last equation can therefore be rewritten:

$$-\left(\frac{G_{n-1} J_{n-1}}{2 l_{n-1}} \right) \theta_{n-1,j+1} + \left(\frac{I_n l_n}{(\Delta t)^2} + \frac{G_n J_n}{2 l_n} + \frac{G_{n-1} J_{n-1}}{2 l_{n-1}} - \frac{\eta_n}{2\Delta t} \right) \theta_{n,j+1}$$
$$= \frac{1}{2}\left(\eta_n \frac{\theta_{n-1,j-1}}{\Delta t} + \tau_{n,j} + \tau_{n,j+1} + \frac{G_n J_n}{l_n}(\theta_{n+1,j} + \theta_{n+1,j+1} - \theta_{n,j}) \right.$$
$$\left. - \frac{G_{n-1} J_{n-1}}{l_{n-1}}(\theta_{n,j} - \theta_{n-1,j}) \right) - \frac{I_n l_n}{(\Delta t)^2}(-2\theta_{n,j} + \theta_{n,j-1})$$

The equilibrium of the top of the last element below the rotor can be written as:

$$I_{rotor}\frac{\theta_{n+1,j+1}-2\theta_{n+1,j}+\theta_{n+1,j-1}}{(\Delta t)^2} = \frac{1}{2}\left(-\eta_{n+1}\frac{\theta_{n+1,j}-\theta_{n+1,j-1}}{\Delta t}+\tau_{n+1,j}-\frac{G_nJ_n}{l_n}\left(\theta_{n+1,j}-\theta_{n,j}\right)\right.$$
$$\left.-\eta_{n+1}\frac{\theta_{n+1,j+1}-\theta_{n+1,j}}{\Delta t}+\tau_{n+1,j+1}-\frac{G_nJ_n}{l_n}\left(\theta_{n+1,j+1}-\theta_{n,j+1}\right)\right)$$

For this equation, we know the $\theta_{n+1,j}$ and $\theta_{n+1,j+1}$ as they are defined by the motor controller, and the unknown are the angle $\theta_{n,j+1}$ and the motor torque $\tau_{n+1,j+1}$. The last equation can be rearranged as:

$$-\frac{1}{2}\frac{G_nJ_n}{l_n}\theta_{n,j+1}-\frac{1}{2}\tau_{n,j+1} = \frac{1}{2}\left(-\eta_{n+1}\frac{\theta_{n+1,j+1}-\theta_{n+1,j-1}}{\Delta t}+\tau_{n,j}-\frac{G_nJ_n}{l_n}\left(\theta_{n+1,j}-\theta_{n,j}+\theta_{n+1,j+1}\right)\right)$$
$$-I_{rotor}\frac{\theta_{n+1,j+1}-2\theta_{n+1,j}+\theta_{n+1,j-1}}{(\Delta t)^2}$$

To determine all the $\theta_{i,j+1}, \forall i<n$, and $\tau_{n,j+1}$ we can solve the following system of equations:

$$\begin{pmatrix} a_{0,0} & a_{0,1} & 0 & 0 & 0 & 0 \\ a_{1,0} & a_{1,1} & a_{1,2} & 0 & 0 & 0 \\ 0 & a_{2,1} & a_{2,2} & a_{2,3} & 0 & 0 \\ 0 & 0 & a_{3,2} & a_{3,3} & a_{3,4} & 0 \\ 0 & 0 & 0 & a_{4,3} & a_{4,4} & 0 \\ 0 & 0 & 0 & 0 & a_{5,4} & a_{5,5} \end{pmatrix}\begin{pmatrix} \theta_{0,j+1} \\ \theta_{1,j+1} \\ \theta_{2,j+1} \\ \theta_{3,j+1} \\ \theta_{4,j+1} \\ \tau_{n,j+1} \end{pmatrix} = \begin{pmatrix} c_0 \\ c_1 \\ c_2 \\ c_3 \\ c_4 \\ c_5 \end{pmatrix}$$

Where $a_{0,0}=\left(\frac{I_0l_0}{(\Delta t)^2}+\frac{G_0J_0}{2l_0}+\frac{\eta_0}{2}\right)$, $a_{0,1}=-\left(\frac{G_0J_0}{2l_0}\right)$, $\forall 0<i<n, a_{i,i-1}=-\frac{G_{i-1}J_{i-1}}{2l_{i-1}}, a_{i,i}=\left(\frac{I_il_i}{(\Delta t)^2}+\frac{G_iJ_i}{2l_i}+\frac{G_{i-1}J_{i-1}}{2l_{i-1}}+\frac{\eta_i}{2\Delta t}\right), a_{i,i+1}=-\frac{G_iJ_i}{2l_i}$, $a_{n,n-1}=-\frac{G_{n-1}J_{n-1}}{2l_{n-1}}$, $a_{n,n}=\frac{I_nl_n}{(\Delta t)^2}+\frac{G_nJ_n}{2l_n}+\frac{G_{n-1}J_{n-1}}{2l_{n-1}}+\frac{\eta_n}{2\Delta t}$, $a_{n+1,n}=-\frac{1}{2}\frac{G_nJ_n}{l_n}$, $a_{n+1,n+1}=-\frac{1}{2}$, $c_0=\frac{1}{2}\left(\eta_0\frac{\theta_{0,j-1}}{\Delta t\Delta t}+\tau_{0,j}+\tau_{0,j+1}+\right.$

$\frac{G_0J_0}{l_0}(\theta_{1,j}-\theta_{0,j})\Big)-\frac{I_0l_0}{(\Delta t)^2}(-2\theta_{0,j}+\theta_{0,j-1})$, $\forall 0<i<n-1, c_i=\frac{1}{2}\Big(\eta_i\frac{\theta_{i,j-1}}{\Delta t}+\tau_{i,j}+\tau_{i,j+1}+$ $\frac{G_iJ_i}{l_i}(\theta_{i+1,j}-\theta_{i,j})-\frac{G_{i-1}J_{i-1}}{l_{i-1}}(\theta_{i,j}-\theta_{i-1,j})\Big)-\frac{I_il_i}{(\Delta t)^2}(-2\theta_{i,j}+\theta_{i,j-1})$ and $c_n=\frac{1}{2}\Big(\eta_n\frac{\theta_{n-1,j-1}}{\Delta t}+$ $\tau_{n,j}+\tau_{n,j+1}+\frac{G_nJ_n}{l_n}(\theta_{n+1,j}+\theta_{n+1,j+1}-\theta_{n,j})-\frac{G_{n-1}J_{n-1}}{l_{n-1}}(\theta_{n,j}-\theta_{n-1,j})\Big)-\frac{I_nl_n}{(\Delta t)^2}(-2\theta_{n,j}+$ $\theta_{n,j-1})$ and $c_{n+1}=\frac{1}{2}\Big(-\eta_{n+1}\frac{\theta_{n+1,j+1}-\theta_{n+1,j-1}}{\Delta t}+\tau_{n,j}-\frac{G_nJ_n}{l_n}(\theta_{n+1,j}-\theta_{n,j}+\theta_{n+1,j+1})\Big)-$ $I_{rotor}\frac{\theta_{n+1,j+1}-2\theta_{n+1,j}+\theta_{n+1,j-1}}{(\Delta t)^2}$

This is a tridiagonal linear system which can efficiently be solved numerically.

If the bottom boundary condition is the bit angle, then the unknown variables are $\tau_{0,j+1}$, $0<i<n$ $\theta_{i,j+1}$ and $\tau_{n,j+1}$:

$$\begin{pmatrix} a_{0,0} & a_{0,1} & 0 & 0 & 0 & 0 \\ 0 & a_{1,1} & a_{1,2} & 0 & 0 & 0 \\ 0 & a_{2,1} & a_{2,2} & a_{2,3} & 0 & 0 \\ 0 & 0 & a_{3,2} & a_{3,3} & a_{3,4} & 0 \\ 0 & 0 & 0 & a_{4,3} & a_{4,4} & 0 \\ 0 & 0 & 0 & 0 & a_{5,4} & a_{5,5} \end{pmatrix}\begin{pmatrix} \tau_{0,j+1} \\ \theta_{1,j+1} \\ \theta_{2,j+1} \\ \theta_{3,j+1} \\ \theta_{4,j+1} \\ \tau_{n,j+1} \end{pmatrix}=\begin{pmatrix} c_0 \\ c_1 \\ c_2 \\ c_3 \\ c_4 \\ c_5 \end{pmatrix}$$

where $a_{0,0}=-\frac{1}{2}$, $a_{0,1}=-\frac{1}{2}\frac{G_0J_0}{l_0}$ and $c_0=\frac{1}{2}\Big(-\frac{\eta_0}{\Delta t}(\theta_{0,j+1}-\theta_{0,j-1})+\tau_{0,j}+\frac{G_0J_0}{l_0}(\theta_{1,j}-\theta_{0,j}-$ $\theta_{0,j+1})\Big)-I_0l_0\frac{\theta_{0,j+1}-2\theta_{0,j}+\theta_{0,j-1}}{(\Delta t)^2}$, $a_{1,1}=\frac{I_1l_1}{(\Delta t)^2}+\frac{\eta_1}{2\Delta t}+\frac{G_0J_0}{2l_0}+\frac{G_1J_1}{2l_1}$, $a_{1,2}=-\frac{G_1J_1}{2l_1}$ and $c_1=$ $\frac{1}{2}\Big(\frac{\eta_1}{\Delta t}\theta_{1,j-1}+\tau_{1,j}+\tau_{1,j+1}-\frac{G_0J_0}{l_0}(\theta_{1,j}-\theta_{0,j}-\theta_{0,j+1})+\frac{G_1J_1}{l_1}(\theta_{2,j}-\theta_{1,j})\Big)-\frac{I_1l_1}{(\Delta t)^2}(-2\theta_{1,j}+$ $\theta_{1,j-1})$ the other coefficients being identical to the formulation based on boundary condition using the bit torque.

B Modelling of accelerometers in Drillbotics 2016

An accelerometer is placed at a distance $r"$ from the center of rotation of a pipe. The pipe rotates with an angular velocity $\dot{\theta}"$ (the first derivative compared to time of the angle $\theta"$). The pipe axis rotates at a distance r' from a center of rotation Ω with an angular velocity $\dot{\theta}'$ (the first derivative compared to time of the angle θ'). And the center of rotation Ω translates compared to the wellbore center Ω_0 (see Figure) in an orthonormal basis defined by the unit vectors $\hat{\imath}$ and $\hat{\jmath}$.

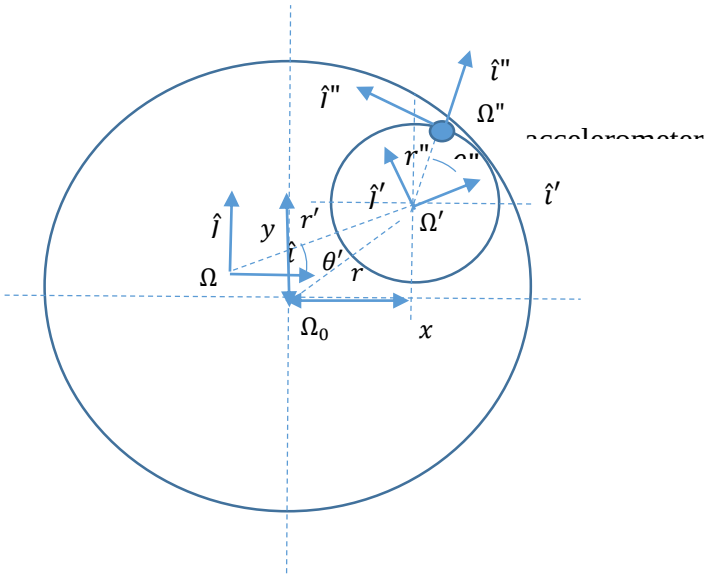

Figure: definition of the variables characterizing the movement of the accelerometer.

The polar coordinate $(r", \theta")$ are related to the geometrical position of the accelerometer and the drill-string , while (r', θ') are associated with the lateral movement of the drill-pipe inside the borehole. The latter can be contributed from either forward whirl, backward whirl or chaotic whirl.

For each of these two rotations, fictitious accelerations can be experienced by a local observer in the rotating frame. These accelerations are:

- Centrifugal acceleration: $-\vec{\omega} \times (\vec{\omega} \times \vec{r})$

- Coriolis acceleration: $-2\vec{\omega} \times \vec{r}$
- Euler acceleration: $-\dot{\vec{\omega}} \times \vec{r}$

However, Ω, r' and θ' are not directly known. Instead, it is most likely that we have the Cartesian coordinates (x and y) of the center line of the drill-pipe compared to the geometrical center of the borehole Ω_0, $\hat{\imath}$ and $\hat{\jmath}$. Ω, r' and θ' describes in fact a co-rotating frame which is sometime referred to as the osculating circle of the motion of the pipe center line with regards to the inertial frame defined by Ω_0, $\hat{\imath}$ and $\hat{\jmath}$. In the osculating circle, the fictitious accelerations are:

$$\gamma_r = \ddot{r}' - r'\dot{\theta}'^2 \; and \; \gamma_\theta = r'\ddot{\theta}' + 2\dot{r}'\dot{\theta}'$$

The curvature in the osculating circle is defined by:

$$\kappa' = \frac{1}{r'} = \frac{\dot{x}\ddot{y} - \dot{y}\ddot{x}}{(\dot{x}^2 + \dot{y}^2)^{3/2}}$$

And the center of the osculating circle is:

$$\begin{cases} x - \dfrac{\dot{y}}{\kappa\sqrt{\dot{x}^2 + \dot{y}^2}} \\ y + \dfrac{\dot{x}}{\kappa\sqrt{\dot{x}^2 + \dot{y}^2}} \end{cases}$$

which means that the angle $\theta' = \tan^{-1}\left(\frac{-\dot{y}}{\dot{x}}\right)$

Regarding the rotation of the accelerometer at the periphery of the pipe, its angle of rotation has to be corrected for the own rotation of the pipe inside the inertial frame. So if α is the angle of rotation of the pipe compared to a fixed referential, then the angle $\theta" = \alpha - \theta'$.

The pipe central line acceleration, seen from the reference frame of the accelerometer is:

$$\begin{pmatrix} \cos\theta" & \sin\theta" \\ -\sin\theta" & \cos\theta" \end{pmatrix} \begin{pmatrix} \gamma_r \\ \gamma_\theta \end{pmatrix}$$

This acceleration is superposed to the fictitious accelerations arising from the pipe rotation around its center line:

$$\gamma_r{}'' = -r''\dot{\theta}''^2 \; and \; \gamma_\theta{}'' = r''\ddot{\theta}''$$

Note that the first and second derivatives of the radius are zero, since the accelerometer does not move radially compared to the pipe.

Furthermore, the pipe may be subject to an axial acceleration. The axial acceleration γ_a will be seen on the axes of the accelerometer as:

$$\begin{cases} 0 \\ 0 \\ \gamma_a \end{cases}$$

The accelerometer is also subject to the gravitational acceleration g which is oriented downward in the global reference frame. The local inclination is denoted β and the rotation angle of the pipe in the inertial frame is α with regards to the upward vertical (see Figure).

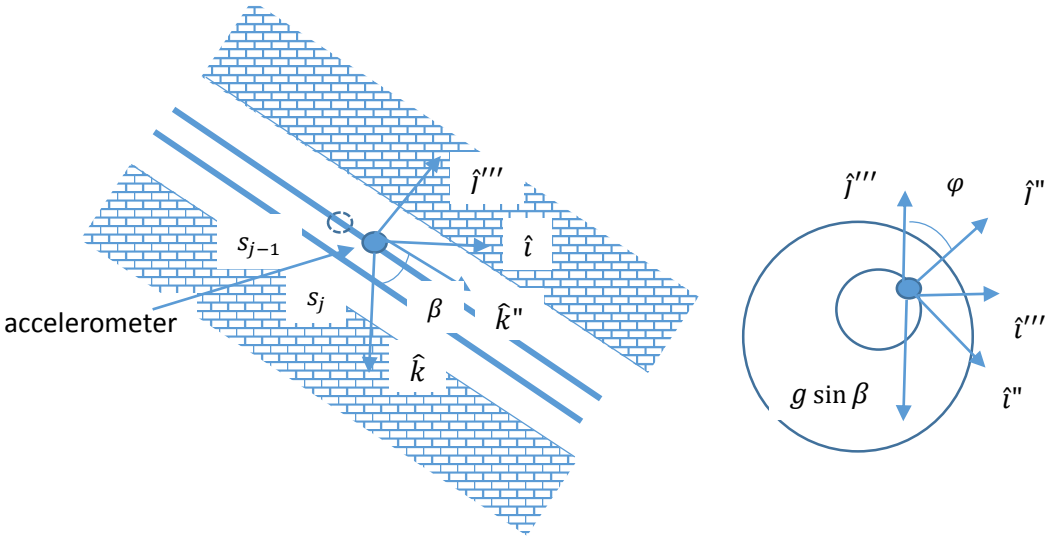

Figure: axial acceleration

Then the gravitation will be seen on the axes of the accelerometer as:

$$\begin{cases} g \sin\beta \sin\varphi \\ g \sin\beta \cos\varphi \\ g \cos\beta \end{cases}$$

The acceleration readings are the sum of the gravitation, axial acceleration, acceleration induced by the pipe rotation around its center line and the one of the pipe center line due to lateral movement.

$$\begin{cases} g\sin\beta\sin\varphi - r^{"}\dot{\theta}^{"2} + \left(\ddot{r}' - r'\dot{\theta}'^{2}\right)\cos\theta" + \left(r'\ddot{\theta}' + 2\dot{r}'\dot{\theta}'\right)\sin\theta" \\ g\sin\beta\cos\varphi + r^{"}\ddot{\theta}' - \left(\ddot{r}' - r'\dot{\theta}'^{2}\right)\sin\theta" + \left(r'\ddot{\theta}' + 2\dot{r}'\dot{\theta}'\right)\cos\theta" \\ g\cos\beta + \gamma_a \end{cases}$$

When there are no lateral and axial vibrations and for a steady rotation, the accelerometers will read:

$$\begin{cases} g\sin\beta\sin\varphi - r^{"}\dot{\theta}^{"2} \\ g\sin\beta\cos\varphi \\ g\cos\beta \end{cases}$$

Over a period of rotation, the average of the first component is the centrifugal force. Then we can subtract that value and extract the amplitude of the sinusoid to obtain the inclination.

For the second equation, the amplitude of the sinusoid should give the inclination.

The third equation does not need time processing to obtain the inclination.

By averaging the three estimations, it should be possible to obtain a more accurate assessment of the inclination.

However, if there are axial and/or lateral vibrations, then the accelerometer signals will contain much more noise. By applying a FFT and a pass band filter around the nominal rotational frequency, it is possible to eliminate the lateral acceleration effects. On the other hand, by measuring the amplitude of the "noise", i.e. eliminating the main rotational frequency, it is possible to estimate the vibration level. If the vibration level goes above a defined threshold, then we can stop the rotation in order to avoid any potential destruction of the drill-string.

C. Simulators

- Detecting buckling using Rayleigh-Ritz method.

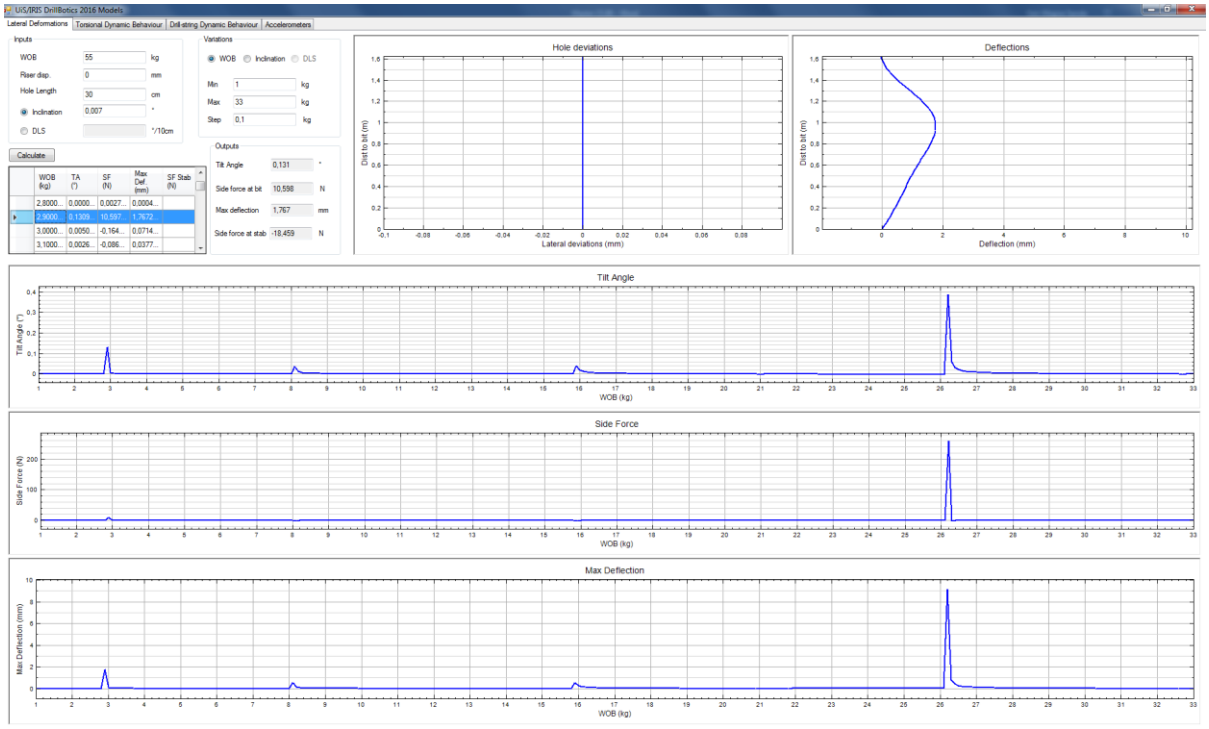

- Estimating the torque on the pipe while applying 22 kg WOB, Using power transmission model.

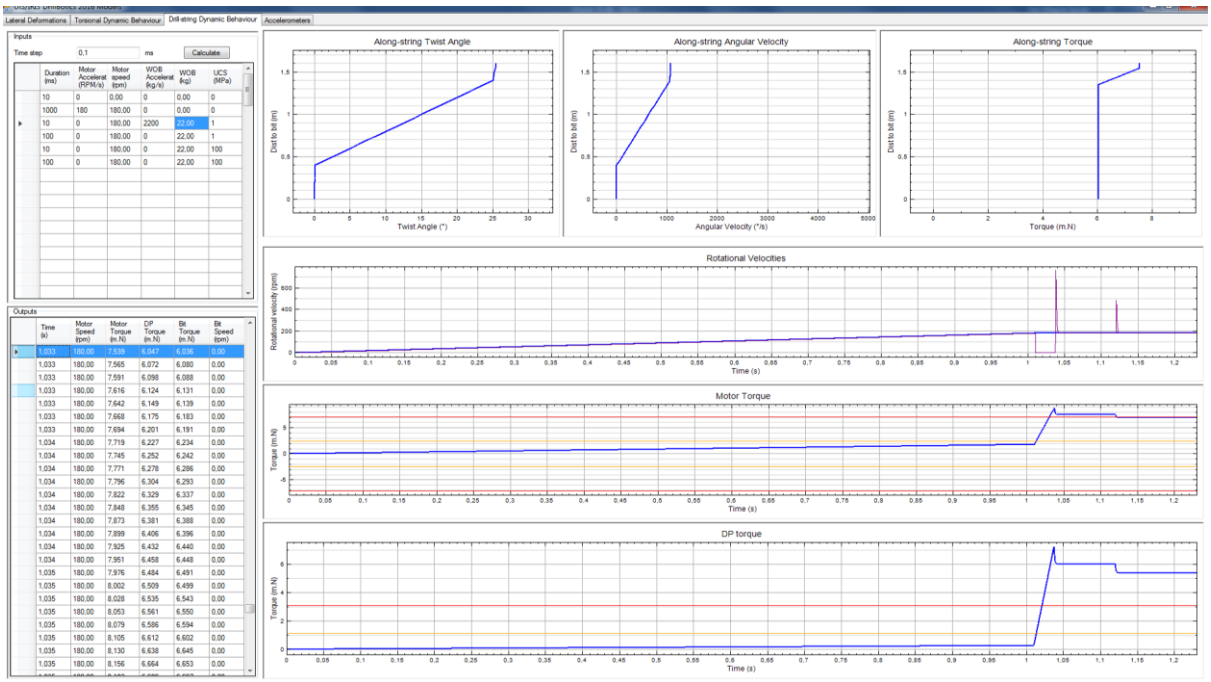

- Simulator for modelling of accelerometers, using a stepper motor that makes noise in acceleration at Y-direction.

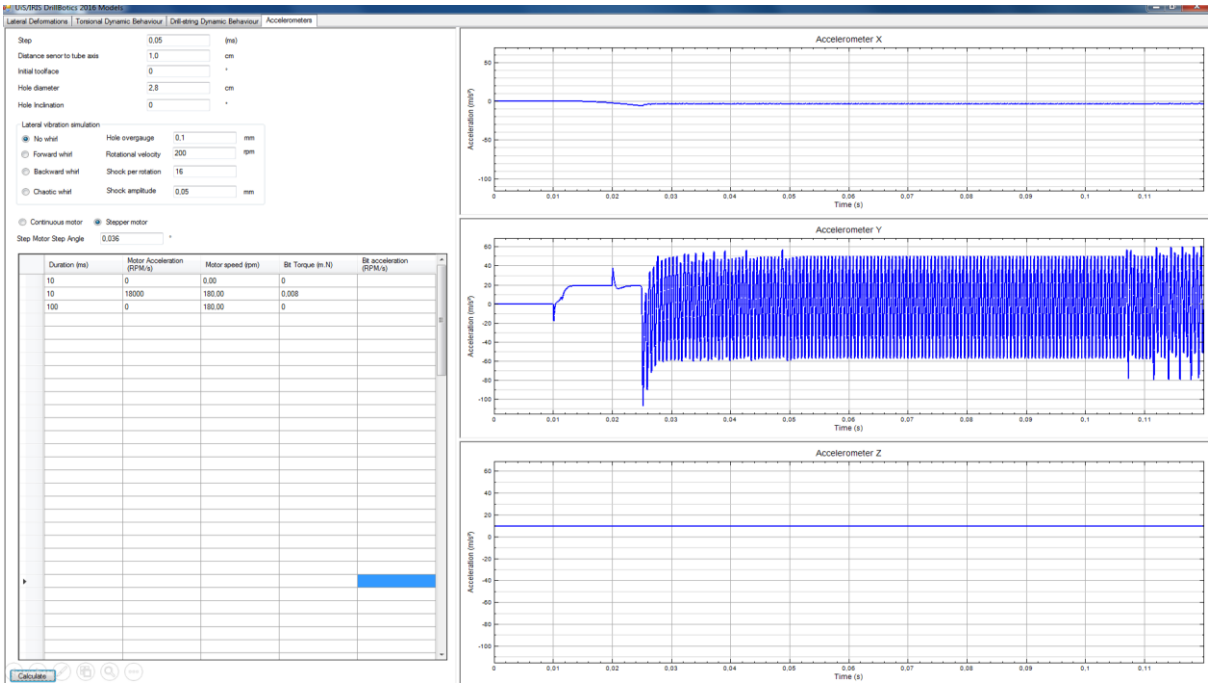

- Using a DC motor for modelling of acceleration, no noise.

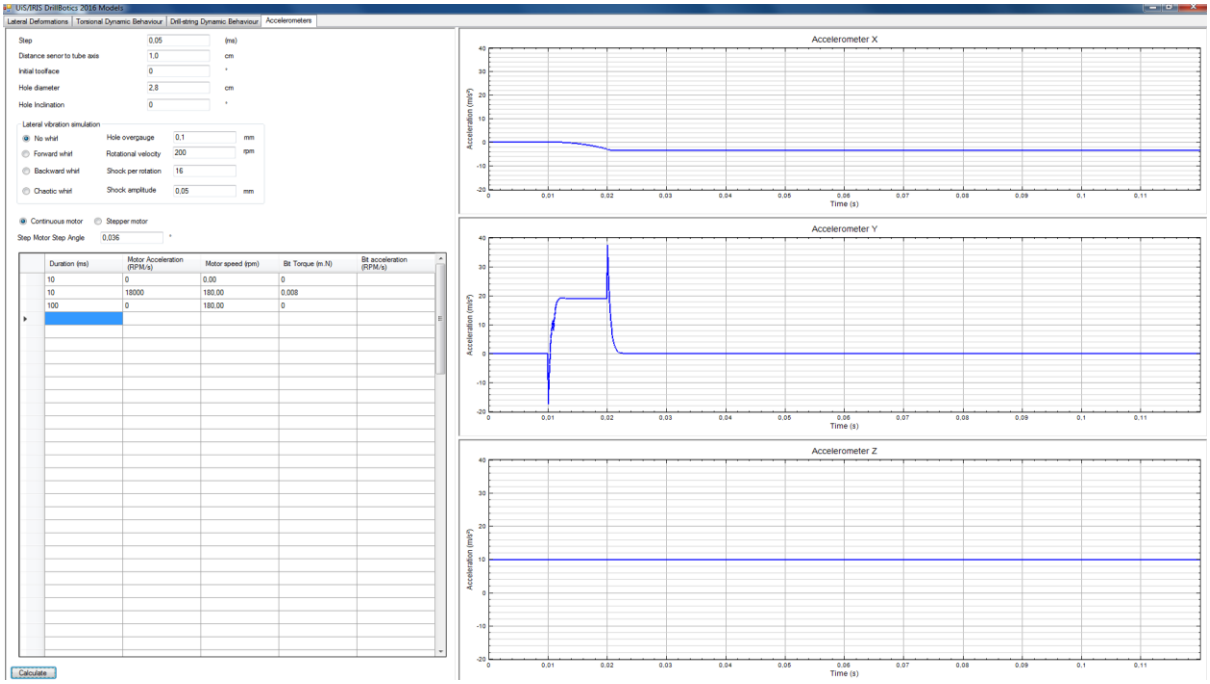

D. Pictures of the design

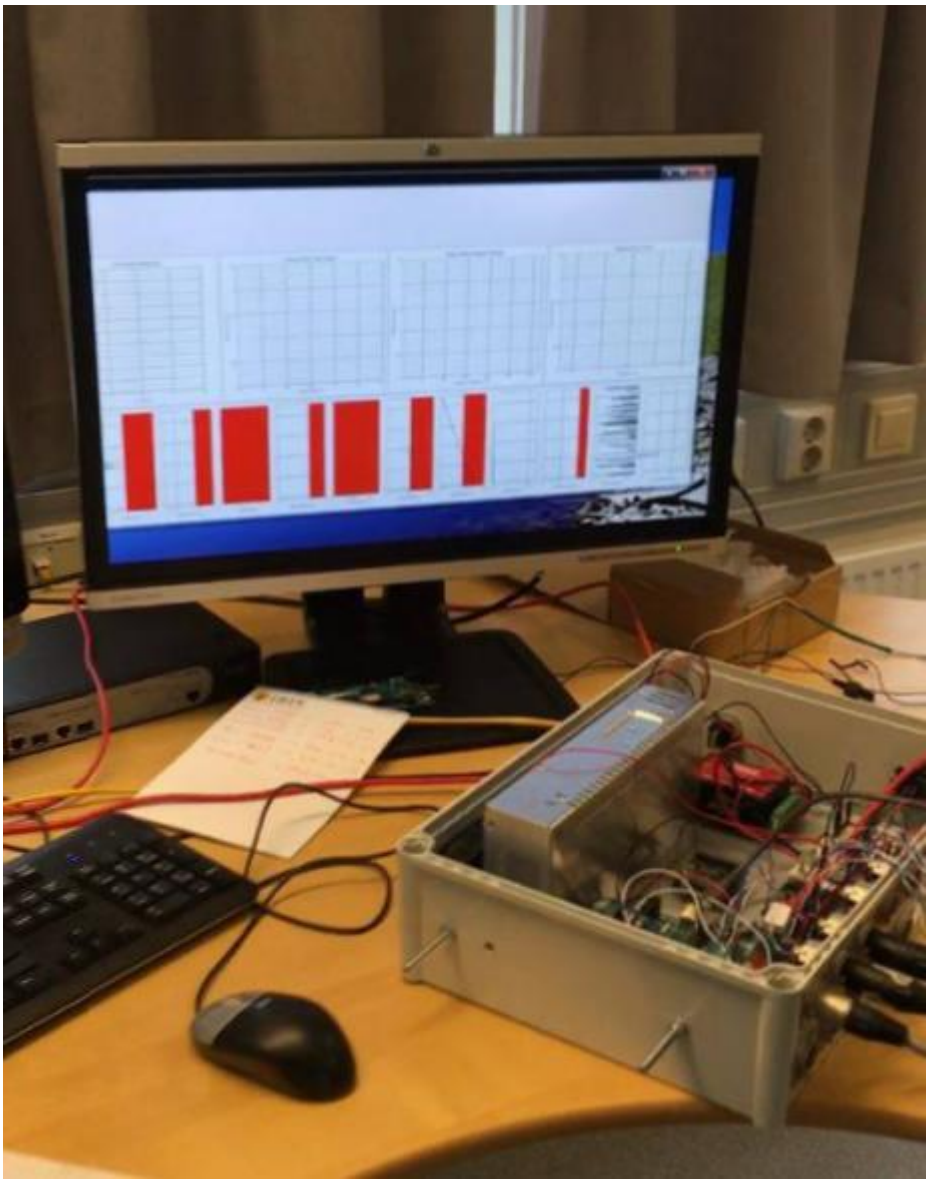

Picture 1: Logging circulation pressure, bit torque, hook load and more in the control panel.

Picture 2: The bottom hole assembly.

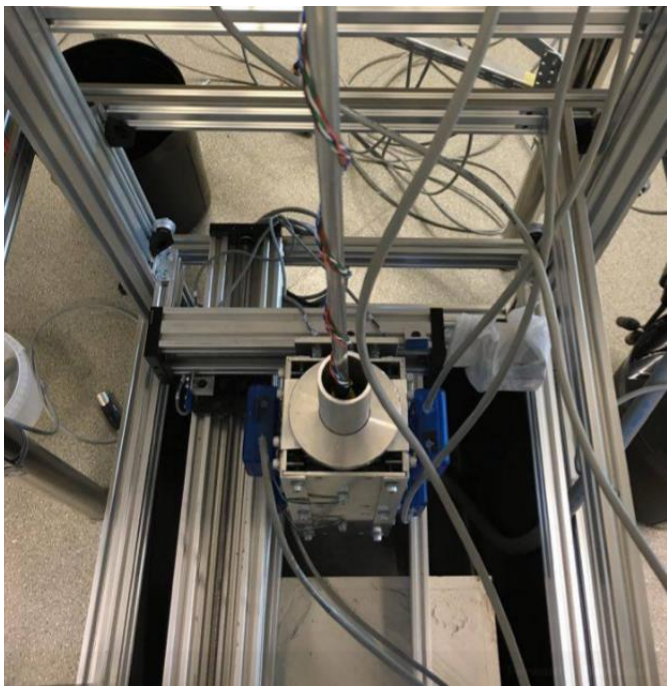

Picture 3: Drill pipe and riser.

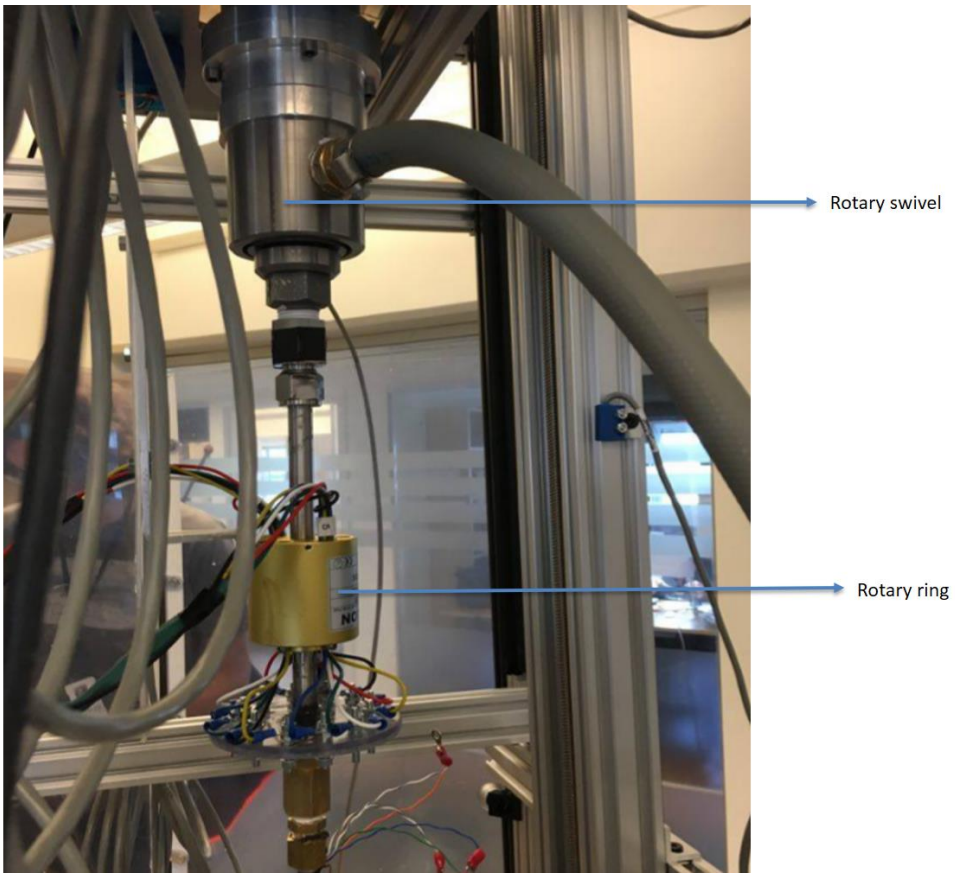

Picture 4: The top part of drill string, rotary swivel and rotary ring.